



THE HONG KONG
POLYTECHNIC UNIVERSITY

香港理工大學

Pao Yue-kong Library

包玉剛圖書館

Copyright Undertaking

This thesis is protected by copyright, with all rights reserved.

By reading and using the thesis, the reader understands and agrees to the following terms:

1. The reader will abide by the rules and legal ordinances governing copyright regarding the use of the thesis.
2. The reader will use the thesis for the purpose of research or private study only and not for distribution or further reproduction or any other purpose.
3. The reader agrees to indemnify and hold the University harmless from and against any loss, damage, cost, liability or expenses arising from copyright infringement or unauthorized usage.

If you have reasons to believe that any materials in this thesis are deemed not suitable to be distributed in this form, or a copyright owner having difficulty with the material being included in our database, please contact lbsys@polyu.edu.hk providing details. The Library will look into your claim and consider taking remedial action upon receipt of the written requests.

The Hong Kong Polytechnic University

Department of Electronic and Information

Engineering

Low Numerical Dispersion Error

ADI-FDTD methods

Sun Man Kin

A thesis submitted in partial fulfilment of the requirements for the

Degree of Doctor of Philosophy

August 2006

CERTIFICATE OF ORIGINALITY

I hereby declare that this thesis is my own work and that, to the best of my knowledge and belief, it reproduces no material previously published or written, nor material that has been accepted for the award of any other degree or diploma, except where due acknowledgment has been made in the text.

_____ (Signed)

SUN MAN KIN _____ (Name of student)

Abstract

The Finite Difference Time Domain (FDTD) method is one of the most popular time domain methods in computational electromagnetics. The FDTD method is easy to implement and a wide band solution can compute from a single run of simulation. However, the application of the FDTD method is limited by the requirement of the computational resources. Such requirement is due to the numerical dispersion error and the Courant-Friedrich-Levy (CFL) stability condition, which relates the choosing of the cell size and the time-step. In recent research, an unconditionally stable FDTD method was proposed—one that can set the time-step to any arbitrary value without compromising the stability of the system. This method applies the Alternating Direction Implicit (ADI) technique to solve the finite difference equations; therefore, it is named the “ADI-FDTD method.” The ADI-FDTD method is useful to simulate a structure with fine features because the time-step can be set to the desired value, based on the signal but not the smallest cell size. However, it suffers a drawback in that the numerical dispersion error is found to increase when the ADI technique is applied.

In this thesis, two modified ADI-FDTD methods are proposed to reduce the numerical dispersion error. The first method is the high-order ADI-FDTD method, which employs the multi-points high-order central difference scheme to approximate the spatial derivative terms. This method is still unconditionally stable and can reduce the numerical dispersion. However, it is found that the numerical dispersion error of the sixth-order ADI-FDTD method is close to the limit of the conventional ADI-FDTD method, and the improvement is found to be relatively insignificant when the time-step is large. This motivated the development of the second method called (2,4) low numerical dispersion

(LD) ADI-FDTD method. This method is based on the fourth-order ADI-FDTD method. The coefficients of finite difference operator are modified by minimizing the error terms in the numerical dispersion relation. This modification does not affect the unconditionally stable property. In addition, the (2,4) LD ADI-FDTD method can provide a significant wide band reduction on the numerical dispersion error for any time-step. Furthermore, there is an alternative scheme that can reduce the numerical dispersion error at a specified propagation angle.

Publications Arising from the Thesis

Journals:

- 1 M. K. Sun and W. Y. Tam, "Stability and Dispersion analysis of ADI-MRTD and ADI High-order schemes," *Microwave and Optical Tech. Lett.*, vol.45, pp. 43-46, Apr. 2005.
- 2 M. K. Sun and W. Y. Tam, "Low Numerical Dispersion Two-Dimensional (2,4) ADI-FDTD Method," *IEEE Trans. Antennas and Propagat.*, vol. 54, pp. 1041-1044, Mar. 2006.

Conference papers:

- 1 M. K. Sun and W. Y. Tam, "Analysis of the Numerical Dispersion of the 2-D ADI-FDTD Method with Higher order scheme," *IEEE Antennas and Propagat. Society International Symp.*, vol.4, pp. 348-351, Jun. 2003.
- 2 M. K. Sun and W. Y. Tam, "An unconditionally stable high-order 2-D ADI-FDTD method," *IEEE Antennas and Propagat. Society International Symp.*, vol.4, pp. 352-355, Jun. 2003.
- 3 M. K. Sun and W. Y. Tam, "A FDTD method based on various explicit finite-difference algorithms," *Proc. Progress in Electromagnetics Research Symp.*, pp. 149, Jan. 2003.
- 4 M. K. Sun and W. Y. Tam, "Analysis of the Numerical Dispersion of the High-order 2-D ADI-FDTD Method," *The 4th IEEE (HK) AP/MTT & LEOS Postgraduate Conf.*, pp.47-50, Oct. 2003.
- 5 M. K. Sun and W. Y. Tam, "Low Numerical Dispersion Algorithm for the 2-D High-order ADI-FDTD method," *The 5th IEEE (HK/Macau) AP/MTT Postgraduate Conf.*, pp.48-51, Sept. 2004.

Acknowledgments

I would like to take this opportunity to express my sincere gratitude toward various bodies.

I am deeply indebted to Dr. W. Y. Tam, who supervised my entire study. His patience, guidance and support made this work possible. Besides, I would like to thanks my colleagues, Canny Y. H. Kwan, Kevin L. F. Lui, C. Y. Li, K. Y. Wong and C. M. Tian, for their friendship support and encouragement. Furthermore, it is my pleasure to acknowledge the Department of Electronic and Information Engineering of the Hong Kong Polytechnic University and the Research Grant Committee of the University Grant Council for their facility and financial support during my study.

Finally, this thesis is dedicated to my parents. Without their never ending support and encouragement, this study would not have the chance to be completed.

Statement of Originality

1 The High-Order ADI-FDTD Method

The high-order ADI-FDTD method is formulated by using the multi-points high-order central finite difference scheme to approximate the spatial derivatives in the ADI-FDTD method. The stability condition is studied, and it has been proven that the high-order ADI-FDTD method is unconditionally stable. In addition, the numerical dispersion relation is derived, and it has been shown that the numerical dispersion error is reduced. Furthermore, the numerical dispersion error of the sixth-order ADI-FDTD method is already close to the limit of the conventional ADI-FDTD method for a given time-step. The stability and numerical dispersion relation are validated by the simulation results.

2 The Low Numerical Dispersion (2,4) ADI-FDTD Method

The Low Numerical Dispersion (2,4) ADI-FDTD method is based on the fourth-order ADI-FDTD method. The finite difference operator is modified by minimizing the error terms in the numerical dispersion relation. The modification does not affect stability condition. In addition, the numerical dispersion relation is derived, and it has been shown that the numerical dispersion error is much smaller than in either the conventional ADI-FDTD method or the FDTD method for any time-step. Furthermore, the complexity of the LD ADI-FDTD method has been studied. When the LU method is used to solve the equations system, the complexity remains as the order of the length of the

computational domain. Finally, the stability and numerical dispersion relation are validated by the simulation results.

Contents

CERTIFICATE OF ORIGINALITY	i
Abstract	ii
Publications Arising from the Thesis	iv
Acknowledgments	vi
Statement of Originality	vii
List of Figures	xii
List of Tables	xv
1 Introduction	1
1.1 Computational Electrodynamics	1
1.2 Time Domain Methods in Computational Electromagnetics	2
1.2.1 The Transmission Line Matrix Method (TLM)	3
1.2.2 The Finite Difference Time Domain Method (FDTD)	3
1.2.3 The Multi-Resolution Time Domain Method (MRTD)	4
1.2.4 Unconditionally Stable ADI-FDTD Method	5

1.2.5	Techniques to Reduce Numerical Dispersion Error	6
1.3	Motivation of the Thesis	6
1.4	Outline	7
2	The ADI-FDTD Method	8
2.1	Introduction	8
2.2	Overview of the FDTD Method	9
2.2.1	Formulation of the FDTD Method	9
2.2.2	Numerical Stability of the FDTD Method	15
2.2.3	Numerical Dispersion of the FDTD Method	16
2.2.4	Limitation of the FDTD Method	17
2.3	Overview of the ADI-FDTD Method	18
2.3.1	Formulation of the ADI-FDTD Method	18
2.3.2	Numerical Stability of the ADI-FDTD Method	22
2.3.3	Numerical Dispersion of the ADI-FDTD Method	25
3	The High-Order ADI-FDTD Method	28
3.1	Introduction	28
3.2	Multi-Points High-Order Central Difference Scheme	29
3.3	The High-Order ADI-FDTD Method	33
3.3.1	Formulation of the High-Order ADI-FDTD Method	33
3.3.2	Numerical Stability of the High-Order ADI-FDTD Method	39
3.3.3	Numerical Dispersion of the High-Order ADI-FDTD Method	40
3.3.4	Simulation and Results	50

3.4	Conclusion	51
4	The (2,4) Low Numerical Dispersion ADI-FDTD Method	55
4.1	Introduction	55
4.2	Overview of the Low Numerical Dispersion Algorithm for the FDTD method	56
4.3	The (2,4) Low Numerical Dispersion ADI-FDTD Method	59
4.3.1	Formulation of the (2,4) LD ADI-FDTD Method	59
4.3.2	Numerical Dispersion of the (2,4) LD ADI-FDTD Method	63
4.3.3	Simulations and Results	68
4.4	Conclusion	79
5	Conclusion and Future Works	81
5.1	Conclusion	81
5.2	Future Works and Discussion	83
5.2.1	(2,4) LD ADI-FDTD Method with PML	83
5.2.2	Modified LD ADI-FDTD Method	86
	Appendices	88
A	Analysis of the Numerical Dispersion Relation of the (2,4) FDTD Method	88
B	Analysis of the Numerical Dispersion Relation of the (2,4) ADI-FDTD Method	91
	Bibliography	95

List of Figures

2.1	Unit cell containing the locations of the discrete electromagnetics field components for the FDTD method.	11
2.2	The use of central difference scheme for the spatial derivatives and leapfrog manner for the temporal derivatives.	13
2.3	Flowchart of the 2-D ADI-FDTD method for a TE wave.	23
2.4	Numerical dispersion errors of the FDTD and ADI-FDTD method with different mesh resolutions at different $CFLN$	27
3.1	The approximation of the spatial derivative $\Phi'(x_0)$	30
3.2	Numerical dispersion errors of the high-order ADI-FDTD method with different order central difference schemes at $\Delta t = T/10$	42
3.3	Numerical dispersion errors of the high-order ADI-FDTD method with different order central difference schemes at $\Delta t = T/20$	43
3.4	Numerical dispersion errors of the high-order ADI-FDTD method with different order central difference schemes at $\Delta t = T/100$	44
3.5	Numerical dispersion errors of the high-order ADI-FDTD method with different order central difference schemes at $CFLN = 0.5$	46

3.6	Numerical dispersion errors of the high-order ADI-FDTD method with different order central difference schemes at $CFLN = 1$	47
3.7	Numerical dispersion errors of the high-order ADI-FDTD method with different order central difference schemes at $CFLN = 2$	48
3.8	Numerical dispersion errors of the high-order ADI-FDTD method with different order central difference schemes at $CFLN = 4$	49
3.9	The 2-D parallel-plate waveguide model.	50
3.10	E_x field at the observation point (10,320) in time domain.	52
3.11	Numerical dispersion errors of the 2 nd - and 6 th -order ADI-FDTD method with different time-steps which are calculated by simulation results.	53
4.1	Numerical dispersion errors of different FDTD methods at $CFLN = 0.75$	60
4.2	Mean absolute numerical dispersion errors with different time-steps at $\Delta = \lambda/50$. (Dashed lines represent the numerical dispersion errors when only the second-order error is considered.)	65
4.3	Mean absolute numerical dispersion errors with different time-steps at $\Delta = \lambda/100$. (Dashed lines represent the numerical dispersion errors when only the second-order error is considered.)	66
4.4	Mean absolute numerical dispersion errors of different methods with different mesh resolutions at $CFLN=1$	69
4.5	Mean absolute numerical dispersion errors of different methods with different mesh resolutions at $CFLN=8$	70
4.6	2-D Free space model.	71

4.7	Normalized phase velocities of the LD ADI-FDTD method with different propagation angles at 500MHz. ($\Delta = 0.015\text{m}$, $CFLN = 4$, and $\theta = 45^\circ$ for the specified angle case)	72
4.8	The non-uniform mesh model with a thin dielectric interface.	74
4.9	Numerical dispersion errors of different methods which are calculated by the simulation results.	75
4.10	H_z field at the observation point in time domain.	76
4.11	Reflected signal power.	77
5.1	Photonic band structure.	84
5.2	Time domain results of the photonic band structure simulation.	85
5.3	Transmission coefficients of the photonic band structure.	85
5.4	Sub-gridding scheme.	86

List of Tables

3.1	Coefficients $a(m)$ of the multi-points high-order central difference scheme. . .	32
3.2	Accuracy limit of the high-order ADI-FDTD method at different time-steps Δt	45
4.1	Mean square errors over all angle \bar{e}^2 of different methods.	64
4.2	Numerical dispersion error $(1 - u_p/c)^2$ for $\Delta t \rightarrow 0$	68
4.3	Comparison of the non-uniform mesh model simulation results.	74
4.4	Computational complexities of solving different equations systems by the LU method.	78

Chapter 1

Introduction

1.1 Computational Electrodynamics

Maxwell's partial differential equations [1] are fundamental physical laws expressed mathematically to govern the time-varying electric and magnetic fields. They are the essentials for the computational electrodynamics [2]. Due to the rapid growth of computer technology, these equations can solve many complex electromagnetics field problems in different applications. These applications include antenna design, high-speed electric circuits modelling, design of micrometer- and nanometer-scale integrated optical devices, and bioelectromagnetics simulations.

In general, based on the solution domain, there are two different methods in computational electrodynamics. One is the frequency domain method, which involves computing the frequency and phase response of a system. The other is the time domain method, which computes the time varying signal inside a computational domain.

Usually, the frequency domain methods [3]-[5] are used to solve a problem that only in-

volves a narrow band of frequency spectrum and when no non-linear elements are involved. When a wide band solution is required, time domain methods are usually used because the computed time-varying signal can be converted to frequency domain to achieve the wide band solution—although a large number of iterations are required if wide band and high frequency solutions are needed. In addition, the time domain method is a better method for handling problems with non-linear elements.

1.2 Time Domain Methods in Computational Electromagnetics

The rapid growth of low-cost but powerful computers has made the time domain method attractive as a versatile problem-solver in computational electromagnetics. In addition, the time domain method is easier to understand and program up since Maxwell's curl equations can be discretized using difference formulas. Furthermore, an added advantage of the time domain method is that a wide band solution can be computed from a single run by Fourier transforming the time varying signal.

Several other attributes of the time domain method make it attractive:

1. Visualization of the time-varying fields helps us study the interaction of the field in a complex structure. For example, such visualization is useful for analyzing the propagation, radiation, and crosstalk of digital pulses in high-speed digital circuits.
2. Excitation of a very short pulse enables us to understand the physics of lightning discharge and the propagating of very high-speed signal in digital circuits.

3. Computation of wide band response of UWB antennas and systems.

In view of the above features, the time domain methods have seen a rapid growth in computational electromagnetics during the last two decades [6]-[20].

1.2.1 The Transmission Line Matrix Method (TLM)

Proposed by P. B. John and R. L. Beurle in 1971, the Transmission Line Matrix (TLM) [6] method is one of the time domain methods in electromagnetics modelling. The TLM method is a physics-based algorithm in which the computational domain is discretized by using a mesh of transmission lines interconnected at nodes. The approach is based on the equivalence between Maxwell's equations and those for the voltage and current on a mesh of continuous two-wire transmission lines, and it solves the electromagnetic field problems by using equivalent electrical circuit networks. The convergence and stability problems associated with the TLM method can be deduced by analyzing the equivalent circuits. The disadvantage of the TLM method is that a large number of iterations are required to generate the field solutions. In addition, the process requires more memory as well as computational time when compared to the Finite Difference Time Domain method.

1.2.2 The Finite Difference Time Domain Method (FDTD)

As mentioned above, the Finite Difference Time Domain (FDTD) method [7]-[10] is another time domain approach that is widely used in computational electromagnetics. It was introduced by K. S. Yee in 1966 [7] to solve Maxwell's time-dependent curl equations, and it applies the finite difference approximation directly to solve the partial differential equations. It is easy to understand and is also versatile in its application to a wide class

of electromagnetics problems.

However, unless multiple processors are used, the FDTD method is often limited to solving electrically small-size problems. This is because the cell size must be sufficiently small to capture the fine features of the geometry and must also be small compared to the wavelength of the signal—usually at least 20 cells per smallest wavelength—to obtain accurate results. Furthermore, the time-step must be small enough to satisfy the Courant-Friedrich-Levy (CFL) condition in order to guarantee numerical stability [11]. Thus, a large model with fine features can place a heavy burden on the method, owing to the small cell size and time-step.

1.2.3 The Multi-Resolution Time Domain Method (MRTD)

In 1996, a Multi-Resolution Time Domain method (MRTD) [12]-[13]—which is based on Battle-Lemarie wavelets—was proposed for efficient time domain computation. It shows an excellent capability to approximate the accurate solution with negligible error, even when using sampling rates in space that approach the Nyquist limit and far smaller than those used to generate accurate solutions in Yee's FDTD algorithm. The MRTD method applies multi-resolution analysis, which uses scaling and wavelet function as a complete set of basis function, in the method of moments type of discretization of Maxwell's equations.

In the MRTD method, the field components are represented in terms of a twofold expansion that utilizes scaling and wavelet functions. In regions that are characterized by smoothly varying fields, the S-MRTD can be used in which the above expansion is only in terms of scaling function. Additional field sampling points are introduced by incorporating wavelets in the field expansions, in regions where the field variations are

strong.

The principal motivation for using the MRTD is to reduce the numerical dispersion and, hence, the required memory for space-gridding. However, the MRTD method is more complex than the FDTD method because of the field expansion—the field at one grid point is related to those at several of the neighboring points. In addition, the stability condition for the MRTD method is stricter than that for the FDTD method, since the ratio of temporal and spatial discretization is five times less than required in the conventional FDTD method [13].

1.2.4 Unconditionally Stable ADI-FDTD Method

The low computation efficiency of the FDTD method, which arises from the requirement that the CFL stability condition must be satisfied, can become a bottleneck in the application of the FDTD method. This motivated the development of an unconditionally stable FDTD method called Alternative Direction Implicit (ADI) FDTD method [14]-[20] in which the time-step can be set to any arbitrary value without compromising the stability of the system.

In contrast to the traditional FDTD method, the ADI-FDTD method employs an implicit finite difference method—namely, the Crank-Nicholson scheme—to approximate the spatial derivatives appearing in Maxwell's equations. The ADI method, which is a two-procedures method, is applied to solve the equations. The spatial derivatives in one direction are treated implicitly first, and then the other direction in the second procedure.

While the ADI-FDTD method is no longer subject to the CFL stability condition, it suffers from a drawback: The numerical dispersion error is found to increase when the

implicit method is employed [21]-[24].

1.2.5 Techniques to Reduce Numerical Dispersion Error

The numerical dispersion error is introduced when the finite difference is applied to approximate the partial derivative of the PDE. It is one of the criteria to choose the cell size as well as the size of the time-step in the FDTD method. An increase in the cell size or the size of time-step results in an increase in the numerical dispersion error.

For the traditional FDTD method, there are several ways available to reduce the numerical dispersion error. One of these is to use a higher-order and more accurate finite differencing scheme to approximate the spatial derivatives that are approximated by a Taylor series expansion [2], [9], [25]-[30]. An alternative way to reduce the numerical dispersion error is to redefine the finite difference operators based on the analysis of the numerical dispersion relation of the FDTD method so as to minimize the error [31]-[32].

1.3 Motivation of the Thesis

By applying the ADI technique, the CFL stability condition can be obviated, and the computational efficiency of the FDTD method can be increased; however, the drawback of this approach is that it increases the numerical dispersion error. The objective of this thesis is to develop an ADI-FDTD method that is not only unconditionally stable but also has low numerical dispersion. Different schemes are implemented in the ADI-FDTD method to accomplish this reduction in the numerical dispersion error, and the accuracy as well as the stability criteria associated with these modifications are investigated in detail.

1.4 Outline

This thesis introduces two new time domain methods that are based on the ADI-FDTD method. Following a general introduction in Chapter 1, the ADI-FDTD method is introduced in Chapter 2. It begins with a discussion of Yee's FDTD method and then formulates the ADI-FDTD method in some detail. This chapter also demonstrates that the numerical dispersion error increases when the ADI method is applied.

Next, the high-order ADI-FDTD method is developed in Chapter 3. A detailed formulation of this new scheme is presented, and it is proved that the method is also unconditionally stable but has less numerical dispersion error. The improvement, however, is found to be relatively insignificant when the time-step is large.

In Chapter 4, we go on to develop the (2,4) low-numerical-dispersion ADI-FDTD method. It is based on the fourth-order ADI-FDTD method, and the finite difference operators are adjusted according to the numerical dispersion relationship. The schemes for choosing the finite difference operators are discussed in detail. The numerical dispersion characteristics of this method are investigated analytically and numerical results presented for validation, as well as discussion of the advantages of the proposed method over the conventional ADI-FDTD method.

In Chapter 5, some conclusions of this study are presented, and future directions as well as some problems encountered in the ADI-FDTD method are discussed.

Chapter 2

The ADI-FDTD Method

2.1 Introduction

The FDTD method is one of the well-known computational techniques for solving electromagnetics problems. In this method, the electromagnetics fields in a finite volume of space are discretized in both time and space. The shape and the material of the structure under simulation can be set arbitrarily inside the discrete domain. However, the FDTD method suffers from a limitation: Huge computational resources are required due to the constraints on choosing the cell size and size of the time-step. According to the sampling theorem, the cell size must be taken as at least half of the minimum wavelength to avoid aliasing. In practice, at least 20 cells per the minimum wavelength are used. In addition, the cell size must be small enough to model the minimum dimension of the structure. After the cell size is chosen, a small time-step must be chosen to satisfy the Courant-Friedrich-Levy (CFL) stability condition, which is proportional to the smallest cell size.

It is difficult to relax the constraint on choosing the cell size because it is limited by the physical dimensions of the structure under simulation. To reduce required computational resources, a novel FDTD method was developed that can use arbitrary time-step without compromising the CFL stability condition. This unconditionally stable FDTD method is based on the traditional FDTD method and an implicit finite difference method called the Crank-Nicholson method. The implicit equations are then solved by the Alternating Direction Implicit (ADI) technique.

In this chapter, the formulation of the FDTD method and the ADI-FDTD method are reviewed. Then, the stability condition and numerical dispersion error of these methods are studied and compared.

2.2 Overview of the FDTD Method

2.2.1 Formulation of the FDTD Method

The algorithm of FDTD method for solving electromagnetics problems was introduced by K. S. Yee in 1966. The continuous electromagnetics fields in a finite volume of space are sampled in discrete manner in time and space. The central difference scheme is then applied to model the differential form of Maxwell's equations.

In a lossless, linear, and isotropic medium, the differential form of Maxwell's equations are

$$\nabla \times \mathbf{E} = -\mu \frac{\partial \mathbf{H}}{\partial t}, \quad (2.1)$$

$$\nabla \times \mathbf{H} = \varepsilon \frac{\partial \mathbf{E}}{\partial t}, \quad (2.2)$$

where μ is magnetic permeability and ε is electrical permittivity.

Then, the vector components of the curl operators in (2.1) and (2.2) are written out to yield the following six scalar equations in the three-dimensional rectangular coordinates system:

$$\frac{\partial H_x}{\partial t} = \frac{1}{\mu} \left\{ \frac{\partial E_y}{\partial z} - \frac{\partial E_z}{\partial y} \right\}, \quad (2.3)$$

$$\frac{\partial H_y}{\partial t} = \frac{1}{\mu} \left\{ \frac{\partial E_z}{\partial x} - \frac{\partial E_x}{\partial z} \right\}, \quad (2.4)$$

$$\frac{\partial H_z}{\partial t} = \frac{1}{\mu} \left\{ \frac{\partial E_x}{\partial y} - \frac{\partial E_y}{\partial x} \right\}, \quad (2.5)$$

$$\frac{\partial E_x}{\partial t} = \frac{1}{\varepsilon} \left\{ \frac{\partial H_z}{\partial y} - \frac{\partial H_y}{\partial z} \right\}, \quad (2.6)$$

$$\frac{\partial E_y}{\partial t} = \frac{1}{\varepsilon} \left\{ \frac{\partial H_x}{\partial z} - \frac{\partial H_z}{\partial x} \right\}, \quad (2.7)$$

$$\frac{\partial E_z}{\partial t} = \frac{1}{\varepsilon} \left\{ \frac{\partial H_y}{\partial x} - \frac{\partial H_x}{\partial y} \right\}. \quad (2.8)$$

In the Yee's algorithm, the electric and magnetic fields in the free-space are sampled in the grid shown in Figure 2.1. It can be noticed that the electric and magnetic field components are interlaced within the unit cell, which is convenience to perform the central difference approximation.

Let any function u of space and time evaluated at discrete point in the grid and time as

$$u(i\Delta x, j\Delta y, k\Delta z, n\Delta t) = u_{i,j,k}^n, \quad (2.9)$$

where Δx , Δy , Δz are the lattice space increments in the x , y , z coordinate directions respectively and Δt is the time increments. i , j , k , and n are integer.

Then, the second-order accurate central difference approximation expression of the spatial and temporal derivatives can be written as

$$\frac{\partial u_{i,j,k}^n}{\partial x} = \frac{u_{i+1/2,j,k}^n - u_{i-1/2,j,k}^n}{\Delta x} + O(\Delta x^2), \quad (2.10)$$

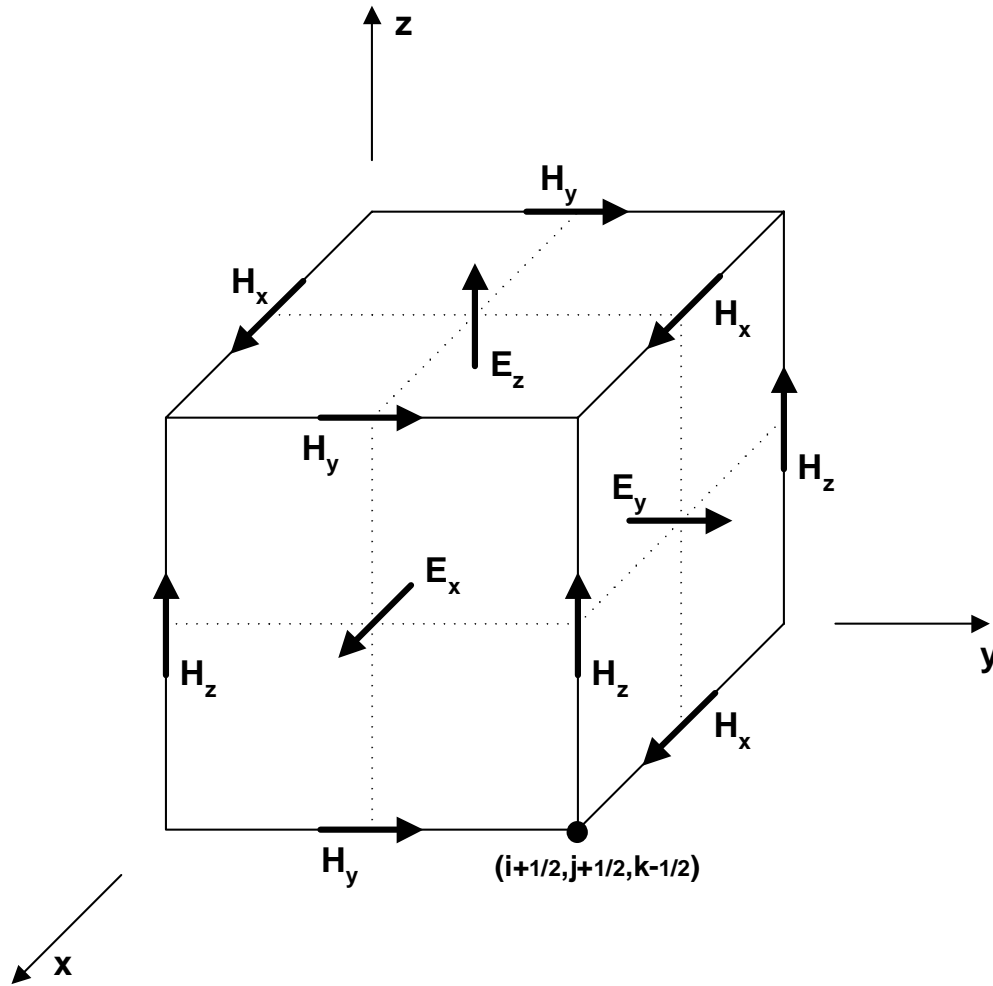


Figure 2.1: Unit cell containing the locations of the discrete electromagnetic field components for the FDTD method.

$$\frac{\partial u_{i,j,k}^n}{\partial t} = \frac{\partial u_{i,j,k}^{n+1/2} - \partial u_{i,j,k}^{n-1/2}}{\Delta t} + O(\Delta t^2). \quad (2.11)$$

An explicit approach in leapfrog manner is used in the Yee's algorithm. The components of the present time-step are derived from the field components at the previous time-step. In addition, the electric and magnetic field components are computed at half time-step alternately. Figure 2.2 shows the use of central difference scheme for the spatial derivatives and leapfrog manner for the temporal derivatives.

The temporal and spatial partial derivatives of the electric and magnetic fields in (2.3) to (2.8) are then approximated by the second-order accurate central difference scheme and the updating equations for Maxwell's equations can be written as

$$\begin{aligned} H_{x,i,j+1/2,k+1/2}^{n+1/2} &= H_{x,i,j+1/2,k+1/2}^{n-1/2} + \frac{\Delta t}{\mu_{i,j+1/2,k+1/2}} \left(\frac{E_{y,i,j+1/2,k+1}^n - E_{y,i,j+1/2,k}^n}{\Delta z} \right) \\ &\quad - \frac{\Delta t}{\mu_{i,j+1/2,k+1/2}} \left(\frac{E_{z,i,j+1,k+1/2}^n - E_{z,i,j,k+1/2}^n}{\Delta y} \right), \end{aligned} \quad (2.12)$$

$$\begin{aligned} H_{y,i+1/2,j,k+1/2}^{n+1/2} &= H_{y,i+1/2,j,k+1/2}^{n-1/2} + \frac{\Delta t}{\mu_{i+1/2,j,k+1/2}} \left(\frac{E_{z,i+1,j,k+1/2}^n - E_{z,i,j,k+1/2}^n}{\Delta x} \right) \\ &\quad - \frac{\Delta t}{\mu_{i+1/2,j,k+1/2}} \left(\frac{E_{x,i+1/2,j,k+1}^n - E_{x,i+1/2,j,k}^n}{\Delta z} \right), \end{aligned} \quad (2.13)$$

$$\begin{aligned} H_{z,i+1/2,j+1/2,k}^{n+1/2} &= H_{z,i+1/2,j+1/2,k}^{n-1/2} + \frac{\Delta t}{\mu_{i+1/2,j+1/2,k}} \left(\frac{E_{x,i+1/2,j+1,k}^n - E_{x,i+1/2,j,k}^n}{\Delta y} \right) \\ &\quad - \frac{\Delta t}{\mu_{i+1/2,j+1/2,k}} \left(\frac{E_{y,i+1,j+1/2,k}^n - E_{y,i,j+1/2,k}^n}{\Delta x} \right), \end{aligned} \quad (2.14)$$

$$\begin{aligned} E_{x,i+1/2,j,k}^{n+1} &= E_{x,i+1/2,j,k}^n + \frac{\Delta t}{\varepsilon_{i+1/2,j,k}} \left(\frac{H_{z,i+1/2,j+1/2,k}^{n+1/2} - H_{z,i+1/2,j-1/2,k}^{n+1/2}}{\Delta y} \right) \\ &\quad - \frac{\Delta t}{\varepsilon_{i+1/2,j,k}} \left(\frac{H_{y,i+1/2,j,k+1/2}^{n+1/2} - H_{y,i+1/2,j,k-1/2}^{n+1/2}}{\Delta z} \right), \end{aligned} \quad (2.15)$$

$$\begin{aligned} E_{y,i,j+1/2,k}^{n+1} &= E_{y,i,j+1/2,k}^n + \frac{\Delta t}{\varepsilon_{i,j+1/2,k}} \left(\frac{H_{x,i,j+1/2,k+1/2}^{n+1/2} - H_{x,i,j+1/2,k-1/2}^{n+1/2}}{\Delta z} \right) \\ &\quad - \frac{\Delta t}{\varepsilon_{i,j+1/2,k}} \left(\frac{H_{z,i+1/2,j+1/2,k}^{n+1/2} - H_{z,i-1/2,j+1/2,k}^{n+1/2}}{\Delta x} \right), \end{aligned} \quad (2.16)$$

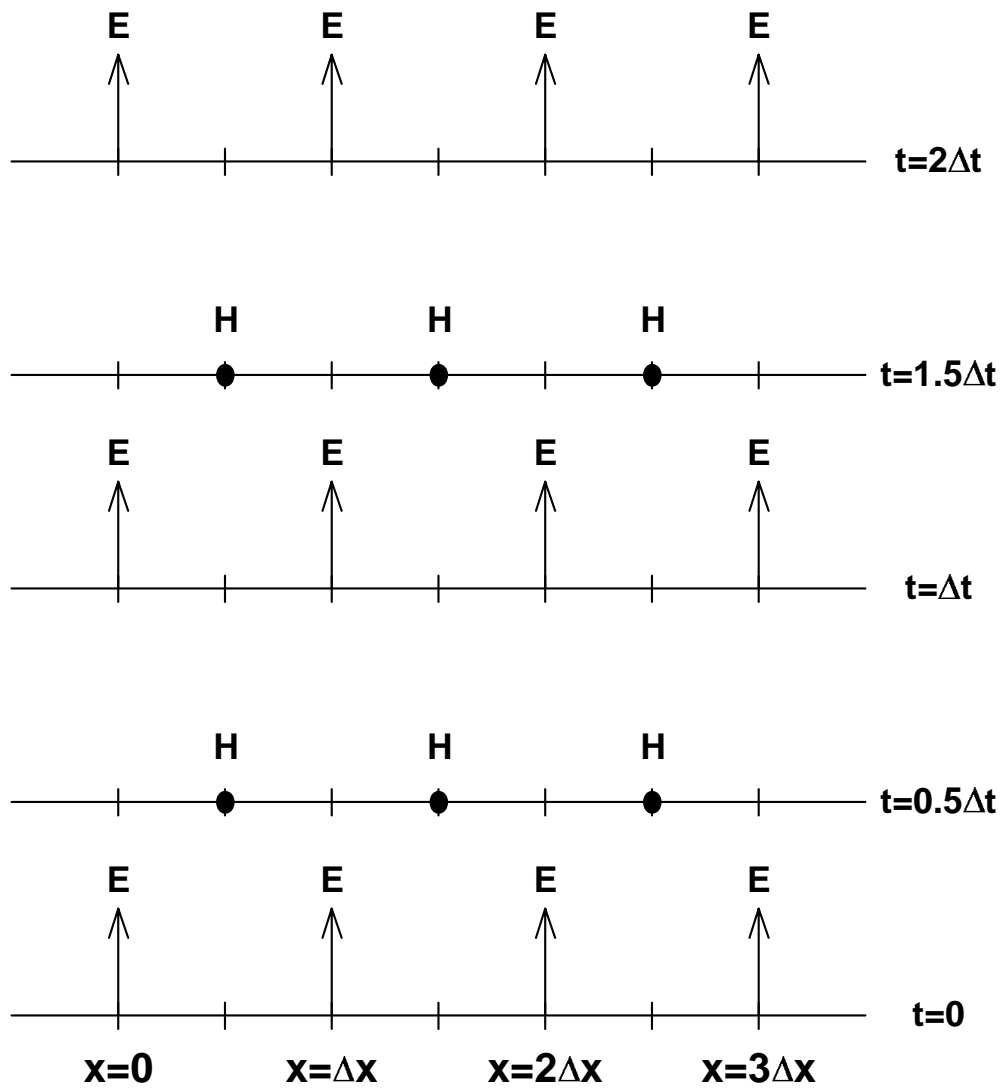


Figure 2.2: The use of central difference scheme for the spatial derivatives and leapfrog manner for the temporal derivatives.

$$\begin{aligned}
E_{z,i,j,k+1/2}^{n+1} = & E_{z,i,j,k+1/2}^n + \frac{\Delta t}{\varepsilon_{i,j,k+1/2}} \left(\frac{H_{y,i+1/2,j,k+1/2}^{n+1/2} - H_{y,i-1/2,j,k+1/2}^{n+1/2}}{\Delta x} \right) \\
& - \frac{\Delta t}{\varepsilon_{i,j,k+1/2}} \left(\frac{H_{x,i,j+1/2,k+1/2}^{n+1/2} - H_{x,i,j-1/2,k+1/2}^{n+1/2}}{\Delta y} \right). \quad (2.17)
\end{aligned}$$

To reduce the complexity of equations, a two-dimensional model for transverse electric (TE) wave is used in the following chapters. To reduce the FDTD method to two dimensions, it is assumed that the electromagnetics field excitation and modelled geometry has no variation in the z -direction. It means that all partial derivatives of the fields with respect to z are zero, and the structure under modelling is extended to infinity in z -direction without any changes in material and shape. Maxwell's equations for the 2-D TE wave in an isotropic loss-free medium in the rectangular coordinates system can be obtained as

$$\frac{\partial E_x}{\partial t} = \frac{1}{\varepsilon} \frac{\partial H_z}{\partial y}, \quad (2.18)$$

$$\frac{\partial E_y}{\partial t} = -\frac{1}{\varepsilon} \frac{\partial H_z}{\partial x}, \quad (2.19)$$

$$\frac{\partial H_z}{\partial t} = \frac{1}{\mu} \left(\frac{\partial E_x}{\partial y} - \frac{\partial E_y}{\partial x} \right). \quad (2.20)$$

Then, the updating equations for the 2-D TE mode Maxwell's equations can be obtained as

$$E_{x,i+1/2,j}^{n+1/2} = E_{x,i+1/2,j}^{n-1/2} + \frac{\Delta t}{\varepsilon_{i+1/2,j}} \left(\frac{H_{z,i+1/2,j+1/2}^n - H_{z,i+1/2,j-1/2}^n}{\Delta y} \right), \quad (2.21)$$

$$E_{y,i,j+1/2}^{n+1/2} = E_{y,i,j+1/2}^{n-1/2} - \frac{\Delta t}{\varepsilon_{i,j+1/2}} \left(\frac{H_{z,i+1/2,j+1/2}^n - H_{z,i-1/2,j+1/2}^n}{\Delta x} \right), \quad (2.22)$$

$$\begin{aligned}
H_{z,i+1/2,j+1/2}^{n+1} = & H_{z,i+1/2,j+1/2}^n + \frac{\Delta t}{\mu_{i+1/2,j+1/2}} \left(\frac{E_{x,i+1/2,j+1}^{n+1/2} - E_{x,i+1/2,j}^{n+1/2}}{\Delta y} \right) \\
& - \frac{\Delta t}{\mu_{i+1/2,j+1/2}} \left(\frac{E_{y,i+1,j+1/2}^{n+1/2} - E_{y,i,j+1/2}^{n+1/2}}{\Delta x} \right). \quad (2.23)
\end{aligned}$$

2.2.2 Numerical Stability of the FDTD Method

The Yee's FDTD method is an explicit numerical method. The choice of size of the time-step is bounded to avoid numerical instability, which is an undesirable possibility with explicit differential equation solvers that can cause the computed result to limitless increase. In addition, the choice of the cell size is also bounded by the structure under simulation and the minimum wavelength of the signal.

The von Neumann method is used to analyze the numerical stability of the Yee's FDTD method. Assume that the trial solution for the 2-D TE wave is given by

$$\Phi_{I,J}^n = \Phi_0 \xi e^{j(k_x I \Delta x + k_y J \Delta y)}, \quad (2.24)$$

where Φ is the field component and k_x, k_y are wavenumber in the x and y directions, respectively. The growth factor ξ describes the time-related behavior of the solution. If the magnitude of the growth factor is greater than one, then the system is unstable. Assume that the solution region is free-space, the updating equations (2.21)-(2.23) are then rewritten as

$$\left(1 - \frac{1}{\xi}\right) E_x^n = j \frac{2\Delta t}{\varepsilon_0 \Delta y} \sin\left(k_y \frac{\Delta y}{2}\right) H_z^n, \quad (2.25)$$

$$\left(1 - \frac{1}{\xi}\right) E_y^n = j \frac{2\Delta t}{\varepsilon_0 \Delta x} \sin\left(k_x \frac{\Delta x}{2}\right) H_z^n, \quad (2.26)$$

$$(\xi - 1) H_z^n = j \frac{2\Delta t}{\mu_0} \left[\frac{1}{\Delta y} \sin\left(k_y \frac{\Delta y}{2}\right) E_x^n - \frac{1}{\Delta x} \sin\left(k_x \frac{\Delta x}{2}\right) E_y^n \right]. \quad (2.27)$$

By eliminating the field components of (2.25)-(2.27), a quadratic equation is obtained as

$$(\xi - 1)(1 - 1/\xi) = -K, \quad (2.28)$$

where

$$K = 4c^2 \Delta t^2 \left[\frac{1}{\Delta x^2} \sin^2\left(k_x \frac{\Delta x}{2}\right) + \frac{1}{\Delta y^2} \sin^2\left(k_y \frac{\Delta y}{2}\right) \right] \quad (2.29)$$

and c is the speed of light. By solving (2.28), the growth factor of the 2-D TE mode FDTD method is found as

$$\xi = \frac{2 - K \pm j\sqrt{K(4 - K)}}{2}. \quad (2.30)$$

Since K is always positive, the magnitude of the growth factor is less than 1 if $K \leq 4$.

It implies that the stability condition for the 2-D TE mode FDTD method is

$$\Delta t \leq \frac{1}{c} \left(\frac{1}{\Delta x^2} + \frac{1}{\Delta y^2} \right)^{-1/2}. \quad (2.31)$$

From (2.31), it can be observed that the upper bound of the time-step is proportional to the cell size. It means that when a small cell size is used, a small time-step is also required to guarantee the numerical stability.

2.2.3 Numerical Dispersion of the FDTD Method

The dispersion relation is used to represent the relationship of the phase velocity of a travelling wave with different frequencies. It can be presented in wavenumber k as

$$k = \frac{\omega}{u_p}, \quad (2.32)$$

where ω is angular frequency and u_p is phase velocity. The theoretical dispersion relation for a 2-D plane wave in free-space is

$$k_x^2 + k_y^2 = \left(\frac{\omega}{c} \right)^2, \quad (2.33)$$

where k_x and k_y are the wavenumber in the x and y directions.

When the FDTD method is applied, the space is sampled into discrete cells. It causes a phase velocity of the numerical wave that is different from the theoretical one. This error is called numerical dispersion error.

The dispersion relation of the FDTD method can be devised from (2.28). Since the growth factor is unity at the stable condition, the growth factor can be expressed in terms of the time-step as

$$\xi = e^{j\omega\Delta t}. \quad (2.34)$$

Then, the dispersion relation of the 2-D FDTD method in free-space can be obtained as

$$\left(\frac{1}{c\Delta t}\right)^2 \sin^2\left(\omega\frac{\Delta t}{2}\right) = \frac{1}{\Delta x^2} \sin^2\left(k_x\frac{\Delta x}{2}\right) + \frac{1}{\Delta y^2} \sin^2\left(k_y\frac{\Delta y}{2}\right). \quad (2.35)$$

It can be observed that when Δx , Δy , and Δt all go to zero, the dispersion of the 2-D FDTD method (2.35) is converted to the theoretical one (2.33). It means that when the cell size is small enough, the numerical solution is close to the analytical solution. This is one of the reasons that small cell size is required in the FDTD method.

2.2.4 Limitation of the FDTD Method

Although the FDTD method is easy to understand and formulate, it is a computational resources-consuming method. Since the FDTD method is a numerical iterative method, the required memory and computational time are dependent on the cell size and the time-step. Smaller cell size or time-step results in more required computational resources. The cell size must be small enough to model the smallest dimension of the structure and in comparison with the smallest wavelength of the signal—usually at least 20 cells per wavelength—in order to make the numerical error negligible, which is shown in the previous section. The size of the time-step is also limited by the stability condition (2.31), which must be proportional to the smallest cell size.

2.3 Overview of the ADI-FDTD Method

When the FDTD method is applied, the selections of the cell size and the size of time-step are limited. The constraint on the choosing of the cell size is difficult to relax because it is due to the physical dimensions of the structure. In 1999, the unconditionally stable ADI-FDTD method was developed, whereby the constraint on choosing of the size of time-step is relaxed and can be set to any arbitrary value while the system remains stable.

2.3.1 Formulation of the ADI-FDTD Method

The ADI-FDTD method uses the same spatial grid as the Yee's method, shown in Figure 2.1. However, the Alternating Direction Implicit (ADI) method is used—instead of the explicit leapfrog method—to solve Maxwell's equations. For Yee's method, the updating equations (2.21)-(2.23) are explicit. All of the field components at the new time instant are computed using the data previously stored. For the ADI-FDTD method, simultaneous equations are used.

The ADI method is used to solve multi-directional partial differential equations. When the ADI method is used, one direction is treated implicitly first, then the other direction in the next step. To demonstrate how to apply the ADI method on the FDTD method, a 2-D model for a TE wave (2.18)-(2.20) in an isotropic loss-free medium is considered as an example.

Since the ADI method treats the equation implicitly in different directions alternately, one discrete time-step is calculated using two procedures. For the first procedure of the ADI-FDTD, the x -direction spatial derivatives are treated implicitly. The updating

equations of the first procedure are

$$E_{x,i+1/2,j}^{n+1/2} = E_{x,i+1/2,j}^n + \frac{\Delta t/2}{\varepsilon} \left(\frac{H_{z,i+1/2,j+1/2}^n - H_{z,i+1/2,j-1/2}^n}{\Delta y} \right), \quad (2.36)$$

$$E_{y,i,j+1/2}^{n+1/2} = E_{y,i,j+1/2}^n - \frac{\Delta t/2}{\varepsilon} \left(\frac{H_{z,i+1/2,j+1/2}^{n+1/2} - H_{z,i-1/2,j+1/2}^{n+1/2}}{\Delta x} \right), \quad (2.37)$$

$$\begin{aligned} H_{z,i+1/2,j+1/2}^{n+1/2} &= H_{z,i+1/2,j+1/2}^n + \frac{\Delta t/2}{\mu} \left(\frac{E_{x,i+1/2,j+1}^n - E_{x,i+1/2,j}^n}{\Delta y} \right) \\ &\quad - \frac{\Delta t/2}{\mu} \left(\frac{E_{y,i+1,j+1/2}^{n+1/2} - E_{y,i,j+1/2}^{n+1/2}}{\Delta x} \right). \end{aligned} \quad (2.38)$$

In the first procedure, the $E_x^{n+1/2}$ components can be computed by (2.36) directly using the data previously stored. The $E_y^{n+1/2}$ and $H_z^{n+1/2}$ components cannot be computed by using (2.37) and (2.38) independently in direct numerical calculation. However, by combining (2.37) and (2.38), a equation for the $H_z^{n+1/2}$ components can be obtained as

$$\begin{aligned} & -\frac{\Delta t^2}{4\varepsilon\mu\Delta x^2} H_{z,i+3/2,j+1/2}^{n+1/2} + \left(1 + \frac{\Delta t^2}{2\varepsilon\mu\Delta x^2} \right) H_{z,i+1/2,j+1/2}^{n+1/2} - \frac{\Delta t^2}{4\varepsilon\mu\Delta x^2} H_{z,i-1/2,j+1/2}^{n+1/2} \\ &= H_{z,i+1/2,j+1/2}^n + \frac{\Delta t}{2\mu} \left(\frac{E_{x,i+1/2,j+1}^n - E_{x,i+1/2,j}^n}{\Delta y} \right) \\ & - \frac{\Delta t}{2\mu} \left(\frac{E_{y,i+1,j+1/2}^n - E_{y,i,j+1/2}^n}{\Delta x} \right). \end{aligned} \quad (2.39)$$

The equation (2.39) can be simplified as

$$a_i u_{i-1} + b_i u_i + c_i u_{i+1} = d_i, \quad (2.40)$$

where u_i represents $H_{z,i-1/2,j-1/2}^{n+1/2}$ which is the unknown variable, a_i, b_i, c_i represent the corresponding coefficients and d_i is the known variable.

Assume that the computational domain has N rows in the x -direction. There will be

N equations by having different suffix i and they can be expressed in matrix form as

$$\begin{bmatrix} a_1 & b_1 & c_1 & 0 & & \cdots & 0 \\ 0 & a_2 & b_2 & c_2 & 0 & & \cdots & 0 \\ \vdots & & \ddots & \ddots & \ddots & & \vdots & \\ 0 & \cdots & 0 & a_{N-1} & b_{N-1} & c_{N-1} & 0 \\ 0 & \cdots & 0 & a_N & b_N & c_N \end{bmatrix} \begin{bmatrix} u_0 \\ u_1 \\ \vdots \\ u_N \\ u_{N+1} \end{bmatrix} = \begin{bmatrix} d_1 \\ d_2 \\ \vdots \\ d_{N-1} \\ d_N \end{bmatrix}. \quad (2.41)$$

This N equations $N + 2$ unknowns system is unsolvable. However, u_0 and u_{N+1} are at the boundary, they are calculated using the boundary conditions by the data at the previous time-step. They become known variables when (2.41) is computed. Then, (2.41) can be rewritten as

$$\mathbf{A}\mathbf{u} = \mathbf{d} - \mathbf{B}_1 u_0 - \mathbf{B}_2 u_{N+1} \quad (2.42)$$

where

$$\mathbf{A} = \begin{bmatrix} b_1 & c_1 & 0 & \cdots & 0 \\ a_2 & b_2 & c_2 & 0 & \cdots & 0 \\ 0 \\ \vdots & \ddots & \ddots & \ddots & \vdots \\ 0 \\ 0 & \cdots & 0 & a_{N-1} & b_{N-1} & c_{N-1} \\ 0 & \cdots & 0 & a_N & b_N \end{bmatrix}, \quad (2.43)$$

$$\mathbf{u} = \begin{bmatrix} u_1 & u_2 & \cdots & u_{N-1} & u_N \end{bmatrix}^T, \quad (2.44)$$

$$\mathbf{d} = \begin{bmatrix} d_1 & d_2 & \cdots & d_{N-1} & d_N \end{bmatrix}^T, \quad (2.45)$$

$$\mathbf{B}_1 = \begin{bmatrix} a_1 & 0 & 0 & \cdots & 0 & 0 \end{bmatrix}^T, \quad (2.46)$$

$$\mathbf{B}_2 = \begin{bmatrix} 0 & 0 & \cdots & 0 & 0 & c_N \end{bmatrix}^T. \quad (2.47)$$

The system becomes a N equations N unknowns solvable system. Since \mathbf{A} is a tri-diagonal sparse matrix, there are many efficient methods to solve the system, such as Gaussian elimination and LU method. The time-consuming calculation \mathbf{A}^{-1} can be avoided.

Then, the $E_y^{n+1/2}$ components can be computed by (2.37), using the $H_z^{n+1/2}$ components.

The second procedure can be formulated similarly, except that the y -direction spatial derivatives are treated implicitly. The updating equations of the second procedure are

$$E_{x,i+1/2,j}^{n+1} = E_{x,i+1/2,j}^{n+1/2} + \frac{\Delta t/2}{\varepsilon} \left(\frac{H_{z,i+1/2,j+1/2}^{n+1} - H_{z,i+1/2,j-1/2}^{n+1}}{\Delta y} \right), \quad (2.48)$$

$$E_{y,i,j+1/2}^{n+1} = E_{y,i,j+1/2}^{n+1/2} - \frac{\Delta t/2}{\varepsilon} \left(\frac{H_{z,i+1/2,j+1/2}^{n+1/2} - H_{z,i-1/2,j+1/2}^{n+1/2}}{\Delta x} \right), \quad (2.49)$$

$$\begin{aligned} H_{z,i+1/2,j+1/2}^{n+1} &= H_{z,i+1/2,j+1/2}^{n+1/2} + \frac{\Delta t/2}{\mu} \left(\frac{E_{x,i+1/2,j+1}^{n+1} - E_{x,i+1/2,j}^{n+1}}{\Delta y} \right) \\ &\quad - \frac{\Delta t/2}{\mu} \left(\frac{E_{y,i+1,j+1/2}^{n+1/2} - E_{y,i,j+1/2}^{n+1/2}}{\Delta x} \right). \end{aligned} \quad (2.50)$$

The E_y^{n+1} components can be computed by (2.49) directly, using the data previously stored. The E_x^{n+1} and H_z^{n+1} components cannot be computed by using (2.48) and (2.50) independently in direct numerical calculation. However, by combining (2.48) and (2.50),

an equation for the H_z^{n+1} components can be obtained as

$$\begin{aligned}
& -\frac{\Delta t^2}{4\varepsilon\mu\Delta y^2}H_{z,i+1/2,j+3/2}^{n+1} + \left(1 + \frac{\Delta t^2}{2\varepsilon\mu\Delta y^2}\right)H_{z,i+1/2,j+1/2}^{n+1} - \frac{\Delta t^2}{4\varepsilon\mu\Delta y^2}H_{z,i+1/2,j-1/2}^{n+1} \\
& = H_{z,i+1/2,j+1/2}^{n+1/2} - \frac{\Delta t}{2\mu} \left(\frac{E_{y,i+1,j+1/2}^{n+1/2} - E_{y,i,j+1/2}^{n+1/2}}{\Delta x} \right) \\
& + \frac{\Delta t}{2\mu} \left(\frac{E_{x,i+1/2,j+1}^{n+1/2} - E_{x,i+1/2,j}^{n+1/2}}{\Delta y} \right). \tag{2.51}
\end{aligned}$$

The equation (2.51) can be written in tri-diagonal matrix form by having different suffix j , and the matrix can be solved after including the boundary conditions. Then, the E_x^{n+1} components can be computed by (2.48) using the H_z^{n+1} components.

The basis flowchart of the ADI-FDTD method is shown in Figure 2.3.

2.3.2 Numerical Stability of the ADI-FDTD Method

The concept of the ADI method is based on the Crank-Nicholson method, which is always stable. The Crank-Nicholson method applies the average of the central difference formulas at the n th and $(n+1)$ th time instant to approximate the spatial derivative at the $(n+1/2)$ th time instant. When the updating equations for the E_x components at the $(n+1/2)$ th (2.36) and $(n+1)$ th (2.48) iteration are combined, it obtains

$$\begin{aligned}
& \frac{E_{x,i+1/2,j}^{n+1} - E_{x,i+1/2,j}^n}{\Delta t} \\
& = \frac{1}{\varepsilon} \left[\frac{1}{2} \left(\frac{H_{z,i+1/2,j+1/2}^{n+1} - H_{z,i+1/2,j-1/2}^{n+1}}{\Delta y} + \frac{H_{z,i+1/2,j+1/2}^n - H_{z,i+1/2,j-1/2}^n}{\Delta y} \right) \right]. \tag{2.52}
\end{aligned}$$

It can be observed that the average of the central difference formulas at the n th and $(n+1)$ th time instant is used to approximate the spatial derivative in y -direction at the $(n+1/2)$ th time instant. Besides, when the updating equations for the E_y components

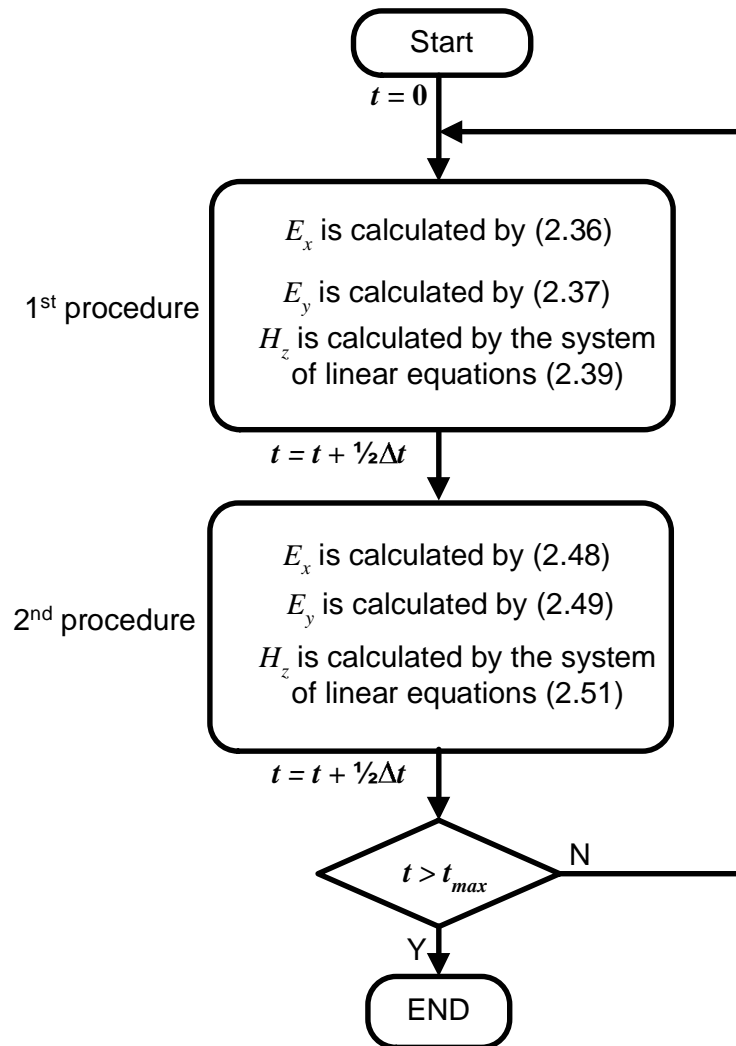


Figure 2.3: Flowchart of the 2-D ADI-FDTD method for a TE wave.

at the n th and $(n + 1/2)$ th (2.37) iteration are combined, it obtains

$$\begin{aligned} & \frac{E_{y,i,j+1/2}^{n+1/2} - E_{y,i,j+1/2}^{n-1/2}}{\Delta t} \\ &= -\frac{1}{\varepsilon} \left[\frac{1}{2} \left(\frac{H_{z,i+1/2,j+1/2}^{n-1/2} - H_{z,i-1/2,j+1/2}^{n-1/2}}{\Delta x} + \frac{H_{z,i+1/2,j+1/2}^{n+1/2} - H_{z,i-1/2,j+1/2}^{n+1/2}}{\Delta x} \right) \right]. \end{aligned} \quad (2.53)$$

It can be also observed that the average of the central difference formulas at the $(n-1/2)$ th and $(n+1/2)$ th time instant is used to approximate the spatial derivative in x -direction at the n th time instant. By the same manner, it can be observed that the averaging method is used at the updating equation for the H_z components.

To analyze the stability of the ADI-FDTD method, the von Neumann method is used. The trial solutions for the 2-D TE wave (2.24) are substituted into the updating equations of the two procedures (2.36)-(2.38), (2.48)-(2.50). Since the complete update cycle includes two procedures, in order to determine the overall growth factor ξ , the updating equations of the two procedures are combined and written as

$$\varepsilon_0 \xi E_x^n + W_y \xi H_z^n = \varepsilon_0 E_x^n - W_y H_z^n, \quad (2.54)$$

$$-W_x W_y \xi E_x^n + \varepsilon_0 \mu_0 \xi E_y^n - W_x W_y \xi H_z^n = -W_x W_y E_x^n + \varepsilon_0 \mu_0 E_y^n - W_x W_y H_z^n, \quad (2.55)$$

$$W_y \xi E_x^n - W_x \xi E_y^n + \mu_0 \xi H_z^n = -W_y E_x^n + W_x E_y^n + \mu_0 H_z^n, \quad (2.56)$$

where

$$W_x = j \frac{\Delta t}{\Delta x} \sin \left(k_x \frac{\Delta x}{2} \right), \quad (2.57)$$

$$W_y = j \frac{\Delta t}{\Delta y} \sin \left(k_y \frac{\Delta y}{2} \right). \quad (2.58)$$

By eliminating the field components of (2.54)-(2.56), it obtains

$$\frac{(\xi - 1)^2}{(\xi + 1)^2} = -K, \quad (2.59)$$

where

$$K = S_x^2 + S_y^2 + S_x^2 S_y^2, \quad (2.60)$$

$$S_x = \frac{c\Delta t}{\Delta x} \sin\left(k_x \frac{\Delta x}{2}\right), \quad (2.61)$$

$$S_y = \frac{c\Delta t}{\Delta y} \sin\left(k_y \frac{\Delta y}{2}\right), \quad (2.62)$$

and c is the speed of light. By solving (2.59), the growth factor of the ADI-FDTD method is found as

$$\xi = \frac{1 - K \pm 2j\sqrt{K}}{1 + K}. \quad (2.63)$$

Since K is always positive, the magnitude of the growth factor is always unity. Therefore, the ADI-FDTD method is unconditionally stable.

2.3.3 Numerical Dispersion of the ADI-FDTD Method

Since the magnitude of the growth factor is always unity, the growth factor can be expressed in terms of the time-step as

$$\xi = e^{j\omega\Delta t}. \quad (2.64)$$

The numerical dispersion relation of the ADI-FDTD method can be derived from (2.59) as

$$S_x^2 + S_y^2 + S_x^2 S_y^2 = \tan^2\left(\frac{\omega\Delta t}{2}\right). \quad (2.65)$$

Before the numerical dispersion error of the ADI-FDTD method is studied, it is assumed that uniform square cell is used, where $\Delta x = \Delta y = \Delta$. Besides, with regard to the 2-D FDTD method, the maximum time-step under CFL stability condition is defined as

$$\Delta t_{CFL} = \frac{\Delta}{c\sqrt{2}} \quad (2.66)$$

and a ratio of time-step is defined as

$$CFLN = \frac{\Delta t}{\Delta t_{CFL}}. \quad (2.67)$$

A larger $CFLN$ means that a larger time-step is applied.

Figure 2.4 shows the numerical dispersion error of the FDTD and ADI-FDTD at different mesh resolutions with different $CFLN$. It can be observed that when the cell size decreases, the numerical dispersion error decreases. In addition, the numerical dispersion error increases when the ADI method is applied. Furthermore, a larger time-step results in higher numerical dispersion error.

Although the ADI method is stable under any arbitrary time-step, the maximum time-step is limited by the numerical dispersion error. It reduces the ability of the ADI-FDTD method to retrench the computational resources.

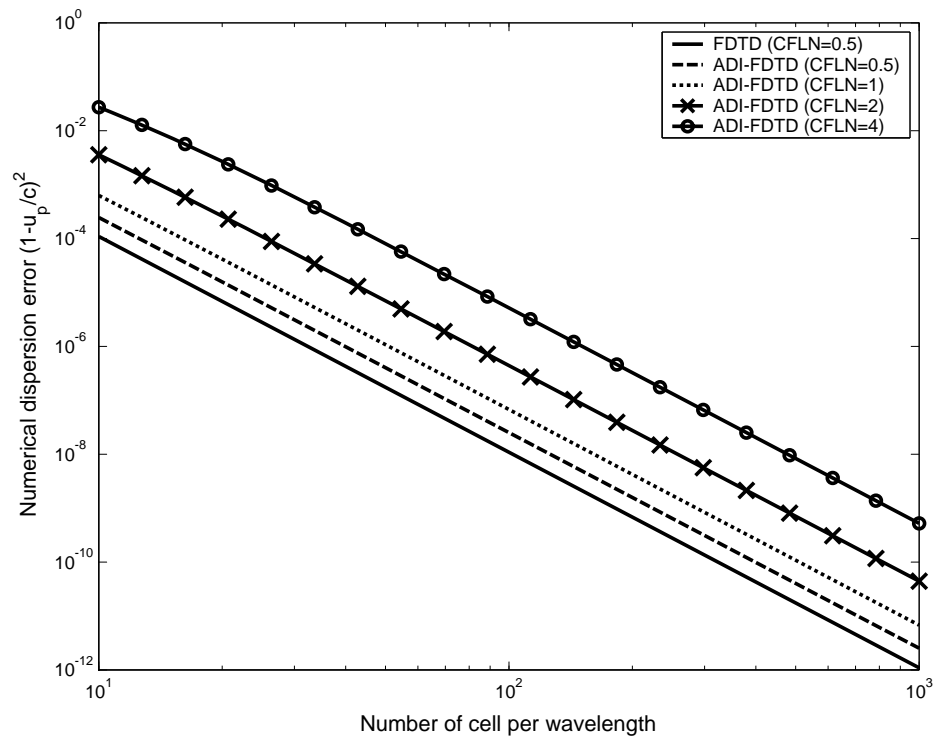


Figure 2.4: Numerical dispersion errors of the FDTD and ADI-FDTD method with different mesh resolutions at different $CFLN$.

Chapter 3

The High-Order ADI-FDTD Method

3.1 Introduction

From the previous chapter, it is found that the ADI method can reduce the required numerical resources of the FDTD method by the unconditionally stable property. However, the numerical dispersion error increases when the ADI method is applied. In addition, larger time-step results in higher numerical dispersion error. It limits the maximum time-step of the ADI-FDTD method.

When we apply the ADI-FDTD method, the numerical dispersion error must be present because of the grid discretization. The obvious way to reduce the numerical dispersion error is to reduce the cell size and the time-step. When both approach to zero, the dispersion relation converges to the theoretical value.

From the previous chapter, the numerical dispersion relation of the ADI-FDTD method is found as

$$S_x^2 + S_y^2 + S_x^2 S_y^2 = \tan^2 \left(\frac{\omega \Delta t}{2} \right), \quad (3.1)$$

where

$$S_x = \frac{c\Delta t}{\Delta x} \sin\left(k_x \frac{\Delta x}{2}\right), \quad (3.2)$$

$$S_y = \frac{c\Delta t}{\Delta y} \sin\left(k_y \frac{\Delta y}{2}\right). \quad (3.3)$$

It can be rewritten as

$$\begin{aligned} & \frac{c^2}{\Delta x^2} \sin^2\left(k_x \frac{\Delta x}{2}\right) + \frac{c^2}{\Delta y^2} \sin^2\left(k_y \frac{\Delta y}{2}\right) + \frac{c^4 \Delta t^2}{\Delta x^2 \Delta y^2} \sin^2\left(k_x \frac{\Delta x}{2}\right) \sin^2\left(k_y \frac{\Delta y}{2}\right) \\ &= \frac{1}{\Delta t^2} \tan^2\left(\frac{\omega \Delta t}{2}\right). \end{aligned} \quad (3.4)$$

By taking the limit of both sides for $\Delta t \rightarrow 0$, $\Delta x \rightarrow 0$ and $\Delta y \rightarrow 0$, it becomes

$$\begin{aligned} & \lim_{\Delta t, \Delta x, \Delta y \rightarrow 0} \frac{c^2}{\Delta x^2} \sin^2\left(k_x \frac{\Delta x}{2}\right) + \frac{c^2}{\Delta y^2} \sin^2\left(k_y \frac{\Delta y}{2}\right) + \frac{c^4 \Delta t^2}{\Delta x^2 \Delta y^2} \sin^2\left(k_x \frac{\Delta x}{2}\right) \sin^2\left(k_y \frac{\Delta y}{2}\right) \\ &= \frac{c^2}{2} (k_x^2 + k_y^2), \end{aligned} \quad (3.5)$$

$$\lim_{\Delta t, \Delta x, \Delta y \rightarrow 0} \frac{1}{\Delta t^2} \tan^2\left(\frac{\omega \Delta t}{2}\right) = \frac{\omega^2}{2}. \quad (3.6)$$

Combining 3.5 and 3.6, we get

$$k_x^2 + k_y^2 = \left(\frac{\omega}{c}\right)^2. \quad (3.7)$$

It is not an efficient way to reduce the numerical dispersion error by reducing the cell size and time-step because both computational time and required memory will be rapidly increased. From other research [25] - [30], using multi-points high-order central difference scheme—instead of two-points second-order central difference scheme—can reduce the numerical dispersion error.

3.2 Multi-Points High-Order Central Difference Scheme

According to the Yee's grid, a one-dimensional diagram for the approximation of the spatial derivative $\Phi'(x_0)$ is shown in Figure 3.1, where Φ is the field component. In

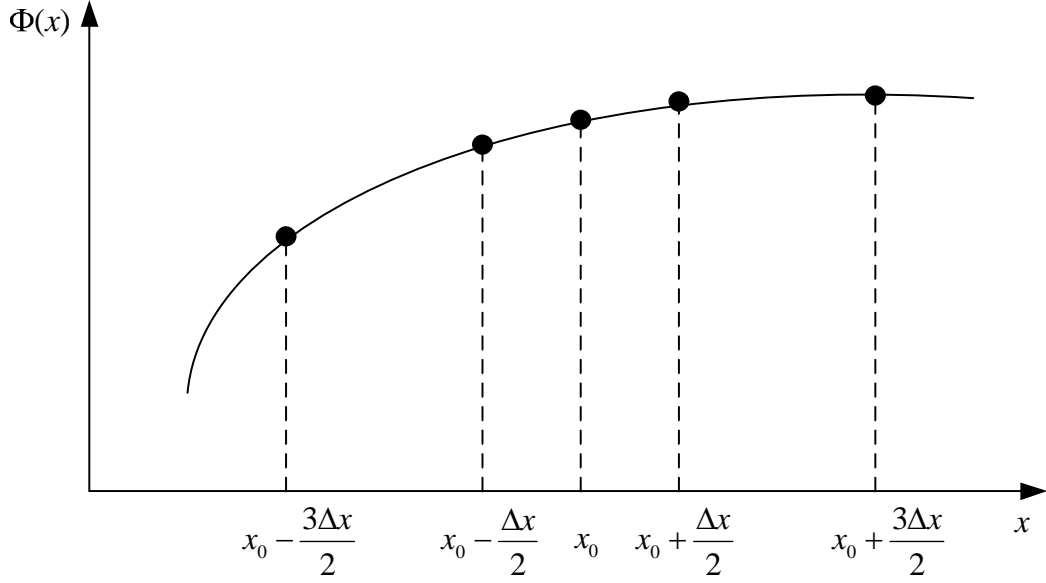


Figure 3.1: The approximation of the spatial derivative $\Phi'(x_0)$.

the Yee's FDTD method and the ADI-FDTD method, the two-points central difference scheme (3.8) is used to approximate the spatial derivatives, where

$$\Phi'(x_0) \simeq \frac{\Phi\left(x_0 + \frac{\Delta x}{2}\right) - \Phi\left(x_0 - \frac{\Delta x}{2}\right)}{\Delta x}. \quad (3.8)$$

By using Taylor series, it can be obtained that

$$\Phi\left(x_0 + \frac{\Delta x}{2}\right) = \Phi(x_0) + \frac{\Delta x}{2}\Phi'(x_0) + \frac{1}{2!}\left(\frac{\Delta x}{2}\right)^2\Phi''(x_0) + \frac{1}{3!}\left(\frac{\Delta x}{2}\right)^3\Phi'''(x_0) + \dots, \quad (3.9)$$

$$\Phi\left(x_0 - \frac{\Delta x}{2}\right) = \Phi(x_0) - \frac{\Delta x}{2}\Phi'(x_0) + \frac{1}{2!}\left(\frac{\Delta x}{2}\right)^2\Phi''(x_0) - \frac{1}{3!}\left(\frac{\Delta x}{2}\right)^3\Phi'''(x_0) + \dots \quad (3.10)$$

Then, by subtracting (3.10) from (3.9), it yields

$$\Phi\left(x_0 + \frac{\Delta x}{2}\right) - \Phi\left(x_0 - \frac{\Delta x}{2}\right) = \Delta x\Phi'(x_0) + O(\Delta x^3), \quad (3.11)$$

or

$$\Phi'(x_0) = \frac{\Phi\left(x_0 + \frac{\Delta x}{2}\right) - \Phi\left(x_0 - \frac{\Delta x}{2}\right)}{\Delta x} + O(\Delta x^2). \quad (3.12)$$

It can be shown that the two-points central difference scheme is of second-order accuracy.

To obtain higher order accuracy, the multi-points central difference scheme [2] can be used. Four-points central difference scheme is taken as an example. By using Taylor series, the four points can be written as

$$\begin{aligned}\Phi\left(x_0 + \frac{\Delta x}{2}\right) &= \Phi(x_0) + \frac{\Delta x}{2}\Phi'(x_0) + \frac{1}{2!}\left(\frac{\Delta x}{2}\right)^2\Phi''(x_0) + \frac{1}{3!}\left(\frac{\Delta x}{2}\right)^3\Phi'''(x_0) \\ &+ \frac{1}{4!}\left(\frac{\Delta x}{2}\right)^4\Phi^4(x_0) + \frac{1}{5!}\left(\frac{\Delta x}{2}\right)^5\Phi^5(x_0) + \dots,\end{aligned}\quad (3.13)$$

$$\begin{aligned}\Phi\left(x_0 - \frac{\Delta x}{2}\right) &= \Phi(x_0) + \frac{\Delta x}{2}\Phi'(x_0) - \frac{1}{2!}\left(\frac{\Delta x}{2}\right)^2\Phi''(x_0) + \frac{1}{3!}\left(\frac{\Delta x}{2}\right)^3\Phi'''(x_0) \\ &- \frac{1}{4!}\left(\frac{\Delta x}{2}\right)^4\Phi^4(x_0) + \frac{1}{5!}\left(\frac{\Delta x}{2}\right)^5\Phi^5(x_0) + \dots,\end{aligned}\quad (3.14)$$

$$\begin{aligned}\Phi\left(x_0 + \frac{3\Delta x}{2}\right) &= \Phi(x_0) + \frac{3\Delta x}{2}\Phi'(x_0) + \frac{1}{2!}\left(\frac{3\Delta x}{2}\right)^2\Phi''(x_0) + \frac{1}{3!}\left(\frac{3\Delta x}{2}\right)^3\Phi'''(x_0) \\ &+ \frac{1}{4!}\left(\frac{3\Delta x}{2}\right)^4\Phi^4(x_0) + \frac{1}{5!}\left(\frac{3\Delta x}{2}\right)^5\Phi^5(x_0) + \dots,\end{aligned}\quad (3.15)$$

$$\begin{aligned}\Phi\left(x_0 - \frac{3\Delta x}{2}\right) &= \Phi(x_0) + \frac{3\Delta x}{2}\Phi'(x_0) - \frac{1}{2!}\left(\frac{3\Delta x}{2}\right)^2\Phi''(x_0) + \frac{1}{3!}\left(\frac{3\Delta x}{2}\right)^3\Phi'''(x_0) \\ &- \frac{1}{4!}\left(\frac{3\Delta x}{2}\right)^4\Phi^4(x_0) + \frac{1}{5!}\left(\frac{3\Delta x}{2}\right)^5\Phi^5(x_0) + \dots.\end{aligned}\quad (3.16)$$

By subtracting (3.14) from (3.13), (3.16) from (3.15) and then adding them together, it yields

$$\begin{aligned}A\left[\Phi\left(x_0 + \frac{\Delta x}{2}\right) - \Phi\left(x_0 - \frac{\Delta x}{2}\right)\right] + B\left[\Phi\left(x_0 + \frac{3\Delta x}{2}\right) - \Phi\left(x_0 - \frac{3\Delta x}{2}\right)\right] \\ = (A + 3B)\Delta x\Phi'(x_0) + (A + 27B)\frac{1}{3!}\left(\frac{\Delta x}{2}\right)^3\Phi'''(x_0) + O(\Delta x^5),\end{aligned}\quad (3.17)$$

where A and B are the coefficients of the four-points central difference scheme. To minimize the error, it sets

$$A + 3B = 1 \quad (3.18)$$

and

$$A + 27B = 0. \quad (3.19)$$

Table 3.1: Coefficients $a(m)$ of the multi-points high-order central difference scheme.

m	2^{nd} order	4^{th} order	6^{th} order	10^{th} order
0	1.000000	1.125000	1.171875	1.211243
1		-0.041667	-0.065104	-0.089722
2			0.004688	0.013843
3				-0.001766
4				0.000119

$a(-1-m) = -a(m)$

By solving (3.18) and (3.19), it obtains

$$\begin{aligned} \Phi'(x_0) = & \frac{\frac{27}{24} \left[\Phi \left(x_0 + \frac{\Delta x}{2} \right) - \Phi \left(x_0 - \frac{\Delta x}{2} \right) \right] + \frac{-1}{24} \left[\Phi \left(x_0 + \frac{3\Delta x}{2} \right) - \Phi \left(x_0 - \frac{3\Delta x}{2} \right) \right]}{\Delta x} \\ & + O(\Delta x^4). \end{aligned} \quad (3.20)$$

It can be found that the four-points central difference scheme is of fourth-order accuracy.

In general, we define that the δ_p is the operator of the multi-points central difference approximation with respect to variable p . For example, the approximation of the spatial derivative of the field component Φ with respect to x is given by

$$\delta_x \Phi_{i,j} = \frac{1}{\Delta x} \sum_{m=-M/2}^{M/2-1} a(m) \Phi_{i+m+1/2,j}, \quad (3.21)$$

where $a(m)$ is the coefficient of the central difference scheme and M is the total number of points used.

The $a(m)$ of different order schemes can be found by the same manner, and they are shown in Table 3.1.

3.3 The High-Order ADI-FDTD Method

3.3.1 Formulation of the High-Order ADI-FDTD Method

For Yee's FDTD method and the ADI-FDTD method, two-points second-order central difference scheme is used to approximate the temporal derivatives and the spatial derivatives. To apply high-order method, only high-order backward difference scheme, which requires huge number of memory, can be used to approximate the temporal derivatives. It is because unknowns in different time instants will be included at an updating equation if high-order central difference or forward difference scheme is used. Mathematically, those updating equations can be solved by forming equations system, however, it will have unknowns from each time instant, and the method is no longer a time-iterative simulation. In addition, for this simulation method, it is unpractical because final values are needed to solve the equations system.

Following the formulation of the ADI-FDTD method in the previous chapter, the high-order ADI-FDTD method [36]-[38] also has two procedures to calculate in one time-step. The two-points second-order central difference scheme is replaced by the multi-points high-order central difference scheme to approximate the spatial derivatives. The temporal derivatives are still approximated by the two-points second-order central difference scheme. The updating equations of the first procedure for a 2-D TE wave in an isotropic loss free medium can be written as

$$E_{x,i+1/2,j}^{n+1/2} = E_{x,i+1/2,j}^n + \frac{\Delta t/2}{\varepsilon} \delta_y H_{z,i+1/2,j+1/2}^n, \quad (3.22)$$

$$E_{y,i,j+1/2}^{n+1/2} = E_{y,i,j+1/2}^n - \frac{\Delta t/2}{\varepsilon} \delta_x H_{z,i+1/2,j+1/2}^{n+1/2}, \quad (3.23)$$

$$H_{z,i+1/2,j+1/2}^{n+1/2} = H_{z,i+1/2,j+1/2}^n + \frac{\Delta t/2}{\mu} \left(\delta_y E_{x,i+1/2,j+1/2}^n - \delta_x E_{y,i+1/2,j+1/2}^{n+1/2} \right), \quad (3.24)$$

where δ_p is defined as the operator of the multi-points central difference approximation with respect to variable p . For example, the approximation of the spatial derivative of the field component Φ with respect to x is given by

$$\delta_x \Phi_{i,j}^n = \frac{1}{\Delta x} \sum_{m=-M}^{M-1} a(m) \Phi_{i+m+1/2,j}^n. \quad (3.25)$$

The $a(m)$ depends on order of the central difference scheme used to approximate the spatial derivatives.

The updating equations of the second procedure can also be obtained as

$$E_{x,i+1/2,j}^{n+1} = E_{x,i+1/2,j}^{n+1/2} + \frac{\Delta t/2}{\varepsilon} \delta_y H_{z,i+1/2,j+1/2}^{n+1}, \quad (3.26)$$

$$E_{y,i,j+1/2}^{n+1} = E_{y,i,j+1/2}^{n+1/2} - \frac{\Delta t/2}{\varepsilon} \delta_x H_{z,i+1/2,j+1/2}^{n+1/2}, \quad (3.27)$$

$$H_{z,i+1/2,j+1/2}^{n+1} = H_{z,i+1/2,j+1/2}^{n+1/2} + \frac{\Delta t/2}{\mu} \left(\delta_y E_{x,i+1/2,j+1}^{n+1} - \delta_x E_{y,i+1,j+1/2}^{n+1/2} \right). \quad (3.28)$$

Similar to the ADI-FDTD method, the high-order ADI-FDTD also forms simultaneous equations by combining the updating equations. It takes fourth-order ADI-FDTD method as an example. The updating equations of the first procedure of the fourth-order ADI-FDTD method are

$$E_{x,i+1/2,j}^{n+1/2} = E_{x,i+1/2,j}^n + \frac{\Delta t/2}{\varepsilon \Delta y} \left[\begin{array}{c} \frac{27}{24} \left(H_{z,i+1/2,j+1/2}^n - H_{z,i+1/2,j-1/2}^n \right) \\ -\frac{1}{24} \left(H_{z,i+1/2,j+3/2}^n - H_{z,i+1/2,j-3/2}^n \right) \end{array} \right], \quad (3.29)$$

$$E_{y,i,j+1/2}^{n+1/2} = E_{y,i,j+1/2}^n - \frac{\Delta t/2}{\varepsilon \Delta x} \left[\begin{array}{c} \frac{27}{24} \left(H_{z,i+1/2,j+1/2}^{n+1/2} - H_{z,i-1/2,j+1/2}^{n+1/2} \right) \\ -\frac{1}{24} \left(H_{z,i+3/2,j+1/2}^{n+1/2} - H_{z,i-3/2,j+1/2}^{n+1/2} \right) \end{array} \right], \quad (3.30)$$

$$H_{z,i+1/2,j+1/2}^{n+1/2} = H_{z,i+1/2,j+1/2}^n + \frac{\Delta t/2}{\mu \Delta y} \left[\begin{array}{c} \frac{27}{24} \left(E_{x,i+1/2,j+1}^n - E_{x,i+1/2,j}^n \right) \\ -\frac{1}{24} \left(E_{x,i+1/2,j+2}^n - E_{x,i+1/2,j-1}^n \right) \end{array} \right]$$

$$-\frac{\Delta t/2}{\mu\Delta x} \left[\begin{array}{c} \frac{27}{24} \left(E_{y,i+1,j+1/2}^{n+1/2} - E_{y,i,j+1/2}^{n+1/2} \right) \\ -\frac{1}{24} \left(E_{y,i+2,j+1/2}^{n+1/2} - E_{y,i-1,j+1/2}^{n+1/2} \right) \end{array} \right]. \quad (3.31)$$

By combining (3.30) and (3.31), an equation for the $H_z^{n+1/2}$ components can be obtained

as

$$\begin{aligned} & -\frac{1}{24^2} \frac{\Delta t^2}{4\varepsilon\mu\Delta x^2} H_{z,i+7/2,j+1/2}^{n+1/2} + \frac{54}{24^2} \frac{\Delta t^2}{4\varepsilon\mu\Delta x^2} H_{z,i+5/2,j+1/2}^{n+1/2} - \frac{783}{24^2} \frac{\Delta t^2}{4\varepsilon\mu\Delta x^2} \frac{27}{24^2} H_{z,i+3/2,j+1/2}^{n+1/2} \\ & + \left(1 + \frac{1460}{24^2} \frac{\Delta t^2}{4\varepsilon\mu\Delta x^2} \right) H_{z,i+1/2,j+1/2}^{n+1/2} - \frac{783}{24^2} \frac{\Delta t^2}{4\varepsilon\mu\Delta x^2} H_{z,i-1/2,j+1/2}^{n+1/2} \\ & + \frac{54}{24^2} \frac{\Delta t^2}{4\varepsilon\mu\Delta x^2} H_{z,i-3/2,j+1/2}^{n+1/2} - \frac{1}{24^2} \frac{\Delta t^2}{4\varepsilon\mu\Delta x^2} H_{z,i-5/2,j+1/2}^{n+1/2} \\ & = H_{z,i+1/2,j+1/2}^n + \frac{\Delta t}{2\mu\Delta y} \left[\frac{27}{24} \left(E_{x,i+1/2,j+1}^n - E_{x,i+1/2,j}^n \right) - \frac{1}{24} \left(E_{x,i+1/2,j+2}^n - E_{x,i+1/2,j-1}^n \right) \right] \\ & - \frac{\Delta t}{2\mu\Delta x} \left[\frac{27}{24} \left(E_{y,i+1,j+1/2}^n - E_{y,i,j+1/2}^n \right) - \frac{1}{24} \left(E_{y,i+2,j+1/2}^n - E_{y,i-1,j+1/2}^n \right) \right]. \quad (3.32) \end{aligned}$$

It can be simplified as

$$a_i u_{i-3} + b_i u_{i-2} + c_i u_{i-1} + d_i u_i + e_i u_{i+1} + f_i u_{i+2} + g_i u_{i+3} = h_i. \quad (3.33)$$

where u_i represents $H_{z,i-1/2,j-1/2}^{n+1/2}$ which is the unknown variable, $a_i, b_i, c_i, d_i, e_i, f_i, g_i$ represent the corresponding coefficients and h_i is the known variable.

Assume that the computational domain has N rows in the x -direction. There will be

N equations by having different suffix i and they can be expressed in matrix form as

$$\begin{bmatrix}
 a_1 & b_1 & c_1 & d_1 & e_1 & f_1 & g_1 & 0 & \cdots & 0 \\
 0 & a_2 & b_2 & c_2 & d_2 & e_2 & f_2 & g_2 & 0 & \cdots & 0 \\
 \vdots & & \ddots & & \vdots \\
 & & & & & & & & & & 0 \\
 0 & \cdots & & 0 & a_N & b_N & c_N & d_N & e_N & f_N & g_N
 \end{bmatrix}
 \begin{bmatrix}
 u_{-2} \\
 u_{-1} \\
 u_0 \\
 u_1 \\
 \vdots \\
 u_N \\
 u_{N+1} \\
 u_{N+2} \\
 u_{N+3}
 \end{bmatrix}
 =
 \begin{bmatrix}
 h_1 \\
 h_2 \\
 \vdots \\
 h_N
 \end{bmatrix}.
 \tag{3.34}$$

This N equations $N + 6$ unknowns system is unsolvable. However, $u_{-2}, u_{-1}, u_0, u_{N+1}, u_{N+2}$ and u_{N+3} are at the boundary, they can be calculated using the data at the previous time-step by the boundary conditions. They become known variables when (3.34) is computed.

Then, (3.34) can be rewritten as

$$\mathbf{A}\mathbf{u} = \mathbf{h} - \mathbf{B}_1 \begin{bmatrix} u_{-2} & u_{-1} & u_0 \end{bmatrix} - \mathbf{B}_2 \begin{bmatrix} u_{N+1} & u_{N+2} & u_{N+3} \end{bmatrix}, \tag{3.35}$$

where

$$\mathbf{A} = \begin{bmatrix} d_1 & e_1 & f_1 & g_1 & 0 & \cdots & 0 \\ c_2 & d_2 & e_2 & f_2 & g_2 & 0 & \cdots & 0 \\ \cdots & \cdots \\ 0 & a_i & b_i & c_i & d_i & e_i & f_i & g_i & 0 \\ \cdots & \cdots \\ 0 & \cdots & 0 & a_{N-1} & b_{N-1} & c_{N-1} & d_{N-1} & e_{N-1} \\ 0 & \cdots & 0 & a_N & b_N & c_N & d_N \end{bmatrix}, \quad (3.36)$$

$$\mathbf{u} = \begin{bmatrix} u_1 & u_2 & \cdots & u_{N-1} & u_N \end{bmatrix}^T, \quad (3.37)$$

$$\mathbf{h} = \begin{bmatrix} h_1 & h_2 & \cdots & h_{N-1} & h_N \end{bmatrix}^T, \quad (3.38)$$

$$\mathbf{B}_1 = \begin{bmatrix} c_1 & b_2 & a_3 & 0 & \cdots & 0 \\ b_1 & a_2 & 0 & \cdots & 0 \\ a_1 & 0 & \cdots & 0 \end{bmatrix}^T, \quad (3.39)$$

$$\mathbf{B}_2 = \begin{bmatrix} 0 & \cdots & 0 & a_N \\ 0 & \cdots & 0 & a_{N-1} & b_N \\ 0 & \cdots & 0 & a_N & b_{N-1} & c_N \end{bmatrix}^T. \quad (3.40)$$

The system becomes an N equations N unknowns solvable system. \mathbf{A} is a hepta-diagonal matrix. Since N is much larger than 7, \mathbf{A} is still a sparse matrix and the system can be

solved using efficient methods. Besides, multi-layers of boundary conditions are required for the high-order ADI-FDTD method. Therefore, for an open region simulation, the perfectly matched layer (PML)[33]-[35],[39]-[44] is one of the possible absorbing boundary conditions for the high-order ADI-FDTD method.

By the similar manner, the updating equations of the second procedure of the fourth-order ADI-FDTD method can be written as

$$E_{x,i+1/2,j}^{n+1} = E_{x,i+1/2,j}^{n+1/2} + \frac{\Delta t/2}{\varepsilon \Delta y} \begin{bmatrix} \frac{27}{24} (H_{z,i+1/2,j+1/2}^{n+1} - H_{z,i+1/2,j-1/2}^{n+1}) \\ -\frac{1}{24} (H_{z,i+1/2,j+3/2}^{n+1} - H_{z,i+1/2,j-3/2}^{n+1}) \end{bmatrix}, \quad (3.41)$$

$$E_{y,i,j+1/2}^{n+1} = E_{y,i,j+1/2}^{n+1/2} - \frac{\Delta t/2}{\varepsilon \Delta x} \begin{bmatrix} \frac{27}{24} (H_{z,i+1/2,j+1/2}^{n+1/2} - H_{z,i-1/2,j+1/2}^{n+1/2}) \\ -\frac{1}{24} (H_{z,i+3/2,j+1/2}^{n+1/2} - H_{z,i-3/2,j+1/2}^{n+1/2}) \end{bmatrix}, \quad (3.42)$$

$$H_{z,i+1/2,j+1/2}^{n+1} = H_{z,i+1/2,j+1/2}^{n+1/2} + \frac{\Delta t/2}{\mu \Delta y} \begin{bmatrix} \frac{27}{24} (E_{x,i+1/2,j+1}^{n+1} - E_{x,i+1/2,j}^{n+1}) \\ -\frac{1}{24} (E_{x,i+1/2,j+2}^{n+1} - E_{x,i+1/2,j-1}^{n+1}) \end{bmatrix} \\ - \frac{\Delta t/2}{\mu \Delta x} \begin{bmatrix} \frac{27}{24} (E_{y,i+1,j+1/2}^{n+1/2} - E_{y,i,j+1/2}^{n+1/2}) \\ -\frac{1}{24} (E_{y,i+2,j+1/2}^{n+1/2} - E_{y,i-1,j+1/2}^{n+1/2}) \end{bmatrix}. \quad (3.43)$$

Then, by combining (3.41) and (3.43), an equation for the H_z^{n+1} components can be obtained as

$$-\frac{1}{24^2} \frac{\Delta t^2}{4\varepsilon\mu\Delta y^2} H_{z,i+1/2,j+7/2}^{n+1} + \frac{54}{24^2} \frac{\Delta t^2}{4\varepsilon\mu\Delta y^2} H_{z,i+1/2,j+5/2}^{n+1} - \frac{783}{24^2} \frac{\Delta t^2}{4\varepsilon\mu\Delta y^2} \frac{27}{24^2} H_{z,i+1/2,j+3/2}^{n+1} \\ + \left(1 + \frac{1460}{24^2} \frac{\Delta t^2}{4\varepsilon\mu\Delta y^2}\right) H_{z,i+1/2,j+1/2}^{n+1} - \frac{783}{24^2} \frac{\Delta t^2}{4\varepsilon\mu\Delta y^2} H_{z,i+1/2,j-1/2}^{n+1} \\ + \frac{54}{24^2} \frac{\Delta t^2}{4\varepsilon\mu\Delta y^2} H_{z,i+1/2,j-3/2}^{n+1} - \frac{1}{24^2} \frac{\Delta t^2}{4\varepsilon\mu\Delta y^2} H_{z,i+1/2,j-5/2}^{n+1} \\ = H_{z,i+1/2,j+1/2}^{n+1/2} - \frac{\Delta t}{2\mu\Delta x} \left[\frac{27}{24} (E_{y,i+1,j+1/2}^{n+1/2} - E_{y,i,j+1/2}^{n+1/2}) - \frac{1}{24} (E_{y,i+2,j+1/2}^{n+1/2} - E_{y,i-1,j+1/2}^{n+1/2}) \right] \\ + \frac{\Delta t}{2\mu\Delta y} \left[\frac{27}{24} (E_{x,i+1/2,j+1}^{n+1/2} - E_{x,i+1/2,j}^{n+1/2}) - \frac{1}{24} (E_{x,i+1/2,j+2}^{n+1/2} - E_{x,i+1/2,j-1}^{n+1/2}) \right]. \quad (3.44)$$

Assume that the computational domain has P columns in the y -direction. There will be P equations by having different suffix j , and they can be solved by the same manner with the first procedure mentioned above.

3.3.2 Numerical Stability of the High-Order ADI-FDTD Method

To analyze the stability of the high-order ADI-FDTD method, the von Neumann method is used. The trial solutions for the 2-D TE wave (2.24) are substituted into the updating equations of the two procedures (3.22)-(3.24), (3.26)-(3.28). Since the only difference between the high-order ADI-FDTD method and the ADI-FDTD method is using different order central difference schemes to approximate the spatial derivatives, the formulation of the numerical stability is very similar.

After substituting the trial solutions into the updating equations of the two procedures, the resulted equations are combined as

$$\varepsilon_0 \xi E_x^n + W_y \xi H_z^n = \varepsilon_0 E_x^n - W_y H_z^n, \quad (3.45)$$

$$-W_x W_y \xi E_x^n + \varepsilon_0 \mu_0 \xi E_y^n - W_x W_y \xi H_z^n = -W_x W_y E_x^n + \varepsilon_0 \mu_0 E_y^n - W_x W_y H_z^n, \quad (3.46)$$

$$W_y \xi E_x^n - W_x \xi E_y^n + \mu_0 \xi H_z^n = -W_y E_x^n + W_x E_y^n + \mu_0 H_z^n, \quad (3.47)$$

where

$$W_x = j \frac{\Delta t}{\Delta x} \sum_{m=0}^{M-1} a(m) \sin \left[k_x \frac{(2m+1) \Delta x}{2} \right], \quad (3.48)$$

$$W_y = j \frac{\Delta t}{\Delta y} \sum_{m=0}^{M-1} a(m) \sin \left[k_y \frac{(2m+1) \Delta y}{2} \right], \quad (3.49)$$

and ξ is the growth factor of the complete update cycle, $a(m)$ is the coefficient of the central difference scheme and k_x and k_y are wavenumber in the x and y directions respectively.

By eliminating the field components of (3.45)-(3.47), it obtains

$$\frac{(\xi - 1)^2}{(\xi + 1)^2} = -K, \quad (3.50)$$

where

$$K = S_x^2 + S_y^2 + S_x^2 S_y^2, \quad (3.51)$$

$$S_x = \frac{c\Delta t}{\Delta x} \sum_{m=0}^{M-1} a(m) \sin \left[k_x \frac{(2m+1)\Delta x}{2} \right], \quad (3.52)$$

$$S_y = \frac{c\Delta t}{\Delta y} \sum_{m=0}^{M-1} a(m) \sin \left[k_y \frac{(2m+1)\Delta y}{2} \right], \quad (3.53)$$

and c is the speed of light. By solving (3.50), the growth factor of the ADI-FDTD method is found as

$$\xi = \frac{1 - K \pm 2j\sqrt{K}}{1 + K}. \quad (3.54)$$

Since K is always positive with any coefficient $a(m)$, the magnitude of the growth factor is always unity. Therefore, the high-order ADI-FDTD method is also unconditionally stable.

3.3.3 Numerical Dispersion of the High-Order ADI-FDTD Method

Since the magnitude of the growth factor is always unity, the growth factor can be expressed in terms of the time-step as

$$\xi = e^{j\omega\Delta t}. \quad (3.55)$$

The numerical dispersion relation of the high-order ADI-FDTD method can be easily derived from (3.50) as

$$S_x^2 + S_y^2 + S_x^2 S_y^2 = \tan^2 \left(\frac{\omega\Delta, t}{2} \right) \quad (3.56)$$

where

$$S_x = \frac{c\Delta t}{\Delta x} \sum_{m=0}^{M-1} a(m) \sin \left[k_x \frac{(2m+1)\Delta x}{2} \right], \quad (3.57)$$

$$S_y = \frac{c\Delta t}{\Delta y} \sum_{m=0}^{M-1} a(m) \sin \left[k_y \frac{(2m+1)\Delta y}{2} \right], \quad (3.58)$$

and c is the speed of light. To solve the equation of numerical dispersion relation, it is assumed that the wave propagates at angle θ with respect to the positive x -direction ($k_x = k\cos\theta$, $k_y = k\sin\theta$). Thus, the numerical solution of the wavenumber $k = \omega/u$ can be obtained, where u is the numerical phase velocity. In addition, it is assumed that square uniform cell is used and the mesh density n is defined as

$$\Delta x = \Delta y = \Delta = \frac{\lambda}{n}, \quad (3.59)$$

where λ is the wavelength of the signal.

The numerical dispersion errors of the high-order ADI-FDTD method at different mesh densities n are shown in Figure 3.2 to 3.4. Those results are for the fixed time-step $\Delta t = T/10$, $T/20$ and $T/100$, respectively, where T is the signal period.

From Figure 3.2 to 3.4, it can be found that the numerical dispersion error of the conventional second-order ADI-FDTD method is much larger than the other methods when the mesh is coarse. In addition, the numerical dispersion error decreases when the mesh density increases. Furthermore, it is observed that the numerical dispersion error is reduced when the high-order central difference scheme is applied.

When the sixth-order ADI-FDTD method is applied, the numerical dispersion error is very close to a constant, even in different mesh densities. In addition, no further improvement is found when the order of the method is higher than six. This is because the high-order central difference scheme can only reduce the numerical dispersion error,

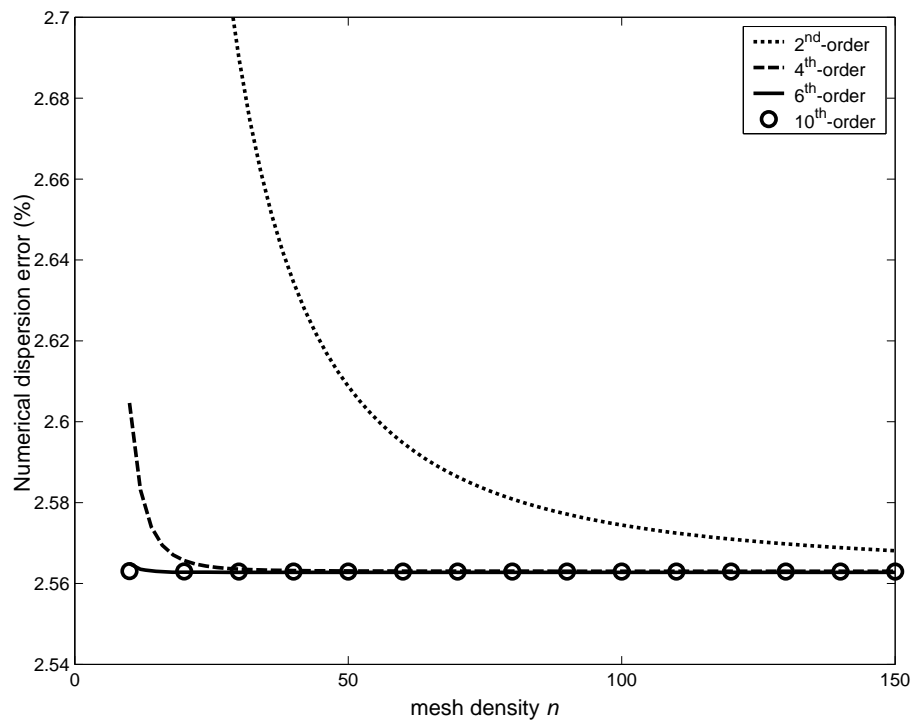


Figure 3.2: Numerical dispersion errors of the high-order ADI-FDTD method with different order central difference schemes at $\Delta t = T/10$.

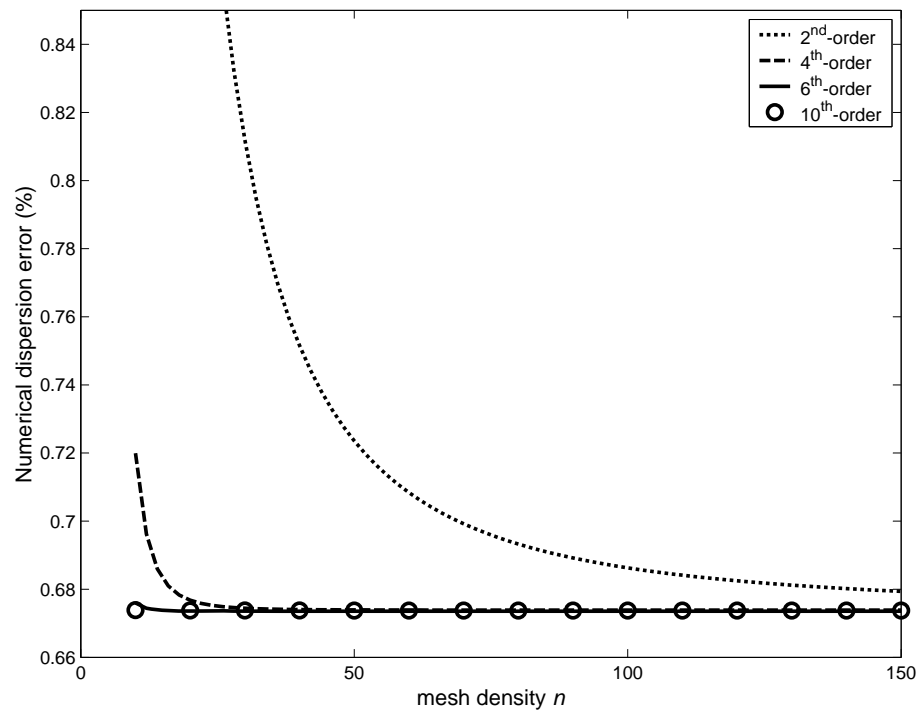


Figure 3.3: Numerical dispersion errors of the high-order ADI-FDTD method with different order central difference schemes at $\Delta t = T/20$.

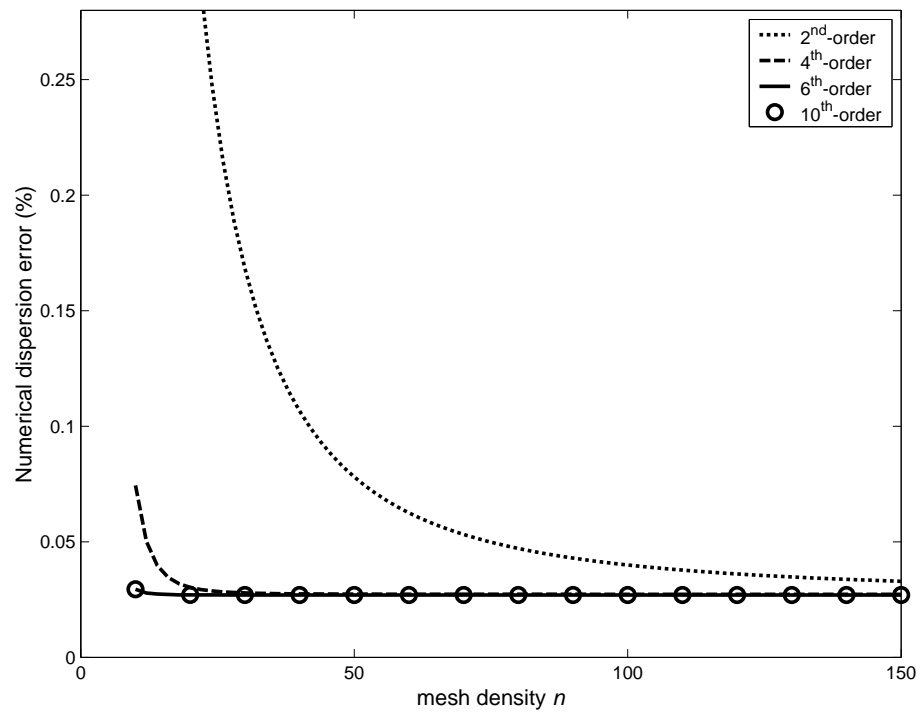


Figure 3.4: Numerical dispersion errors of the high-order ADI-FDTD method with different order central difference schemes at $\Delta t = T/100$.

Table 3.2: Accuracy limit of the high-order ADI-FDTD method at different time-steps Δt .

Δt	accuracy limit (%)
$T/10$	2.564
$T/20$	0.669
$T/100$	0.026

which is caused by approximating the spatial derivative but not the temporal derivative.

The constant is the accuracy limit of the high-order ADI-FDTD method. To calculate the constant, we take the limit of the numerical dispersion relation for the cell size going to zero, it obtains

$$\frac{c^2 \Delta t^2}{4} (k_x^2 + k_y^2) + \frac{c^4 \Delta t^4}{16} k_x^2 k_y^2 = \tan^2 \left(\frac{\omega \Delta t}{2} \right). \quad (3.60)$$

Therefore, the error does not depend on the approximation of the spatial derivatives.

Since (3.60) is not equal to the theoretical one, it can calculate the accuracy limit of the high-order ADI-FDTD method for a given time-step. The accuracy limit for the time-step $\Delta t = T/10, T/20$ and $T/100$ are computed and shown in Table 3.2. The results are close to that from the figures.

Figure 3.5 to 3.8 show the numerical dispersion errors of the high-order ADI-FDTD method with different order central difference schemes at different $CFLN$. From these figures, it can be observed that the numerical dispersion errors are reduced when the high-order central difference schemes are applied. However, the improvement diminishes when the order of scheme is higher than 4. In addition, the slope of the numerical dispersion error plot in the log-log diagram is 2. This means that the numerical dispersion error of

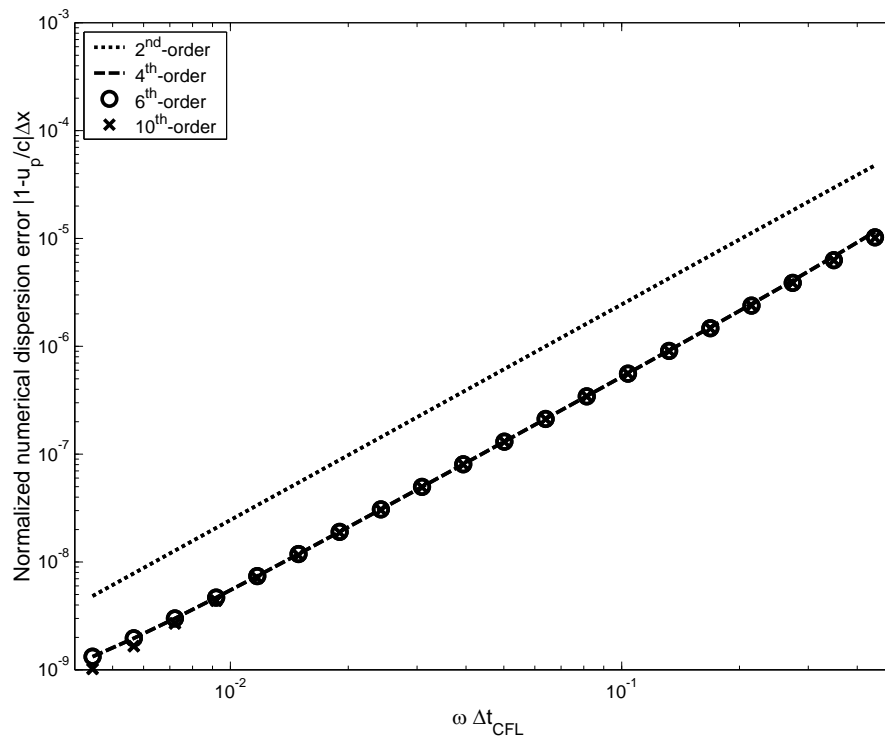


Figure 3.5: Numerical dispersion errors of the high-order ADI-FDTD method with different order central difference schemes at $CFLN = 0.5$.

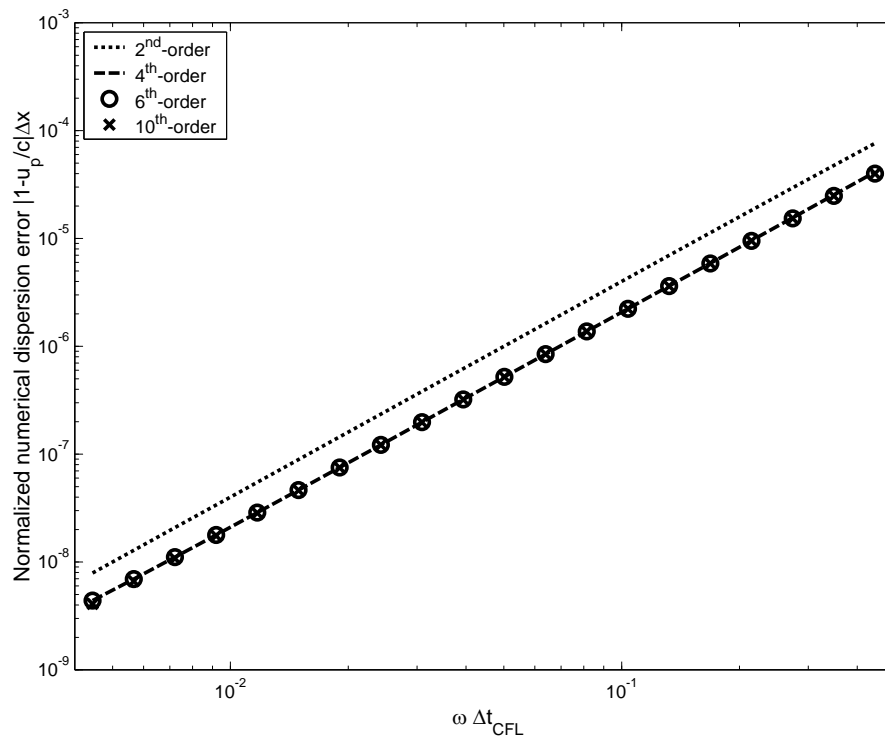


Figure 3.6: Numerical dispersion errors of the high-order ADI-FDTD method with different order central difference schemes at $CFLN = 1$.

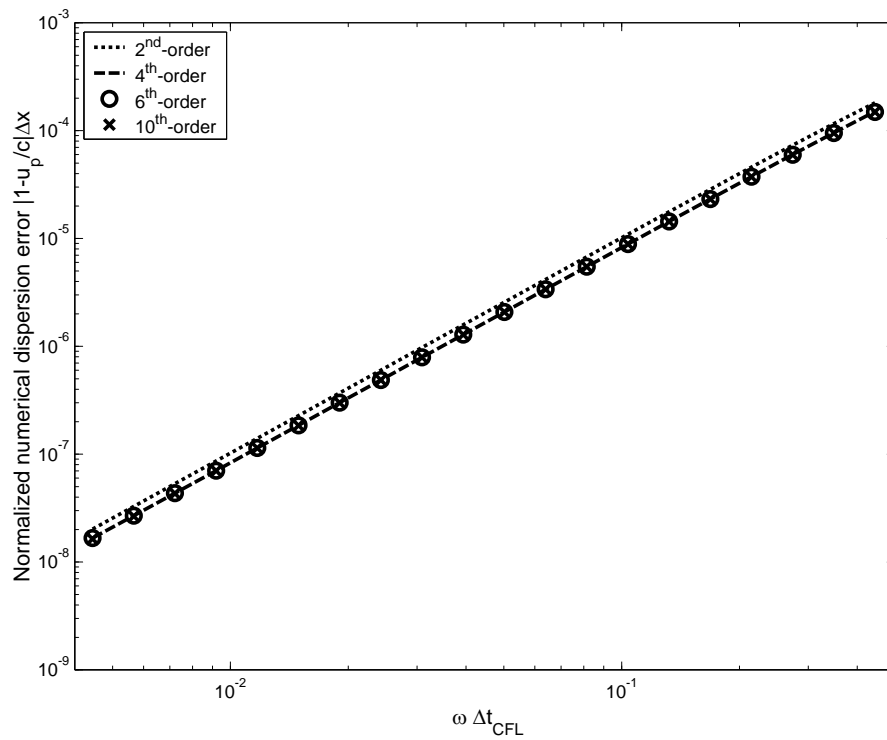


Figure 3.7: Numerical dispersion errors of the high-order ADI-FDTD method with different order central difference schemes at $CFLN = 2$.

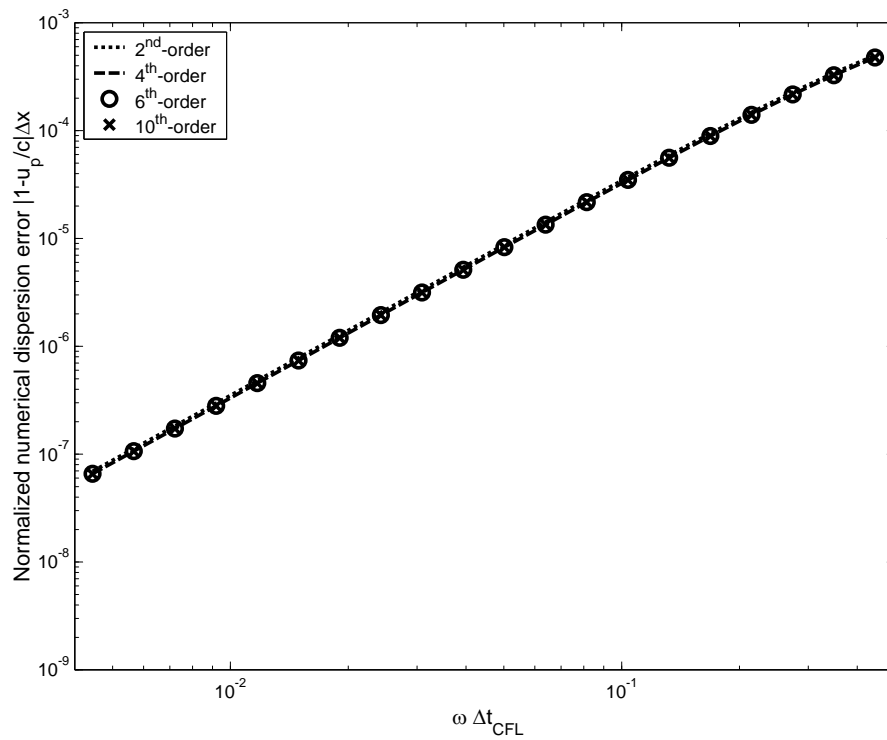


Figure 3.8: Numerical dispersion errors of the high-order ADI-FDTD method with different order central difference schemes at $CFLN = 4$.

the high-order ADI-FDTD method is $O(\Delta t^2)$. Furthermore, the improvement of applying the high-order central difference scheme becomes insignificant when the $CFLN$ is large. It is because the high-order central difference scheme is applied only to approximate the spatial derivatives. The numerical dispersion error that is caused by the approximation of the temporal derivatives dominates when the $CFLN$ is large.

3.3.4 Simulation and Results

To demonstrate the validity and examine the performance of the high-order ADI-FDTD method, the propagation of the TE wave in a short-circuited parallel-plate waveguide model, which is shown in Figure 3.9, is simulated. This model is chosen because the numerical dispersion error can be easily found by the data from two observation points. In addition, the perfect electric conductor (PEC) is used as the boundaries such that the stability is not affected by the modelling of the boundary. For simplicity, square uniform cells are used.

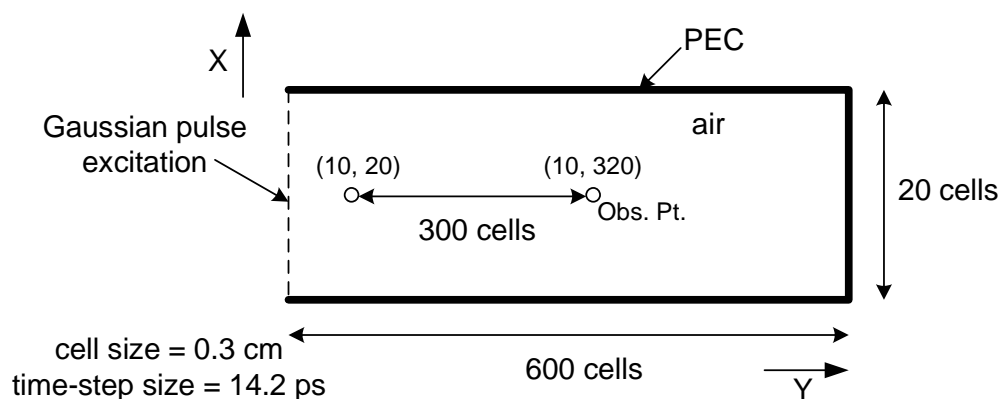


Figure 3.9: The 2-D parallel-plate waveguide model.

From the analytical study, it is found that the numerical dispersion error of the ADI-FDTD method is reduced when the high-order central difference scheme is applied. How-

ever, there is no further improvement when the order of the scheme is higher than 6. Therefore, the sixth-order ADI-FDTD is used at the simulation. Besides, the simulation is performed at different sizes of time-step.

The E_x field at the observation point (10,320) is shown in Figure 3.10. It can be observed that when the time-step is larger than the CFL stability condition, the method remains stable but the numerical dispersion increases.

The numerical dispersion error is estimated by the data from the two observation points [45] and plotted in Figure 3.11. It can be shown that the numerical dispersion error of the ADI-FDTD method is larger than the FDTD method and increases when the $CFLN$ is increased. In addition, the numerical dispersion error of the sixth-order ADI-FDTD method is smaller than that of the conventional second-order ADI-FDTD method under the same time-step. The results agree with the analytical study.

3.4 Conclusion

The high-order ADI-FDTD method is formulated in this chapter. The multi-points high-order central difference scheme is applied to approximate the spatial derivatives. The unconditionally stable property of the high-order ADI-FDTD method is proved by the analytical method and simulation examples. In addition, the numerical dispersion error of the high-order ADI-FDTD method is smaller than that of the conventional second-order ADI-FDTD method under the same time-step. However, it is found that there is no further improvement when the order of the finite difference scheme is higher than 6, and the improvement diminishes when the time-step is increased. This is because the high-order central difference scheme only reduces the error that is caused by the approximation

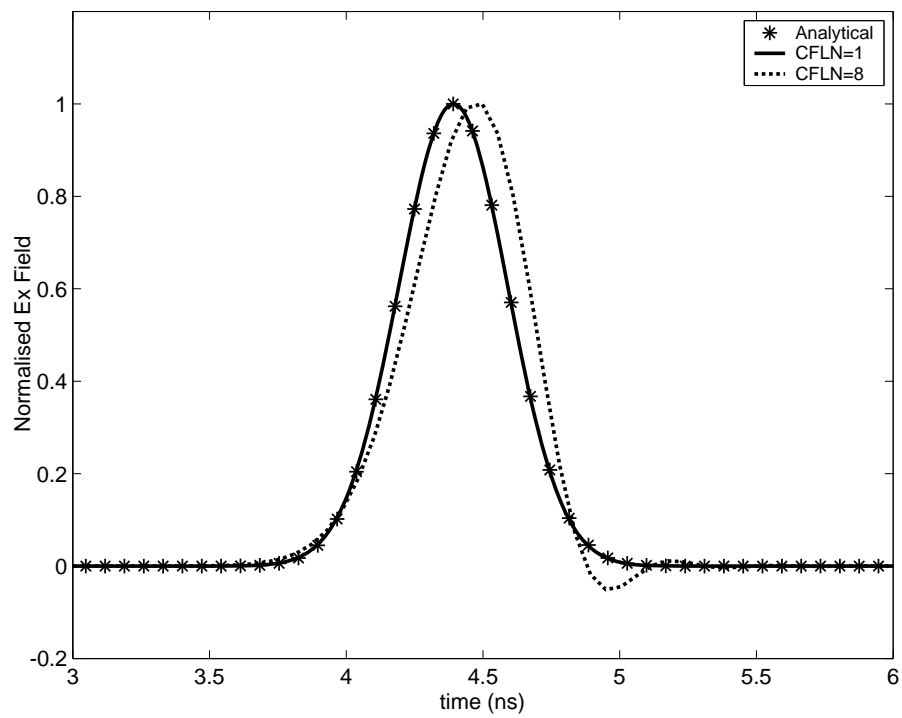


Figure 3.10: E_x field at the observation point (10,320) in time domain.

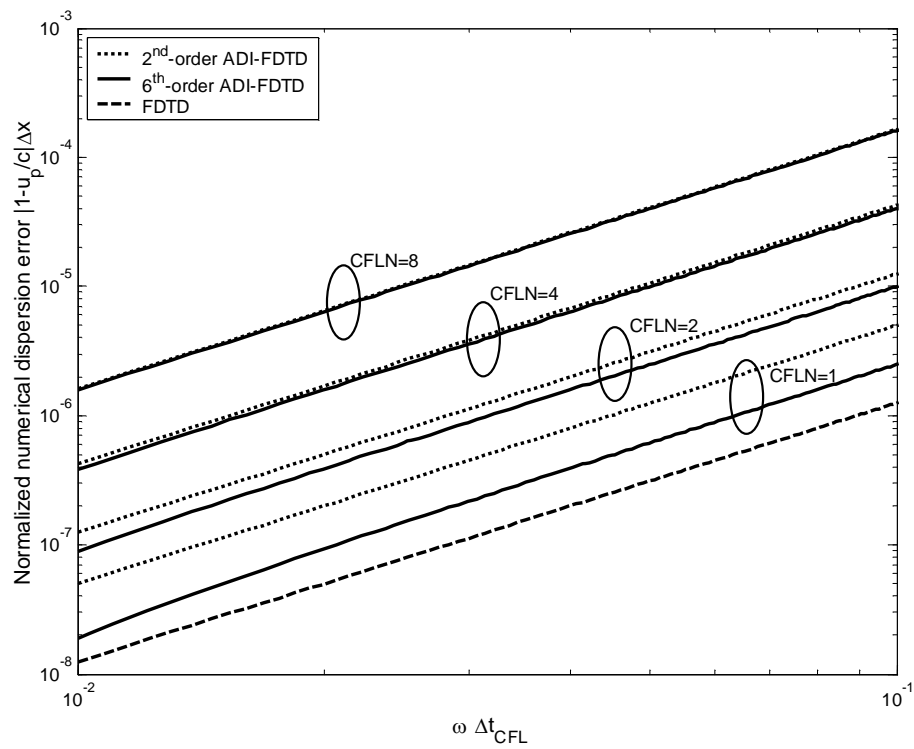


Figure 3.11: Numerical dispersion errors of the 2nd- and 6th-order ADI-FDTD method with different time-steps which are calculated by simulation results.

of the spatial derivative and the error that is caused by the approximation of the temporal derivatives dominates when the $CFLN$ is large.

Chapter 4

The (2,4) Low Numerical Dispersion ADI-FDTD Method

4.1 Introduction

In the previous chapter, it is shown that the numerical dispersion error can be reduced by applying the multi-points high-order central difference scheme to approximate the spatial derivatives. However, when the time-step is increased, the improvement becomes relatively insignificant. This is because the high-order scheme can only reduce the numerical dispersion error, which is caused by approximating the spatial derivatives with the finite difference scheme but not the temporal derivatives. In addition, the multi-points high-order central difference scheme cannot be applied to the temporal derivative because the method will become practically unsolvable.

The simplest high-order FDTD method for electromagnetics simulation is Fang's (2,4) scheme. The (2,4) high-order FDTD method uses two-points second-order central differ-

ence scheme to approximate the temporal derivatives and four-points fourth-order central difference scheme to approximate the spatial derivatives. The finite difference operator of the fourth-order central difference scheme is computed by Taylor series, shown in previous chapter.

In 2004, a low numerical dispersion (LD) algorithm based on the (2,4) high-order FDTD method was proposed [31]. The finite difference operator is determined by minimizing the error terms, which are caused by approximating the spatial derivatives and temporal derivatives with finite difference scheme, in the numerical dispersion relation.

In this chapter, a (2,4) low numerical dispersion ADI-FDTD method is developed based on the idea of [31]. The formulation of the novel method is shown. The numerical dispersion error is investigated and compared to the conventional ADI-FDTD method as well as to the FDTD method.

4.2 Overview of the Low Numerical Dispersion Algorithm for the FDTD method

For the conventional (2,4) FDTD method, the four-points central difference scheme is applied to approximate the spatial derivatives, and the finite difference operator is computed by Taylor series. The finite difference operator is determined by cancelling the second-order error terms and the error of the approximation of the spatial derivative becomes $O(\Delta x^4)$. However, two-points central difference scheme is still applied to approximate the temporal derivative. The overall error of the (2,4) FDTD method remains at $O(\Delta t^2)$. Besides, the size of the time-step is linear proportional to the cell size under the stability

condition. Therefore, the overall error of the (2,4) FDTD method is also equivalent to $O(\Delta x^2)$.

The idea of the low numerical dispersion algorithm is minimizing the overall second-order error in the numerical dispersion relation by adjusting the coefficients of the finite difference operator but is not reducing the order of the accuracy.

To construct the low numerical dispersion algorithm, the four-points central difference scheme is considered. For example, the approximation of the spatial derivative of the field component Φ with respect to x is

$$\frac{\partial \Phi_{i,j}}{\partial x} = \frac{C_1 \left(\Phi_{i+\frac{1}{2},j} - \Phi_{i-\frac{1}{2},j} \right) + C_2 \left(\Phi_{i+\frac{3}{2},j} - \Phi_{i-\frac{3}{2},j} \right)}{\Delta x}, \quad (4.1)$$

where C_1 and C_2 are the coefficients of the finite difference operator.

In the previous chapter, the numerical dispersion relation of the FDTD method is formulated. By the same manner, the numerical dispersion relation of the 2-D (2,4) FDTD method for TE wave in free-space can be formulated as

$$\sin^2 \left(\frac{\omega \Delta t}{2} \right) = S_x^2 + S_y^2, \quad (4.2)$$

where

$$S_x = \frac{c \Delta t}{\Delta x} \left[C_1 \sin \left(\frac{\widetilde{k}_x \Delta x}{2} \right) + C_2 \sin \left(\frac{3 \widetilde{k}_x \Delta x}{2} \right) \right], \quad (4.3)$$

$$S_y = \frac{c \Delta t}{\Delta y} \left[C_1 \sin \left(\frac{\widetilde{k}_y \Delta y}{2} \right) + C_2 \sin \left(\frac{3 \widetilde{k}_y \Delta y}{2} \right) \right], \quad (4.4)$$

c is the speed of light, and \widetilde{k}_x and \widetilde{k}_y are numerical wavenumbers in the x and y directions, respectively. For a propagation angle θ , the numerical wavenumbers can be written as $\widetilde{k}_x = \widetilde{k} \cos \theta$, $\widetilde{k}_y = \widetilde{k} \sin \theta$.

To analyze the numerical dispersion relation, the trigonometric terms in (4.2) are expanded using Taylor series and assume that the numerical wavenumber is equal to the

theoretical one, in which $\tilde{k} = k = \omega/c$. In addition, it is assumed that uniform square cell is used. Furthermore, with regard to the 2-D FDTD method, the maximum time-step under the Courant-Friedrich-Levy stability condition is defined as

$$\Delta t_{CFL} = \frac{\Delta}{c\sqrt{2}} \quad (4.5)$$

and a ratio of the time-step is defined as

$$CFLN = \frac{\Delta t}{\Delta t_{CFL}}, \quad (4.6)$$

where $CFLN$ must be smaller than 1 to guarantee the stability of the FDTD method.

Therefore, the numerical dispersion relation (4.2) can be rewritten as

$$\begin{aligned} \frac{\omega^2}{c^2} = & (C_1 + 3C_2)^2 k^2 - (C_1 + 3C_2)(C_1 + 27C_2) (\cos^4 \theta + \sin^4 \theta) \frac{k^4 \Delta^2}{12} \\ & + \frac{CFLN^2 k^4 \Delta^2}{24}, \end{aligned} \quad (4.7)$$

where terms with the order of the cell size greater than 2 are neglected. The details of the formulation are shown in Appendix A.

To determine the coefficient C_1 and C_2 so that the numerical dispersion error is minimized, two conditions are formulated from equation (4.7). By equalizing the zero-order terms in both sides of (4.7), the first condition is obtained as

$$C_1 + 3C_2 = 1. \quad (4.8)$$

This condition guarantees the second-order accuracy.

Then, the second-order terms in the numerical dispersion relation (4.7) are defined as the error of k^2 and can be written as

$$e = - (C_1 + 3C_2)(C_1 + 27C_2) (\cos^4 \theta + \sin^4 \theta) \frac{k^4 \Delta^2}{12} + \frac{CFLN^2 k^4 \Delta^2}{24}. \quad (4.9)$$

Therefore, by minimizing the mean square error over all angles, the second condition for determining the coefficients can be formulated as

$$C_1 + 27C_2 = \frac{12}{19}CFLN^2. \quad (4.10)$$

By combining the first condition (4.8) and the second condition (4.10), C_1 and C_2 can be determined for a given $CFLN$.

The numerical dispersion errors of different FDTD methods at $CFLN = 0.75$ are plotted in Figure 4.1. The coefficients of the finite difference operator for the fourth-order FDTD method are ($C_1 = 27/24, C_2 = -1/24$) and that for the LD FDTD method is ($C_1 = 657/608, C_2 = -49/1824$). It is shown that the numerical dispersion errors of both FDTD methods are $O(\Delta t^2)$. However, the numerical dispersion error of the LD FDTD method is much smaller than that of the conventional second-order FDTD method and the fourth-order FDTD method.

4.3 The (2,4) Low Numerical Dispersion ADI-FDTD Method

4.3.1 Formulation of the (2,4) LD ADI-FDTD Method

The (2,4) LD ADI-FDTD method [46] is formulated based on the idea of [31], which is minimizing the overall second-order error by adjusting the finite difference operator in the numerical dispersion relation. Since the ADI-FDTD method is unconditionally stable, the low numerical dispersion algorithm is very useful for the ADI-FDTD method. It is because the time-step of the ADI-FDTD method can be set to any arbitrary value, which is

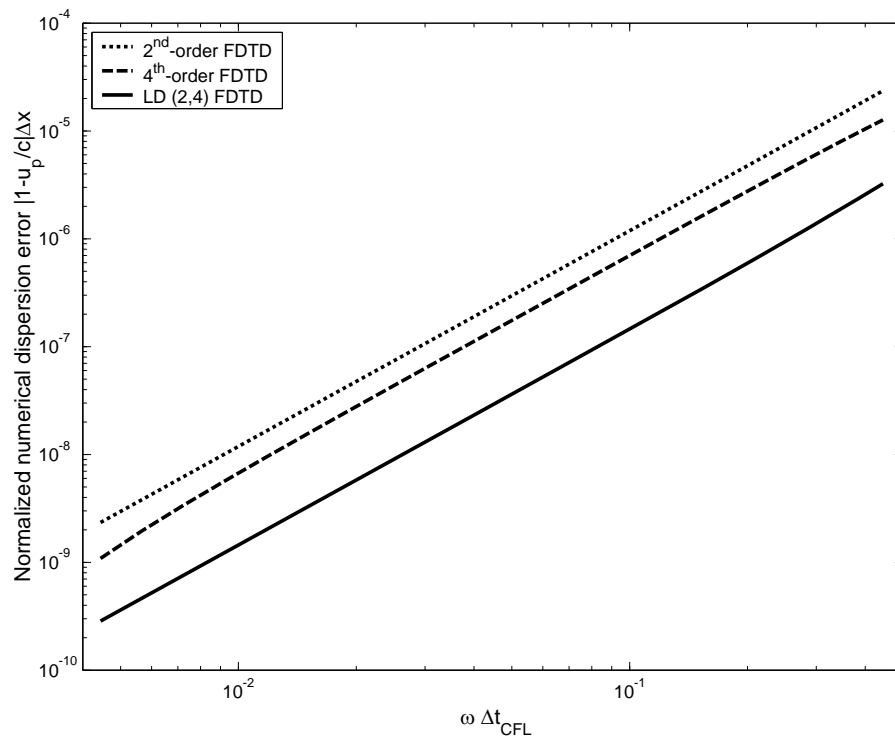


Figure 4.1: Numerical dispersion errors of different FDTD methods at $CFLN = 0.75$.

always larger than that under the stability condition. Therefore, the numerical dispersion error, which is caused by approximating the temporal derivatives, is dominated. The low numerical dispersion algorithm can reduce the error terms of the numerical dispersion relation but not the approximation formula of the individual spatial derivative, which is used in the high-order FDTD method.

The updating equations of the (2,4) LD ADI-FDTD method are same as the fourth-order ADI-FDTD method, and the difference is that the finite difference operators are determined according to the numerical dispersion relation. We consider the numerical dispersion relation of the (2,4) ADI-FDTD method, which is derived in the previous chapter, as

$$\tan^2\left(\frac{\omega\Delta t}{2}\right) = S_x^2 + S_y^2 + S_x^2 S_y^2, \quad (4.11)$$

where

$$S_x = \frac{c\Delta t}{\Delta x} \left[C_1 \sin\left(\frac{\widetilde{k}_x\Delta x}{2}\right) + C_2 \sin\left(\frac{3\widetilde{k}_x\Delta x}{2}\right) \right], \quad (4.12)$$

$$S_y = \frac{c\Delta t}{\Delta y} \left[C_1 \sin\left(\frac{\widetilde{k}_y\Delta y}{2}\right) + C_2 \sin\left(\frac{3\widetilde{k}_y\Delta y}{2}\right) \right], \quad (4.13)$$

c is the speed of light, and \widetilde{k}_x and \widetilde{k}_y are numerical wavenumbers in the x and y directions, respectively. For a propagation angle θ , the numerical wavenumbers can be written as $\widetilde{k}_x = \widetilde{k} \cos \theta$, $\widetilde{k}_y = \widetilde{k} \sin \theta$.

Then, the trigonometric terms in (4.11) are expanded using Taylor series and the numerical dispersion relation can be rewritten as

$$\begin{aligned} \frac{\omega^2}{c^2} &= (C_1 + 3C_2)^2 k^2 - (C_1 + 3C_2)(C_1 + 27C_2) \frac{(\cos^4 \theta + \sin^4 \theta) k^4 \Delta^2}{12} \\ &+ \left((C_1 + 3C_2)^4 \frac{\cos^2 \theta \sin^2 \theta}{8} - \frac{1}{12} \right) CFLN^2 k^4 \Delta^2, \end{aligned} \quad (4.14)$$

where terms with the order of the cell size greater than 2 are neglected. The details of formulation are shown in Appendix B.

To determine the coefficient C_1 and C_2 so that the numerical dispersion error is minimized, we can formulate two conditions from equation (4.14). By equalizing the zero-order terms in both sides of (4.14), the first condition is obtained as

$$C_1 + 3C_2 = 1. \quad (4.15)$$

This condition guarantees the second-order accuracy.

Then, the second-order terms in the numerical dispersion relation (4.14) are defined as the error of k^2 and can be written as

$$e = \left[\left(\frac{3}{2} \sin^2 \theta \cos^2 \theta - 1 \right) CFLN^2 - (C_1 + 27C_2) (\cos^4 \theta + \sin^4 \theta) \right] \frac{k^4 \Delta^2}{12}. \quad (4.16)$$

After that, we can formulate the second condition to determine C_1 and C_2 by setting the error to zero. However, from the expression of the error, it is necessary to consider the propagation angle. This subsequently leads to two alternative cases to determine the coefficients of the finite difference operator. For the first case, a propagation angle is specified. We then have

$$\left(\frac{3}{2} \sin^2 \theta \cos^2 \theta - 1 \right) CFLN^2 - (C_1 + 27C_2) (\cos^4 \theta + \sin^4 \theta) = 0. \quad (4.17)$$

In this case, the numerical dispersion error at the specified propagation angle is minimized.

For the second case, we determine the coefficients by minimizing the mean square error over all angles. We then have the second condition as

$$C_1 + 27C_2 = -\frac{81}{76} CFLN^2. \quad (4.18)$$

By combining the first condition (4.15) and one of the cases of the second condition (4.17) or (4.18), C_1 and C_2 can be determined for a given $CFLN$.

To reduce the complexity of the equations, the formulation is shown in the two-dimensional case. The LD method can be extended to the three-dimensional case straightforwardly. The only difference is that the formulation starts from the numerical dispersion relation of (2,4) ADI-FDTD method in three-dimensional case as

$$\tan^2\left(\frac{\omega\Delta t}{2}\right) = S_x^2 + S_y^2 + S_z^2 - S_x^2 S_y^2 - S_x^2 S_z^2 - S_y^2 S_z^2 + S_x^2 S_y^2 S_z^2, \quad (4.19)$$

where

$$S_x = \frac{c\Delta t}{\Delta x} \left[C_1 \sin\left(\frac{\widetilde{k}_x \Delta x}{2}\right) + C_2 \sin\left(\frac{3\widetilde{k}_x \Delta x}{2}\right) \right], \quad (4.20)$$

$$S_y = \frac{c\Delta t}{\Delta y} \left[C_1 \sin\left(\frac{\widetilde{k}_y \Delta y}{2}\right) + C_2 \sin\left(\frac{3\widetilde{k}_y \Delta y}{2}\right) \right], \quad (4.21)$$

$$S_z = \frac{c\Delta t}{\Delta z} \left[C_1 \sin\left(\frac{\widetilde{k}_z \Delta z}{2}\right) + C_2 \sin\left(\frac{3\widetilde{k}_z \Delta z}{2}\right) \right]. \quad (4.22)$$

Then, the formulation is the same as that described previously, which starts from expanding the trigonometric terms using the Taylor series.

In Chapter 3.3.2, it is shown that the high-order ADI-FDTD method is unconditionally stable and that the stability condition is not affected by the coefficients of the finite difference operator. Therefore, the LD ADI-FDTD method is also unconditionally stable when the coefficients are modified.

4.3.2 Numerical Dispersion of the (2,4) LD ADI-FDTD Method

For the conventional fourth-order ADI-FDTD method, which is shown in the previous chapter, the coefficients of the finite difference operator are $C_1 = 27/24$ and $C_2 = -1/24$.

Therefore, the error of the fourth-order ADI-FDTD method can be formulated from (4.16)

as

$$e_{ADI} = CFLN^2 k^4 \Delta^2 \left(-\frac{1}{12} + \frac{\cos^2 \theta \sin^2 \theta}{8} \right). \quad (4.23)$$

In addition, with regard to the LD ADI-FDTD method, the error can also be formulated by substituting the general case of the second condition (4.18) into (4.16) as

$$e_{LD-ADI} = CFLN^2 k^4 \Delta^2 \left(-\frac{1}{912} + \frac{1}{152} \cos 4\theta \right). \quad (4.24)$$

Furthermore, the error of the LD FDTD method is formulated in the previous section as

$$e_{LD-FDTD} = CFLN^2 k^4 \Delta^2 \left(\frac{1}{456} - \frac{1}{76} \cos 4\theta \right). \quad (4.25)$$

To compare the performance of different methods, the mean square errors over all angles are calculated according to

$$\overline{e^2} = \frac{1}{2\pi} \int_0^{2\pi} e(\theta)^2 d\theta. \quad (4.26)$$

Table 4.1: Mean square errors over all angle $\overline{e^2}$ of different methods.

Simulation method	Mean square error $\overline{e^2}$
4 th -order ADI-FDTD	$4.706 \times 10^{-3} CFLN^2 k^4 \Delta^2$
(2,4) LD ADI-FDTD	$2.284 \times 10^{-5} CFLN^2 k^4 \Delta^2$
(2,4) LD FDTD	$9.137 \times 10^{-5} CFLN^2 k^4 \Delta^2$

The mean square errors over all angle $\overline{e^2}$ of different methods are shown in Table 4.1.

It can be found that the LD ADI-FDTD method has a wide-band error reduction of about 99.5% for any time-step when it compares with the fourth-order ADI-FDTD method. In

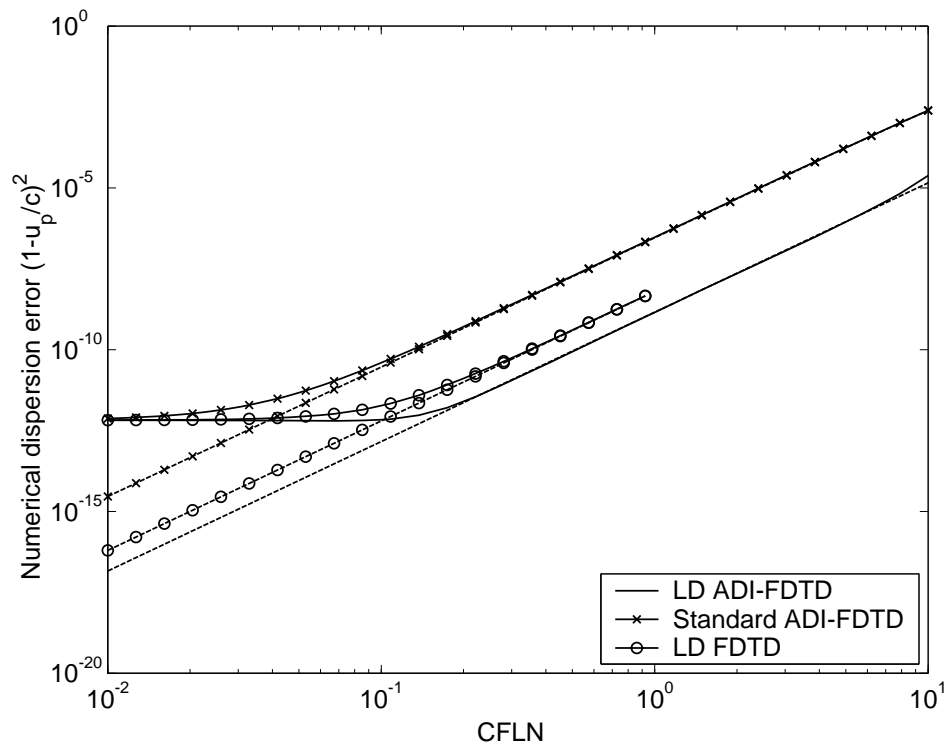


Figure 4.2: Mean absolute numerical dispersion errors with different time-steps at $\Delta = \lambda/50$. (Dashed lines represent the numerical dispersion errors when only the second-order error is considered.)

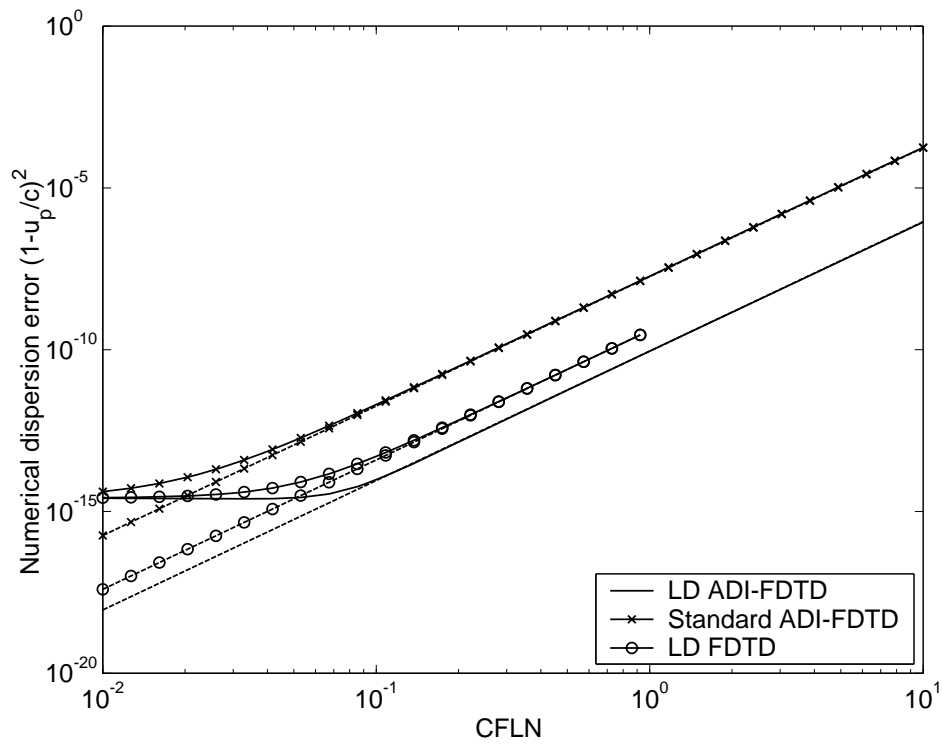


Figure 4.3: Mean absolute numerical dispersion errors with different time-steps at $\Delta = \lambda/100$. (Dashed lines represent the numerical dispersion errors when only the second-order error is considered.)

addition, the mean square error of the LD ADI-FDTD method is only a quarter that of the LD FDTD method.

Figure 4.2 and 4.3 show the numerical dispersion errors of different methods with different time-steps, when the mesh resolution is $\lambda/50$ and $\lambda/100$. It shows that the numerical dispersion errors for different methods are second-order when the time-step is large. In addition, the LD ADI-FDTD method shows a significant reduction on the numerical dispersion error when it compares with the conventional ADI-FDTD method and the LD FDTD method with different $CFLN$. Furthermore, when the time-step is decreased, the numerical dispersion errors of different methods approach to a constant. It is because the terms with order greater than 2 have been neglected during the formulation. If the general case is used in second condition, the second-order error decreases when the $CFLN$ decreases. The error terms with the order of cell size larger than two become dominant. Since the coefficients of the finite difference operator are the same for different methods ($C_1 = 9/8$, $C_2 = -1/24$) when the time-step is reduced to zero, the high-order error of all methods is

$$e_{high-order} = \frac{9}{960} (\cos^6 \theta + \sin^6 \theta) k^6 \Delta^4. \quad (4.27)$$

The details of the formulation can be found in Appendix A and B. In addition, the numerical dispersion errors, when the time-step is reduced to zero, are shown in Table 4.2.

To show the improvement is wide-band and for all $CFLN$, the numerical dispersion errors of different methods with different number of cells per wavelength are plotted in Figure 4.4 and 4.5, when the $CFLN$ is equal to 1 ($C_1 = 765/608$, $C_2 = -157/1824$) and 8 ($C_1 = 1467/152$, $C_2 = -1315/456$), respectively. It can be observed that the LD ADI-

Table 4.2: Numerical dispersion error $(1 - u_p/c)^2$ for $\Delta t \rightarrow 0$.

Δ	Simulated results	Analytical results
$\lambda/50$	0.6581×10^{-12}	0.6558×10^{-12}
$\lambda/100$	0.2571×10^{-14}	0.2550×10^{-14}

FDTD method can provide a constant improvement over the conventional ADI-FDTD method and the LD FDTD method at all frequencies for different $CFLN$.

4.3.3 Simulations and Results

In order to validate the new algorithm, two numerical examples are presented. One of the examples is a uniform mesh free-space model, and the other is a non-uniform mesh inhomogeneous medium model. Both of them are simulated by the conventional ADI-FDTD method and the LD ADI-FDTD method for comparison.

To demonstrate the specified angle case, a free-space model, which is shown in Figure 4.6, for 2-D TE wave propagation with uniform mesh $\Delta = 0.015\text{m}$ and $CFLN = 4$ is simulated. A Gaussian pulse is excited at the center of the computational domain, and the observation points are specially arranged such that the phase velocities at different propagation angles can be calculated. The finite difference operator of the LD ADI-FDTD method is determined in the general case ($C_1 = 495/152, C_2 = -343/456$) and also the specified angle case with $\theta = 45^\circ$ ($C_1 = 29/8, C_2 = -7/8$). The normalized phase velocities with different propagation angles at 500MHz are plotted in Figure 4.7. It can be observed that the curve of the normalized phase velocity of the LD ADI-FDTD method is closer to 1 and flatter than that from the conventional ADI-FDTD method for both cases. For the general case, the mean numerical dispersion error of the LD ADI-FDTD

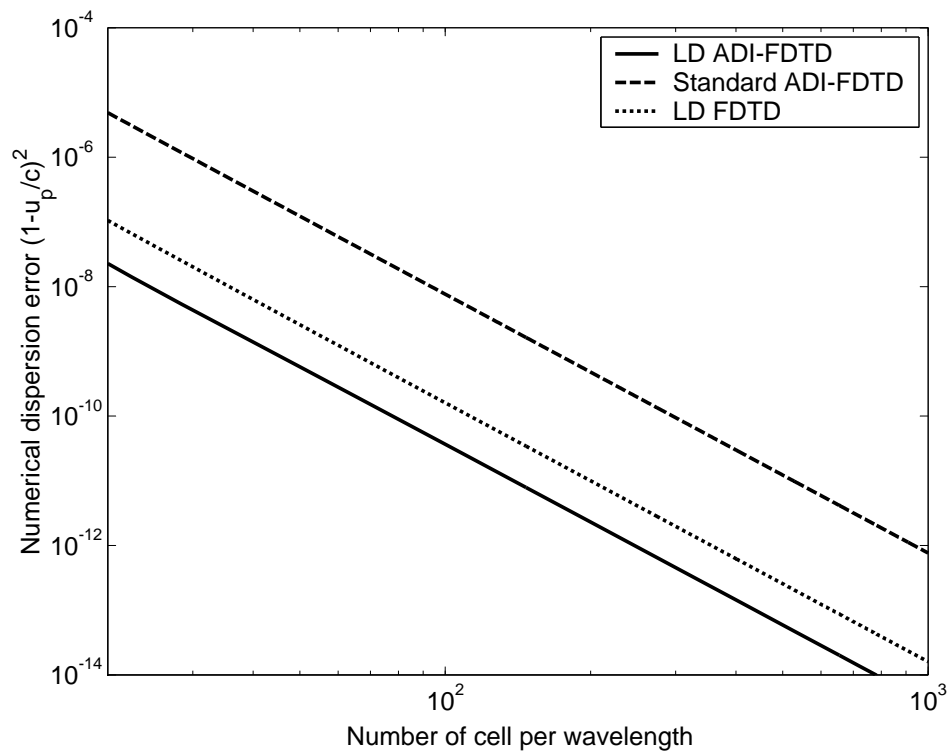


Figure 4.4: Mean absolute numerical dispersion errors of different methods with different mesh resolutions at $CFLN=1$.

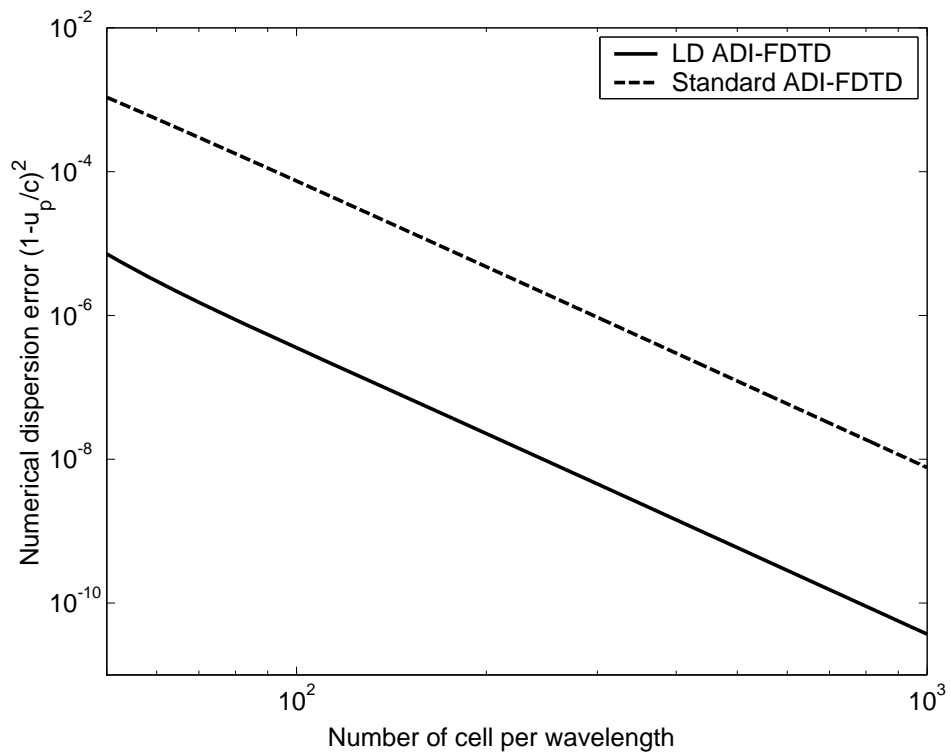


Figure 4.5: Mean absolute numerical dispersion errors of different methods with different mesh resolutions at $CFLN=8$.

method is zero. For the specified angle case, the curve of the LD ADI-FDTD method is shifted, such that the normalized phase velocity at $\theta = 45^\circ$ is closer to 1. This means that the numerical dispersion error at the specified angle is minimum. In addition, the simulation results agree with the theoretical evaluation.

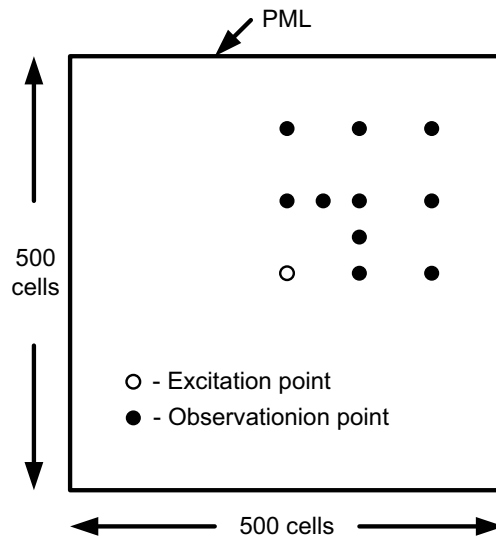


Figure 4.6: 2-D Free space model.

The non-uniform mesh model with a thin dielectric interface with periodic boundary [47] is shown in Figure 4.8. The cell size is set as $50\text{mm} \times 50\text{mm}$ at air and $5\text{mm} \times 50\text{mm}$ at the dielectric medium. The average permittivity is used at the surface of the dielectric medium. The time-step is set as 0.2357 ns , which is 20 times that under the stability condition ($CFLN = 20$). The coefficients of the finite difference operator are determined based on the general case locally. For the fine mesh region, the $CFLN$ equals to 20 and $C_1 = 8271/152, C_2 = -8119/456$. For the coarse mesh region, the $CFLN$ equals to 2 and $C_1 = 63/78, C_2 = -25/114$. A Gaussian pulse is excited at the left boundary and the right boundary is terminated by the PML with the thickness equals to 10 cells. The pulse

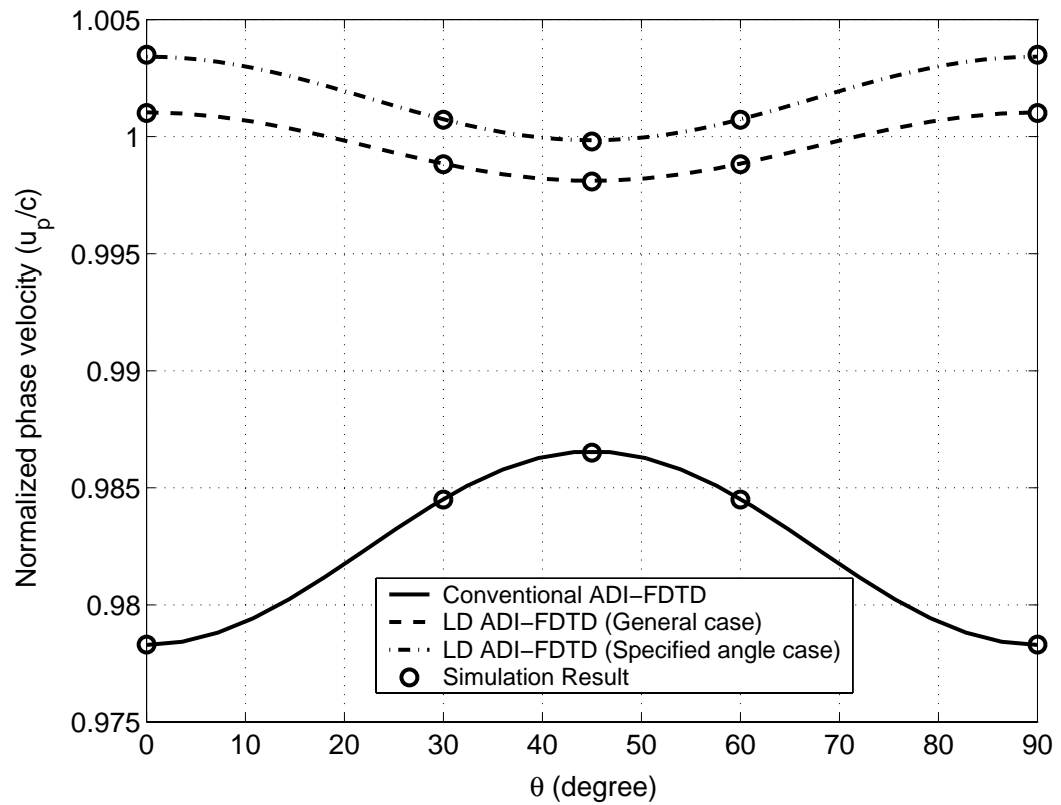


Figure 4.7: Normalized phase velocities of the LD ADI-FDTD method with different propagation angles at 500MHz. ($\Delta = 0.015\text{m}$, $CFLN = 4$, and $\theta = 45^\circ$ for the specified angle case)

propagates in y -direction and normally incidents on the dielectric interface. In addition, the simulation is also carried out using the LD FDTD method and time-step equals to 0.01178 ns for reference. The H_z field at the Observation Point A in time domain is shown in Figure 4.10. It can be observed that the first half of the signal is the incident wave, and the other half is the reflected wave. The signal, which is computed by the conventional ADI-FDTD method, is dispersed much than the other two methods. The results in the LD ADI-FDTD method and the LD FDTD method are in good agreement.

The numerical dispersion errors of different methods are calculated by the first half of the signal, which is the incident wave, from the two observation points and plotted in Figure 4.9. It can be shown that the LD ADI-FDTD method provides a wide-band constant improvement over the fourth-order ADI-FDTD method and the LD FDTD method.

Analytically, the minimum reflected power is operated at 200 MHz for this dielectric interface. By applying Fourier transformation to the reflected wave, the reflected power is computed and shown in Figure 4.11. It is shown that the results from the LD ADI-FDTD method and the LD FDTD method agree very well, and the minimum reflected power is occurred at 199.9 MHz. For the conventional ADI-FDTD method, the minimum reflected power is occurred at 198.5 MHz.

The simulations of the non-uniform mesh model are performed by different methods on the Intel Pentium 4 1.8GHz PC and the simulation programs are written by Matlab. There are 15×1000 non-uniform cells in the computational domain. The cell size mainly is $50\text{mm} \times 50\text{mm}$. Instead, the dielectric interface is modelled by fine mesh with the cell size equals to $50\text{mm} \times 5\text{mm}$. The fine mesh region is allocated about 5% of the total number of cells. The simulation period is 235.6 ns. The computational time and

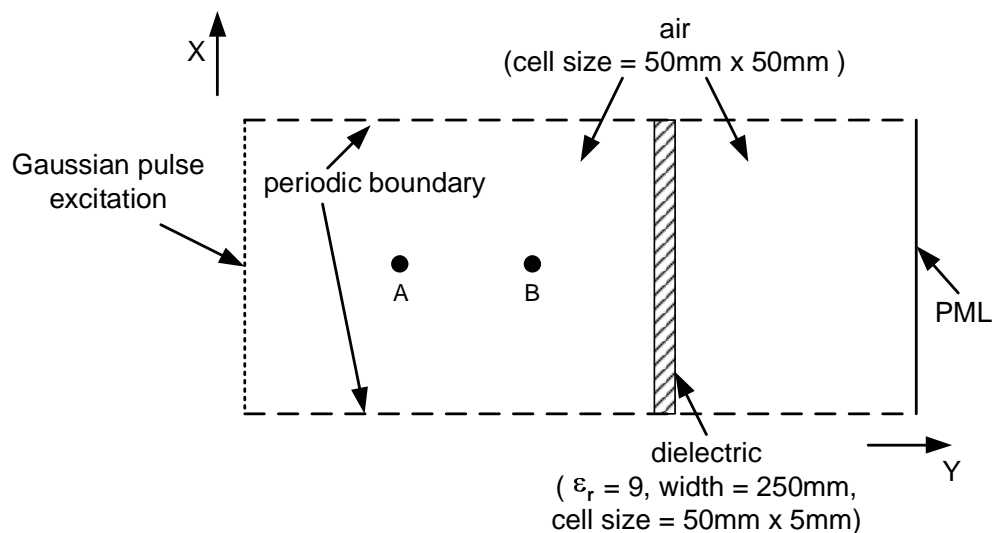


Figure 4.8: The non-uniform mesh model with a thin dielectric interface.

simulation results for different methods are shown in Table 4.3. It can be found that the total number of iterations of the ADI-FDTD method is 1/20 of that of the FDTD method. In addition, the computational time is reduced to about 30% that of the FDTD method. Furthermore, since the ADI-FDTD method is a two-step method, the number of samples in time domain is double of the number of iterations.

Table 4.3: Comparison of the non-uniform mesh model simulation results.

Simulation method	Δt (ns)	No. of iterations	CPU time (s)	Result* (MHz)
(2,2) FDTD	0.01178	20000	581.72	199.96
(2,4) LD FDTD	0.01178	20000	637.83	199.97
(2,2) ADI-FDTD	0.2357	1000	168.60	198.52
(2,4) ADI-FDTD	0.2357	1000	201.78	198.53
(2,4) LD ADI-FDTD	0.2357	1000	205.13	199.88

* Frequency of minimum reflected power occurred. (Analytical result = 200MHz)

In addition, the computational time of the two different (2,4) ADI-FDTD methods is

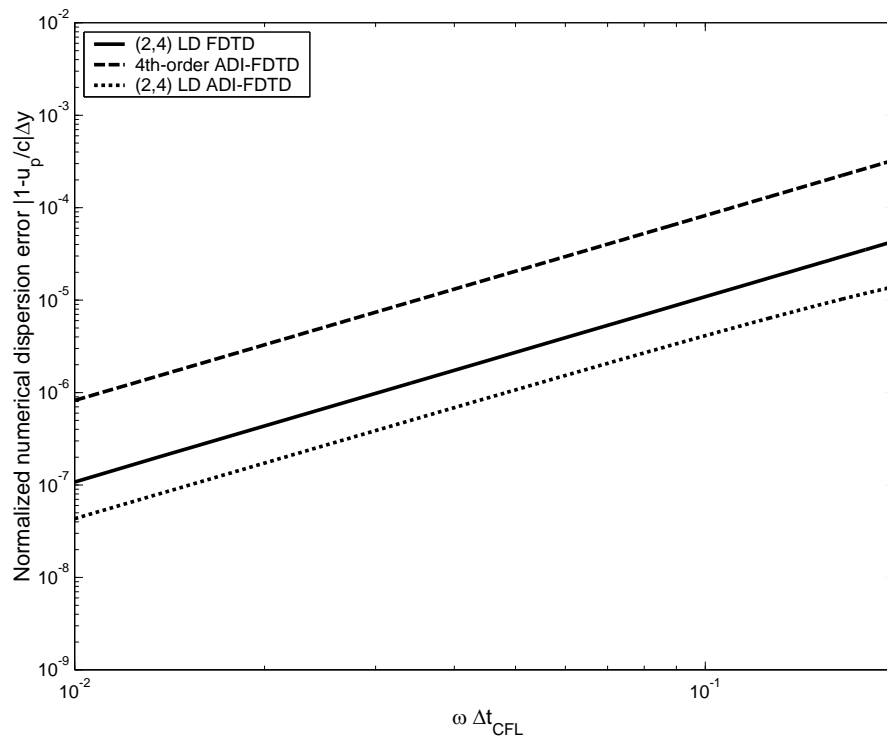


Figure 4.9: Numerical dispersion errors of different methods which are calculated by the simulation results.

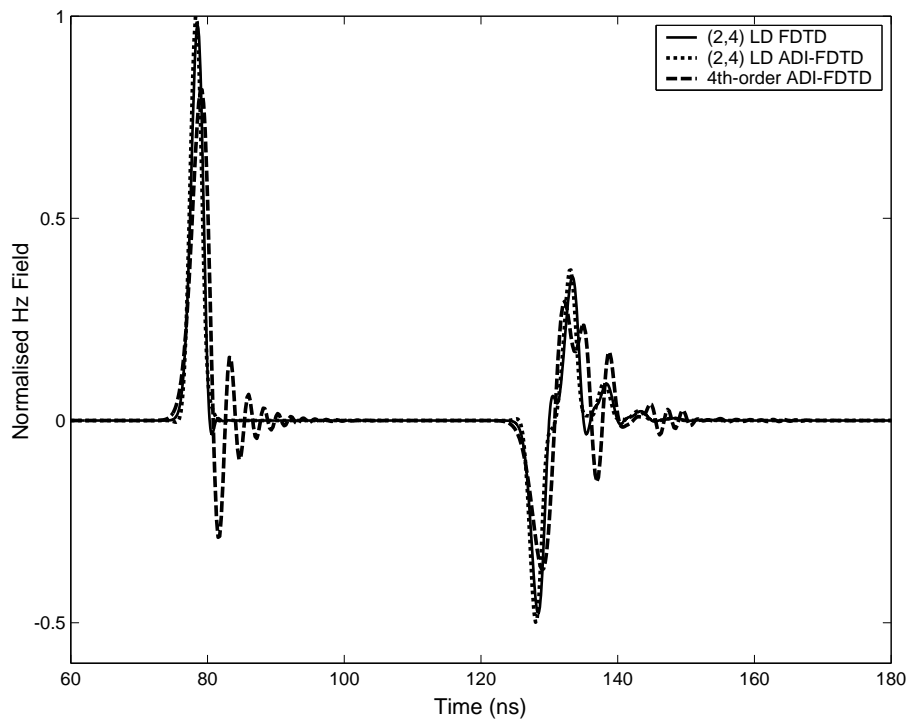


Figure 4.10: H_z field at the observation point in time domain.

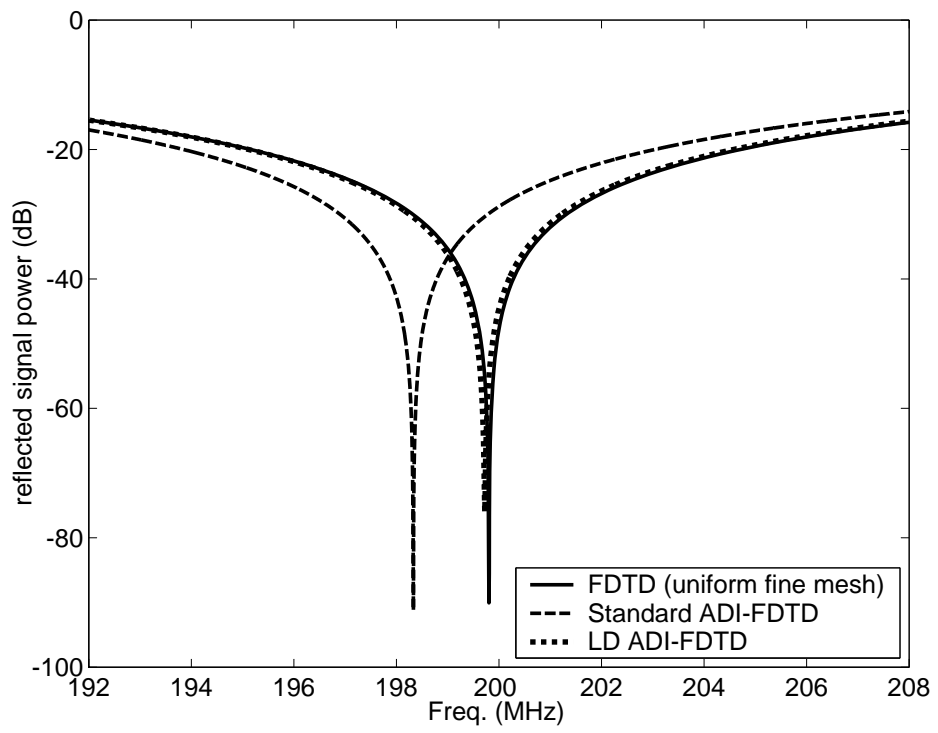


Figure 4.11: Reflected signal power.

about 15% more than that of the conventional (2,2) ADI-FDTD method. This is because the square matrix of the equations system to be solved for the conventional (2,2) ADI-FDTD method is a tri-diagonal matrix and that for the (2,4) ADI-FDTD method is a hepta-diagonal matrix, which has seven diagonal non-zero components. However, both of them are still sparse matrix since the matrix size is $N \times N$, where N is the number of rows of the computational domain. For this simulation, the largest square matrix to be solved is 1000×1000 .

Table 4.4: Computational complexities of solving different equations systems by the *LU* method.

Simulation method	Style of square matrix	Computational complexity (\times , $+$)*	
		<i>LU</i> factorization	Forward- & back-substitution
(2,2) ADI-FDTD	Tri-diagonal	$(2N, N)$	$(3N, N)$
(2,4) ADI-FDTD	Hepta-diagonal	$(12N, 9N)$	$(7N, 6N)$

* \times - number of multiplications

+ - number of additions

There are many methods to solve the equations system, and the *LU* method [48] is used in this simulation. The *LU* method includes three procedures: the *LU* factorization, forward-substitution, and back-substitution. Table 4.4 shows the computational complexities of solving different equations systems. For the *LU* factorization, the number of numerical operations needed for the hepta-diagonal matrix system is 7 times that for the tri-diagonal matrix system. However, the components in the diagonal matrix are the function of the material constant, cell-size and time-step—which are constant during the simulation—the *LU* factorization is calculated only once before the iteration process. For

the forward- and back-substitution, the number of numerical operations needed for the hepta-diagonal matrix system is about 3 times that of the tri-diagonal matrix system, but it is still order of N .

To reduce the computational time, parallel-computing is one of the most common methods used for the FDTD method. It computes individual cells by different processes simultaneously. For ADI-FDTD method, only the field components—which are not computed by solving the equations system—can use the similar scheme. Therefore, one of three field components for 2-D case and three of six field components for 3-D case cannot use the parallel-computing in form of individual cells, but they can use it in form of individual rows or columns. This is because those equation systems are formulated from individual rows or columns.

4.4 Conclusion

The (2,4) low numerical dispersion ADI-FDTD method is developed in this chapter. It is based on the (2,4) fourth-order ADI-FDTD method and the finite difference operator is determined by minimizing the errors terms, which are caused by approximating the spatial derivatives and temporal derivatives with finite difference scheme, in the numerical dispersion relation. The new method provides a wide-band error reduction of about 99.5% as compared to the conventional ADI-FDTD method. In addition, the error of the new method is only a quarter that of the LD FDTD method.

For the LD ADI-FDTD method, we need to solve an equations system with hepta-diagonal matrix, and more computational time is required. However, the complexity is still order of N for a $N \times N$ matrix when the LU method is used. In addition, in the

2-D non-uniform mesh simulation example, the LD ADI-FDTD method spends only 15% more computational time to have a much accurate result as compared to the conventional ADI-FDTD method.

Chapter 5

Conclusion and Future Works

5.1 Conclusion

The ADI-FDTD method has become attractive because of its unconditionally stable property. It is very useful for a non-uniform mesh model with small dimensional structure. This is because, for the conventional FDTD method, the size of the time-step is bounded by the smallest cell size. The required computational resources become very large when small time-step is used. When the ADI-FDTD method is applied, the time-step can be set to the desired value, and the required computational resources can be reduced. However, there is a drawback in that the numerical dispersion error increases when the ADI technique is applied. Besides, larger time-step results larger numerical dispersion error. To enhance the usefulness and effectiveness of the ADI-FDTD method, two modified ADI-FDTD method are developed to reduce the numerical dispersion error.

The first one is the high-order ADI-FDTD method. The multi-points high-order central difference scheme is applied to approximate the spatial derivatives of the ADI-FDTD

method. It is proved, analytically and practically, that the method is still unconditionally stable when the high-order central difference scheme is applied. In addition, it is found that the numerical dispersion error is reduced. Furthermore, the numerical dispersion error is very close to the accuracy limit of the conventional ADI-FDTD method for a given time-step when the sixth-order central difference scheme is applied. However, when the chosen time-step is much larger than that under the stability condition, the improvement becomes relatively insignificant. This is because the high-order scheme can only reduce the numerical dispersion error, which is caused by approximating the spatial derivatives but not the temporal derivatives. This reason motivates the development of the second method.

The second method is the (2,4) low numerical dispersion (LD) ADI-FDTD method. It is based on the fourth-order (2,4) ADI-FDTD method. The coefficients of the finite difference operator are determined by minimizing the error terms in the numerical dispersion relation but not in the approximation formula of the individual derivative. Since the stability condition of the high-order ADI-FDTD method is not affected by the coefficients of the finite difference operator, the LD ADI-FDTD method is unconditionally stability. From the numerical analysis and simulation results, it is shown that the LD ADI-FDTD method provides a wide-band error reduction of about 99.5% for any time-step when compared to the conventional ADI-FDTD method. In addition, the error of the LD ADI-FDTD method is only a quarter that of the LD FDTD method. Furthermore, there is an alternative method that can reduce numerical dispersion error at a specified propagation angle.

For the LD ADI-FDTD method, we need to solve an equations system with hepta-

diagonal matrix. The required computational time is longer than that of the conventional ADI-FDTD method. However, the complexity is still order of N , where N is the length of the computational domain, when the LU method is used. In addition, the LU factorization is calculated only once before the iteration process. This is because the components in the square matrix are the function of the cell size, time-step and material constants, which are constant in the simulation.

5.2 Future Works and Discussion

5.2.1 (2,4) LD ADI-FDTD Method with PML

In open-region problem simulations, absorbing boundary conditions (ABC) are needed to terminate the boundary for the FDTD, ADI-FDTD or LD ADI-FDTD method. There are many research studies [39]-[44] on applying perfectly matched layer (PML) as ABC for the ADI-FDTD method, but most of the simulations are in free-space, small structure, and observing near the PML. Therefore, it does not require too much iteration. Recently, some researchers [49]-[50] find that the ADI-FDTD open-region simulation will be unstable when more iterations are run. In addition, it is demonstrated that the ADI-FDTD method with PML is unstable at [51]. Similar problem is found when the PML is applied to the LD ADI-FDTD method.

The LD ADI-FDTD method is applied to simulate a photonic band structure, which presents in [52]. The non-uniform mesh is used, and the fine mesh is applied at the area with the tube. The time-step is 1.18 ns, and the other configurations of the simulation are shown in Figure 5.1. We run the iteration 1750 times, and 3500 samples are taken.

Figure 5.2 shows the E_z fields at the observation point. It can be found that the system becomes unstable after 3000 samples are taken when the incident wave already passed the observation point and is absorbed by the PML. By the data before instability occurred, the transmission coefficient in dB is calculated and plotted in Figure 5.3. It is shown that the results are close to the measured results.

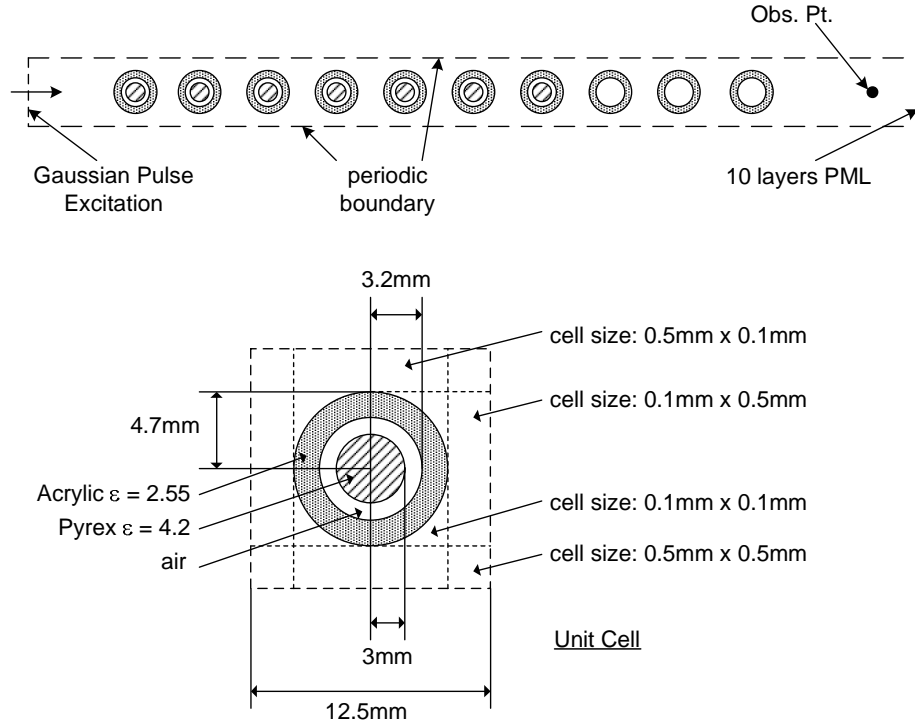


Figure 5.1: Photonic band structure.

One of the possible reasons to cause the instability is that the LD ADI-FDTD and PML region are computed by different sets of equations. The difference of their characteristic generates a small error at the interface between the two regions. In addition, the condition numbers of equations systems in the simulation are between 9322-19648, which are defined as ill-conditioned [48] and which have a large effect on the solution when there is a small error in the coefficients or in the solution process. In the future, the solutions for the instability of the open-region LD ADI-FDTD or ADI-FDTD simulation with ABC are

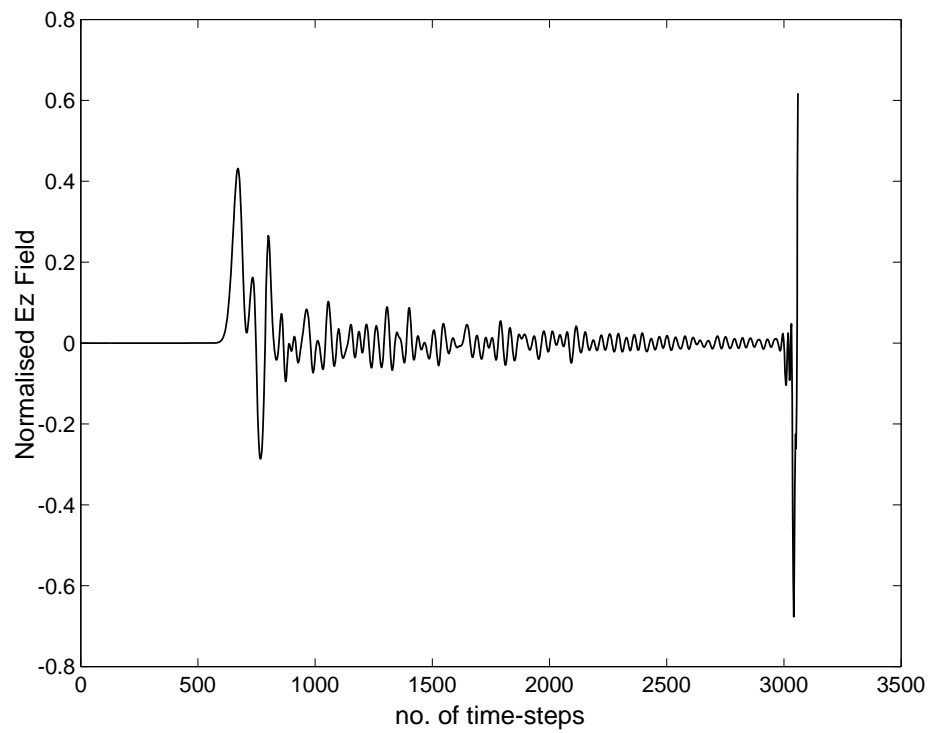


Figure 5.2: Time domain results of the photonic band structure simulation.

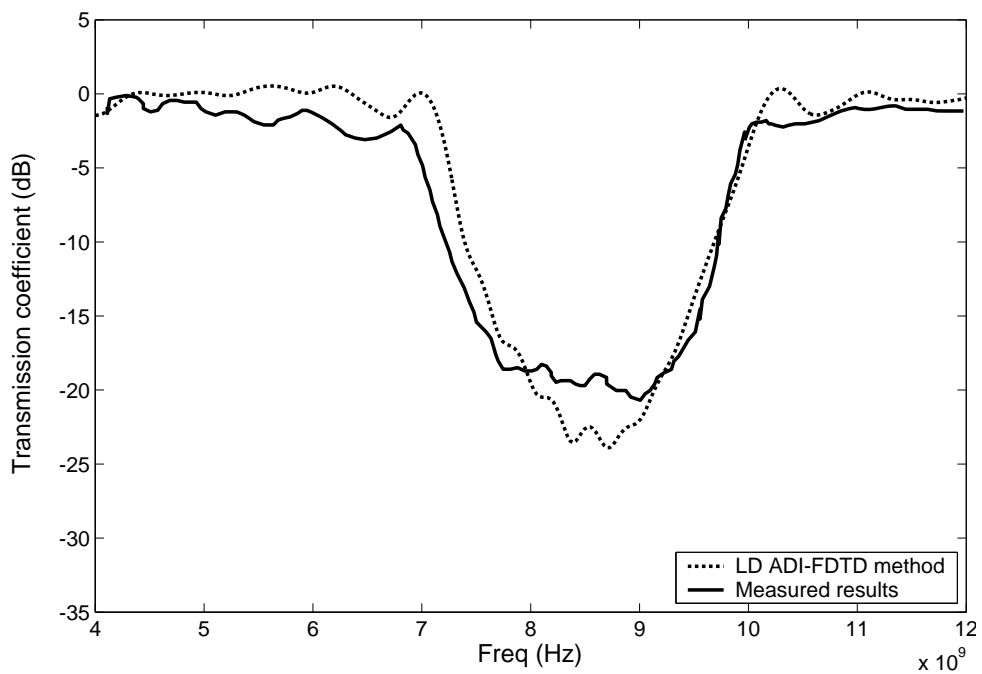


Figure 5.3: Transmission coefficients of the photonic band structure.

valuable research topics.

5.2.2 Modified LD ADI-FDTD Method

Applying the LD ADI-FDTD Method within a Sub-Gridded Model

In most of the structures, only small parts require fine mesh to model. Therefore, it can use sub-gridding scheme, shown in Figure 5.4, to model the structure.

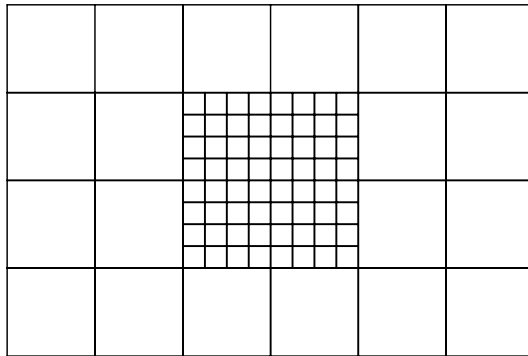


Figure 5.4: Sub-gridding scheme.

With this kind of structure, we can use the conventional FDTD method to compute the coarse region and use the LD ADI-FDTD method in the fine region with a same time-step. It can greatly reduce the size of the computational region of ADI method, which requires paying extra computational cost for the implicit method.

However, an extra error is introduced when the interfaces between the fine and coarse regions are calculated by spatial and temporal interpolation. The temporal interpolation is also required—and even the same time-step is used in both regions—because the leapfrog algorithm is used in the FDTD method but not in the LD ADI-FDTD method. In addition, computing the two regions by different equations will lead to instability, which likens the ADI-FDTD method to PML.

Non-Orthogonal Gridding

To model some structures, it is more convenient for using non-orthogonal grid, such as cylindrical coordinate, to model than the rectangular grid. It was shown that the ADI-FDTD method can be applied to the cylindrical coordinate system [53]. According to the updating equations in [53], the numerical dispersion relation of the ADI-FDTD method in the cylindrical coordinate system can be formulated, and we can devise the low numerical dispersion algorithm for it from this relation, as described in the previous chapter.

Appendix A

Analysis of the Numerical Dispersion Relation of the (2,4) FDTD Method

The numerical dispersion relation of the 2-D (2,4) FDTD method for TE wave in free space is found as

$$\sin^2\left(\frac{\omega\Delta t}{2}\right) = S_x^2 + S_y^2, \quad (\text{A.1})$$

where

$$S_x = \frac{c\Delta t}{\Delta x} \left[C_1 \sin\left(\frac{\widetilde{k}_x\Delta x}{2}\right) + C_2 \sin\left(\frac{3\widetilde{k}_x\Delta x}{2}\right) \right], \quad (\text{A.2})$$

$$S_y = \frac{c\Delta t}{\Delta y} \left[C_1 \sin\left(\frac{\widetilde{k}_y\Delta y}{2}\right) + C_2 \sin\left(\frac{3\widetilde{k}_y\Delta y}{2}\right) \right], \quad (\text{A.3})$$

and c is the speed of light, and \widetilde{k}_x and \widetilde{k}_y are numerical wavenumbers in the x and y directions, respectively. For a propagation angle θ , the numerical wavenumbers can be written as $\widetilde{k}_x = \widetilde{k} \cos \theta$, $\widetilde{k}_y = \widetilde{k} \sin \theta$.

To analyze the numerical dispersion relation, it is assumed that the numerical wavenumber is equal to the theoretical one, in which $\widetilde{k} = k = \omega/c$. In addition, uniform square cell is assumed ($\Delta x = \Delta y = \Delta$). Furthermore, with regard to the 2-D FDTD method,

the maximum time-step under the Courant-Friedrich-Levy (CFL) stability condition is defined as

$$\Delta t_{CFL} = \frac{\Delta}{c\sqrt{2}} \quad (\text{A.4})$$

and a ratio of time-step is defined as

$$CFLN = \frac{\Delta t}{\Delta t_{CFL}}. \quad (\text{A.5})$$

Therefore, the relation of the cell size and the time-step can be written as

$$\Delta t = CFLN \frac{\Delta}{c\sqrt{2}}. \quad (\text{A.6})$$

Then, the trigonometric terms in (A.1) are expanded using the Taylor series

$$\sin x = \sum_{n=0}^{\infty} (-1)^n \frac{x^{2n+1}}{(2n+1)!} = x - \frac{x^3}{3!} + \frac{x^5}{5!} - + \dots \quad (\text{A.7})$$

The numerical dispersion relation (A.1) becomes

$$\begin{aligned} LHS &= \left(\frac{\omega\Delta t}{2}\right)^2 - \frac{1}{3}\left(\frac{\omega\Delta t}{2}\right)^4 + \frac{2}{45}\left(\frac{\omega\Delta t}{2}\right)^6 + \dots, \\ RHS &= c^2\Delta t^2 \left\{ \begin{aligned} &(C_1 + 3C_2)^2 \frac{k^2}{4} - (C_1 + 3C_2)(C_1 + 27C_2) (\cos^4\theta + \sin^4\theta) \frac{k^4\Delta^2}{48} \\ &+ \left[\frac{(C_1+3C_2)(C_1+243C_2)}{3840} + \frac{(C_1+27C_2)^2}{48^2} \right] (\cos^6\theta + \sin^6\theta) k^6\Delta^4 + \dots \end{aligned} \right\}. \end{aligned} \quad (\text{A.9})$$

Then, we neglect the terms with the order greater than 2 and replace Δt with Δ by (A.6).

The numerical dispersion relation of the (2,4) FDTD method becomes

$$\frac{\omega^2}{c^2} = (C_1 + 3C_2)^2 k^2 - (C_1 + 3C_2)(C_1 + 27C_2) (\cos^4\theta + \sin^4\theta) \frac{k^4\Delta^2}{12} + \frac{CFLN^2 k^4 \Delta^2}{24}. \quad (\text{A.10})$$

To guarantees the second-order accuracy, the first condition, which is used to determine the coefficients, can be written as

$$C_1 + 3C_2 = 1. \quad (\text{A.11})$$

The second-order terms in the numerical dispersion relation (A.10) are defined as the error of k^2 and can be written as

$$e = -(C_1 + 3C_2)(C_1 + 27C_2) \left(\cos^4 \theta + \sin^4 \theta \right) \frac{k^4 \Delta^2}{12} + \frac{CFLN^2 k^4 \Delta^2}{24}. \quad (\text{A.12})$$

Then, the mean square error over all angles is calculated according to

$$\overline{e^2} = \frac{1}{2\pi} \int_0^{2\pi} e(\theta)^2 d\theta, \quad (\text{A.13})$$

and the second condition can be formulated by minimizing the mean square error as

$$C_1 + 27C_2 = \frac{12}{19} CFLN^2. \quad (\text{A.14})$$

The C_1 and C_2 can be determined for a given $CFLN$ by combining the two conditions.

In addition, the numerical dispersion error of the LD-FDTD method can be rewritten by substituting the two conditions (A.11),(A.14) into (A.12) as

$$e_{LD-FDTD} = CFLN^2 k^4 \Delta^2 \left(\frac{1}{456} - \frac{1}{76} \cos 4\theta \right), \quad (\text{A.15})$$

where the trigonometric function is simplified.

Furthermore, the fourth-order terms in the numerical dispersion relation (A.1) are defined as

$$e_{high-order} = \left[\frac{(C_1 + 3C_2)(C_1 + 243C_2)}{960} + \frac{(C_1 + 27C_2)^2}{576} \right] (\cos^6 \theta + \sin^6 \theta) k^6 \Delta^4 - \frac{CFLN^4 k^6 \Delta^4}{1440}. \quad (\text{A.16})$$

The high-order error term dominates when the time-step is very small. Therefore, when $CFLN$ trends to zero, $C_1 = 9/8$, $C_2 = -1/24$ and the high-order error term becomes

$$e_{high-order} = \frac{9}{960} (\cos^6 \theta + \sin^6 \theta) k^6 \Delta^4. \quad (\text{A.17})$$

Appendix B

Analysis of the Numerical

Dispersion Relation of the (2,4)

ADI-FDTD Method

The numerical dispersion relation of the 2-D (2,4) ADI-FDTD method for TE wave in free-space is found as

$$\tan^2\left(\frac{\omega\Delta t}{2}\right) = S_x^2 + S_y^2 + S_x^2 S_y^2, \quad (\text{B.1})$$

where

$$S_x = \frac{c\Delta t}{\Delta x} \left[C_1 \sin\left(\frac{\widetilde{k}_x \Delta x}{2}\right) + C_2 \sin\left(\frac{3\widetilde{k}_x \Delta x}{2}\right) \right], \quad (\text{B.2})$$

$$S_y = \frac{c\Delta t}{\Delta y} \left[C_1 \sin\left(\frac{\widetilde{k}_y \Delta y}{2}\right) + C_2 \sin\left(\frac{3\widetilde{k}_y \Delta y}{2}\right) \right], \quad (\text{B.3})$$

and c is the speed of light, and \widetilde{k}_x and \widetilde{k}_y are numerical wavenumbers in the x and y directions, respectively. For a propagation angle θ , the numerical wavenumbers can be written as $\widetilde{k}_x = \widetilde{k} \cos \theta$, $\widetilde{k}_y = \widetilde{k} \sin \theta$.

To analyze the numerical dispersion relation, it is assumed that the numerical wavenumber is equal to the theoretical one, in which $\tilde{k} = k = \omega/c$. In addition, uniform square cell is assumed ($\Delta x = \Delta y = \Delta$). Furthermore, with regard to the 2-D FDTD method, the maximum time-step under the Courant-Friedrich-Levy (CFL) stability condition is defined as

$$\Delta t_{CFL} = \frac{\Delta}{c\sqrt{2}} \quad (\text{B.4})$$

and a ratio of time-step is defined as

$$CFLN = \frac{\Delta t}{\Delta t_{CFL}}. \quad (\text{B.5})$$

Therefore, the relation of the cell size and the time-step can be written as

$$\Delta t = CFLN \frac{\Delta}{c\sqrt{2}}. \quad (\text{B.6})$$

Then, the trigonometric terms in (B.1) are expanded using the Taylor series

$$\sin x = \sum_{n=0}^{\infty} (-1)^n \frac{x^{2n+1}}{(2n+1)!} = x - \frac{x^3}{3!} + \frac{x^5}{5!} - + \dots, \quad (\text{B.7})$$

$$\tan x = \sum_{n=1}^{\infty} \frac{B_{2n} (-4)^n (1-4^n)}{(2n!)} x^{2n-1} = x + \frac{x^3}{3} + \frac{2x^5}{15} + \dots, \quad (\text{B.8})$$

where the B is the Bemoulli number.

The numerical dispersion relation (B.1) becomes

$$LHS = \left(\frac{\omega\Delta t}{2}\right)^2 + \frac{2}{3}\left(\frac{\omega\Delta t}{2}\right)^4 + \frac{17}{45}\left(\frac{\omega\Delta t}{2}\right)^6 + \dots, \quad (\text{B.9})$$

$$RHS = c^2 \Delta t^2 \left\{ \begin{array}{l} (C_1 + 3C_2)^2 \frac{k^2}{4} - (C_1 + 3C_2)(C_1 + 27C_2) (\cos^4 \theta + \sin^4 \theta) \frac{k^4 \Delta^2}{48} \\ + \left[\frac{(C_1 + 3C_2)(C_1 + 243C_2)}{3840} + \frac{(C_1 + 27C_2)^2}{48^2} \right] (\cos^6 \theta + \sin^6 \theta) k^6 \Delta^4 \\ + \dots \end{array} \right\}$$

$$+c^4 \Delta t^4 \left\{ \begin{array}{l} + \frac{(C_1+3C_2)^4}{16} (\cos^2 \theta \sin^2 \theta) k^4 \\ - \frac{(C_1+3C_2)^3(C_1+27C_2)}{192} (\cos^2 \theta \sin^4 \theta + \cos^4 \theta \sin^2 \theta) k^6 \Delta^2 \\ + \dots \end{array} \right\}. \quad (\text{B.10})$$

Then, we neglect the terms with the order greater than two and replace Δt with Δ by (B.6). The numerical dispersion relation of the (2,4) ADI-FDTD method becomes

$$\begin{aligned} \frac{\omega^2}{c^2} &= (C_1 + 3C_2)^2 k^2 - (C_1 + 3C_2)(C_1 + 27C_2) \frac{(\cos^4 \theta + \sin^4 \theta) k^4 \Delta^2}{12} \\ &+ \left((C_1 + 3C_2)^4 \frac{\cos^2 \theta \sin^2 \theta}{8} - \frac{1}{12} \right) CFLN^2 k^4 \Delta^2. \end{aligned} \quad (\text{B.11})$$

To guarantee the second-order accuracy, the first condition, which is used to determine the coefficients, can be written as

$$C_1 + 3C_2 = 1. \quad (\text{B.12})$$

The second-order terms in the numerical dispersion relation (B.11) are defined as the error of k^2 and can be written as

$$e = \left[\left(\frac{3}{2} \sin^2 \theta \cos^2 \theta - 1 \right) CFLN^2 - (C_1 + 27C_2) (\cos^4 \theta + \sin^4 \theta) \right] \frac{k^4 \Delta^2}{12}. \quad (\text{B.13})$$

Then, the second condition, which is used to determine the coefficients, can be formulated by setting the error to zero for a given propagation angle as

$$\left(\frac{3}{2} \sin^2 \theta \cos^2 \theta - 1 \right) CFLN^2 - (C_1 + 27C_2) (\cos^4 \theta + \sin^4 \theta) = 0. \quad (\text{B.14})$$

In addition, it can calculate the mean square error over all angles according to

$$\overline{e^2} = \frac{1}{2\pi} \int_0^{2\pi} e(\theta)^2 d\theta, \quad (\text{B.15})$$

and then the second condition can be formulated by minimizing the mean square error as

$$C_1 + 27C_2 = -\frac{81}{76} CFLN^2. \quad (\text{B.16})$$

The C_1 and C_2 can be determined for a given $CFLN$ by combining the first condition and either one of the second condition.

Besides, numerical dispersion error of the (2,4) LD ADI-FDTD method can be re-written by substituting the two conditions (B.12),(B.16) into (B.13) as

$$e_{LD-ADI} = CFLN^2 k^4 \Delta^2 \left(-\frac{1}{912} + \frac{1}{152} \cos 4\theta \right), \quad (\text{B.17})$$

where the trigonometric function is simplified.

Furthermore, the fourth-order terms in the numerical dispersion relation (B.1) are defined as

$$\begin{aligned} e_{high-order} = & \left[\frac{(C_1 + 3C_2)(C_1 + 243C_2)}{960} + \frac{(C_1 + 27C_2)^2}{576} \right] (\cos^6 \theta + \sin^6 \theta) k^6 \Delta^4 \\ & - \frac{(C_1 + 3C_2)^3 (C_1 + 27C_2)}{384} (\cos^2 \theta \sin^4 \theta + \cos^4 \theta \sin^2 \theta) CFLN^2 k^6 \Delta^4 \\ & - \frac{17}{2880} CFLN^4 k^6 \Delta^4. \end{aligned} \quad (\text{B.18})$$

The high-order error term dominates when the time-step is very small. Therefore, when $CFLN$ trends to zero, $C_1 = 9/8$, $C_2 = -1/24$ and the high-order error term becomes

$$e_{high-order} = \frac{9}{960} (\cos^6 \theta + \sin^6 \theta) k^6 \Delta^4. \quad (\text{B.19})$$

Bibliography

- [1] David K. Cheng, *Field and Wave Electromagnetics*, Addison Wesley, Second Edition, pp. 307-347, 1989.
- [2] Matthew N. O. Sadiku, *Numerical Techniques in Electromagnetics*, CRC Press, Second Edition, 2001.
- [3] R. F. Harrington, *Field Computation by Moment Methods*, Macmillan, 1968.
- [4] H. Nakano, S. R. Kerner and N. G. Alexopoulos, "The Moment Method Solution for Printed Wire Antennas of Arbitrary Configuration," *IEEE Trans. Antennas and Propagat.*, vol. 36, pp. 1667-1637, Dec. 1988.
- [5] A. Kgalil. A. B. Yakovlev and M. B. Steer, "Efficient Method of Moments Formulation for the Modeling Planar Conductive Layers in a Shielded Guided-Wave Structure," *IEEE Trans. Microwave Theory and Tech.*, vol. 47, pp. 1730-1736, Sept. 1999.
- [6] P. B. Johns and R. L. Beurle, "Numerical Solution of Two-Dimensional Scattering Problems Using a Transmission Line Matrix," *IEEE Proc.*, vol. 118, pp. 1203-1208, 1971.

- [7] K. S. Yee, "Numerical Solution of initial boundary value problems involving Maxwell's equations in isotropic medium," *IEEE Trans. Antennas and Propagat.*, vol. 14, pp. 302-307, May 1966.
- [8] A. Taflove, *Computational Electrodynamics: The Finite-Difference Time-Domain Method*, Artech House, 1995.
- [9] A. Taflove, *Advance in Computational Electrodynamics: The Finite-Difference Time-Domain Method*, Artech House, 1998.
- [10] J. Fang, "Time domain computation for Maxwell's equations," Ph.D dissertation, Univ. California at Berkeley, Berkeley, CA, 1989.
- [11] M. N. O. Sadiku, S. O. Agbo and V. Bommel, "Stability Criterion for Finite-Difference Time-Domain Algorithm," *IEEE Southeastcon'90 Proc.*, vol. 1, pp. 1-4, Apr. 1990.
- [12] M. Krumpholz and L. P. B. Katehi, "New Prospects for Time Domain Analysis," *IEEE Microwave Guided Wave Lett.*, vol. 5, pp. 382-384, Nov. 1995.
- [13] M. Krumpholz and L. P. B. Katehi, "MRTD: New Time Domain Schemes based on Multiresolution Analysis," *IEEE Trans. Microwave Theory and Tech.*, vol. 44, pp. 555-571, Apr. 1996.
- [14] T. Namiki, "A New FDTD Algorithm based on Alternating-Direction Implicit Method," *IEEE Trans. Microwave Theory and Tech.*, vol. 47, pp. 2003-2007, Oct. 1999.

- [15] T. Namiki and K. Ito, "Numerical simulation using ADI-FDTD method to estimate shielding effectiveness of thin conductive enclosures," *IEEE Trans. Microwave Theory and Tech.*, vol. 49, pp. 1060-1066, Jun. 2001.
- [16] T. Namiki and K. Ito, "Numerical simulation of microstrip resonators and filters using the ADI-FDTD method," *IEEE Trans. Microwave Theory and Tech.*, vol. 49, pp. 665-670, Apr. 2001.
- [17] G. Sun and C. W. Trueman, "Some Fundamental Characteristics of the One-Dimensional Alternate-Direction-Implicit Finite-Difference Time-domain Method," *IEEE Trans. Microwave Theory and Tech.*, vol. 52, pp. 46-52, Jan. 2004.
- [18] A. P. Zhao, "Two Special Notes on the implementation of the Unconditionally Stable ADI-FDTD Method," *Microwave and Optical Tech. Letters*, vol. 33, pp. 273-277, May 2002.
- [19] T. Namiki, "3-D ADI-FDTD Method - Unconditionally Stable Time-Domain Algorithm for Solving Full Vector Maxwell's Equations," *IEEE Trans. Microwave Theory and Tech.*, vol. 48, pp. 1743-1748, Oct. 2000.
- [20] F. Zheng, Z. Chen and J. Zhang, "Toward the Development of a Three-Dimensional Unconditionally Stable Finite-Difference Time-Domain Method," *IEEE Trans. Microwave Theory and Tech.*, vol. 48, pp. 1550-1558, Sept. 2000.
- [21] G. Sun and C. W. Trueman, "Analysis and Numerical Experiments on the Numerical Dispersion of Two-Dimensional ADI-FDTD," *IEEE Antennas and Wireless Propagat. Letters*, vol. 2, pp. 78-81, Jul. 2003.

- [22] F. Zheng and Z. Chen, "Numerical dispersion analysis of the unconditionally stable 3-D ADI-FDTD method," *IEEE Trans. Microwave Theory and Tech.*, vol. 49, pp. 1006-1009, May 2001.
- [23] T. Namiki and K. Ito, "Investigation of Numerical Errors of the Two-Dimensional ADI-FDTD Method," *IEEE Trans. Microwave Theory and Tech.*, vol. 48, pp. 1950-1956, Nov. 2000.
- [24] S. Ju and H. Kim, "Investigation of an Unconditionally Stable Compact 2D ADI-FDTD Algorithm: Formulations, Numerical Stability, and Numerical Dispersion," *IEEE Antennas and Propagat. Society International Symp.*, vol. 3, pp. 16-21, Jun. 2002.
- [25] E. Turkel and A. Yefet, "On the construction of a high order difference scheme for complex domains in a Cartesian grid," *Applied Numerical Mathematics*, vol. 33, pp. 113-124, 2000.
- [26] A. Yefet and E. Turkel, "Fourth order compact implicit method for the Maxwell equations with discontinuous coefficients," *Applied Numerical Mathematics*, vol. 33, pp. 125-134, 2000.
- [27] T. Namiki and K. Ito, "Accuracy Improvement Technique applied to Non-uniform FDTD cells using high-order implicit scheme," *IEEE Antennas and Propagat. Society International Symp.*, vol. 1, pp.56-59, 2001.
- [28] W. Y. Tam, "Comments on New Prospects for Time Domain Analysis", *IEEE Microwave and Guided wave Letters*, vol. 6, pp. 422, Nov. 1996.

- [29] J. Zhang and Z. Chen, "Low-dispersive Super High-order FDTD schemes," *IEEE Antennas and Propagat. Society International Symp.*, vol. 3, pp. 1510-1513, 2000.
- [30] J. L. Young, D. Gaitonde and J. J. S. Shang, "Toward the construction of a Fourth-order Difference scheme for Transient EM wave Simulation: Staggered Grid Approach," *IEEE Trans. Antennas and Propagat.*, vol. 45, pp. 1573-1580, Nov. 1997.
- [31] T. T. Zygiridis and T. D. Tsiboukis, "Low-Dispersion Algorithms Based on the Higher Order (2,4) FDTD Method," *IEEE Trans. Microwave Theory and Tech.*, vol. 52, pp. 1321-1327, Apr. 2004.
- [32] T. T. Zygiridis and T. D. Tsiboukis, "A Dispersion-Reduction Scheme for the Higher Order (2,4) FDTD Method," *IEEE Trans. Magnetics*, vol. 40, pp. 1464-1467, Mar. 2004.
- [33] J. P. Berenger, "A Perfectly Matched Layer for the Absorption of Electromagnetic Waves," *Journal of Computat. Phys.*, vol. 114, pp. 185-200, Oct. 1994.
- [34] S. A. Cummer, "A Simple, Nearly Perfectly Matched Layer for General Electromagnetic Media," *IEEE Microwave and Wireless Components Letters*, vol. 13, pp. 128-130, Mar. 2003.
- [35] D. S. Katz, E. T. Thiele and A. Taflove, "Validation and Extension to Three Dimensions of the Berenger PML Absorbing Boundary Condition for FD-TD meshes," *IEEE Microwave and Guided Wave Letters*, vol. 4, pp. 268-270, Aug. 1994.

- [36] M. K. Sun and W. Y. Tam, "An unconditionally stable high-order 2-D ADI-FDTD method," *IEEE Antennas and Propagat. Society International Symp.*, vol.4, pp. 352-355, Jun. 2003.
- [37] M. K. Sun and W. Y. Tam, "Analysis of the Numerical Dispersion of the 2-D ADI-FDTD Method with Higher order scheme," *IEEE Antennas and Propagat. Society International Symp.*, vol.4, pp. 348-351, Jun. 2003.
- [38] M. K. Sun and W. Y. Tam, "Stability and Dispersion analysis of ADI-MRTD and ADI High-order schemes," *Microwave and Optical Tech. Lett.*, vol.45, pp. 43-46, Apr. 2005.
- [39] S. Wang and F. L. Teixeira, "An Efficient PML Implementation for the ADI-FDTD Method," *IEEE Microwave and Wireless Components Letters*, vol. 13, pp. 72-74, Feb. 2003.
- [40] A. P. Zhao, "Comments on An Efficient PML Implementation for the ADI-FDTD Method," *IEEE Microwave and Wireless Components Letters*, vol. 14, pp. 248, May 2004.
- [41] G. Liu and S. D. Gedney, "Perfectly Matched Layer Media for an Unconditionally Stable Three-Dimensional ADI-FDTD method," *IEEE Microwave and Guided Wave Letters*, vol. 10, pp. 261-263, Jul. 2000.
- [42] A. P. Zhao, "Uniaxial Perfectly Matched Layer Media for an Unconditionally Stable 3-D ADI-FD-TD Method," *IEEE Microwave and Wireless Components Letters*, vol. 12, pp. 497-499, Dec. 2002.

- [43] A. Zhu, S. Gedney, G. Liu and J. A. Roden, "A Novel Perfectly Matched Layer Method for An Unconditionally Stable ADI-FDTD Method," *IEEE Antennas and Propagat. Society International Symp.*, vol. 4, pp. 146-149, 2001.
- [44] S. D. Gedney, G. Liu, J. A. Roden and A. Zhu, "Perfectly Matched Layer Media With CFS for an Unconditionally Stable ADI-FDTD Method," *IEEE Trans. Antennas and Propagat.*, vol. 49, pp. 1554-1558, Nov. 2001.
- [45] X. Zhang, J. Fang and K. K. Mei, "Calculations of the Dispersive Characteristics of Microstrips by the Time Domain Finite Difference Method," *IEEE Trans. Microwave Theory and Tech.*, vol. 36, pp. 263-266, Feb. 1988.
- [46] M. K. Sun and W. Y. Tam, "Low Numerical Dispersion Two-Dimensional (2,4) ADI-FDTD Method," *IEEE Trans. Antennas and Propagat.*, vol. 54, pp. 1041-1044, Mar. 2006.
- [47] S. Wang, J. Chen and P. Ruchhoeft, "An ADI-FDTD Method for Periodic Structure," *IEEE Trans. Antennas and Propagat.*, vol. 58, pp. 2343-2346, Jul. 2005.
- [48] E. Kreyszig, *Advanced Engineering Mathematics*, John Wiley & Sons, Seventh Edition, 1993.
- [49] M. H. Kermani, X. Wu and O. M. Ramahi, "Instable ADI-FDTD Open-Region Simulation," *IEEE Antennas and Propagat. Society International Symp.*, vol. 1, pp. 595-598, Jun. 2004.

- [50] M. H. Kermani and O. M. Ramahi, "Unstable 3D ADI-FDTD Open-Region Simulation," *IEEE Antennas and Propagat. Society International Symp.*, vol. 1b, pp. 142-145, Jul. 2005.
- [51] J. N. Hwang and F. C. Chen, "A Rigorous Stability Analysis of Instability in ADI-FDTD Method with PML," *IEEE Antennas and Propagat. Society International Symp.*, pp. 1739-1742, Jul. 2006.
- [52] P. K. Kelly, J. G. Maloney, B. L. Shirley and R. L. Moore, "Photonic Band Structures of Finite Thickness: Theory and Experiment," *IEEE Antennas and Propagat. Society International Symp.*, vol. 2, pp. 718-721, Jun. 1994.
- [53] C. G. Yuan and Z. Z. Chen, "A Three-Dimensional Unconditionally Stable ADI-FDTD method in the Cylindrical Coordinate System," *IEEE Trans. Microwave Theory and Tech.*, vol. 50, pp. 2401-2405, Oct. 2002.